Hadronization of partons

S. Albino

II. Institut für Theoretische Physik, Universität Hamburg, Luruper Chaussee 149, 22761 Hamburg, Germany

(Published 13 September 2010)

The description of inclusive production of single unpolarized light hadrons using fragmentation functions in the framework of the factorization theorem is reviewed. The factorization of observables into perturbatively calculable quantities and these universal fragmentation functions are summarized and some improvements beyond the standard fixed order approach are discussed. The extraction of fragmentation functions for light charged ($\pi^{\pm}$, $K^{\pm}$, and $p/\bar{p}$) and neutral (K_S^0 and $\Lambda/\bar{\Lambda}$) hadrons using these theoretical tools is discussed through global fits to experimental data from reactions at various colliders, in particular from accurate e^+e^- reactions at the Large Electron-Position Collider (LEP), and the subsequent successful predictions of other experimental data, such as data gathered at Hadron Electron Ring Accelerator (HERA), the Tevatron, and the Relativistic Heavy Ion Collider (RHIC), from these fitted fragmentation functions as allowed by factorization universality. These global fits also impose competitive constraints on $\alpha_s(M_Z)$. Emphasis is placed on the need for accurate data from $pp(\bar{p})$ and ep reactions in which the hadron species is identified in order to constrain the separate fragmentation functions of the gluon and each quark flavor for each hadron species.

DOI: 10.1103/RevModPhys.82.2489 PACS number(s): 12.38.Cy, 12.39.St, 13.66.Bc, 13.87.Fh

CONTENTS

I. INTRODUCTION

Fragmentation functions (FFs) constitute one of the most important free inputs required for a comprehensive description of most collider processes to which perturbative QCD is applicable, being a necessary ingredient in any sufficiently complete calculation of processes involving detected hadrons in the final state. They quantify the hadronization of quarks and gluons which must eventually occur in every process in which hadrons are produced. While parton distribution functions (PDFs), another important free input, are relevant for collisions involving at least one hadron, most importantly at present for pp collisions at the CERN Large Hadron Collider (LHC) FFs are relevant in principle for all collisions even those without any initial state hadrons such as electron-positron collisions at the future International Linear Collider. Furthermore, while knowledge and application of PDFs are limited to the types of hadrons that can be practically used in the initial state, being almost exclusively nucleons, FFs can be constrained by, and/or used for the predictions of, measurements of the inclusive productions of neutral and charged hadron species ranging from the almost massless to the very heavy. Such a large range of processes provides a large range of information on hadronization, and hence contributes to our understanding of nonperturbative physics in general, and allows for a particularly incontrovertible phenomenological determination of the applicability and limitations of various approximations used in the context of QCD factorization. Such data are also sufficiently accurate to allow for competitive extractions of $\alpha_s(M_Z)$, the strong coupling constant of QCD evolved for convenience to the Z-pole mass M_Z, and the remaining of the most important free inputs, which improves the accuracy of perturbative QCD calculations in general and imposes constraints on new physics. We note here that while other inputs such as higher twist, multihadron FFs, fracture functions, etc. become important in certain kinematic limits, FFs are always necessary for a complete description of inclusive hadron production.

In this article, we review the progress in understanding the hadronization of partons, embodied in FFs, and their application to inclusive hadron production. The concept of fragmentation was first introduced by Field and Feynman (1977) to explain the limited transverse momenta and energy fraction scaling of hadrons in jets produced in e^+e^- collisions, as well as the presence of a few high transverse momentum ($p_T \gtrsim 2$ GeV) hadrons in hadron-hadron collisions. In the latter case, the collision of a pointlike constituent particle of one hadron with that of another produces a pair of particles whose directions of motion are opposite to one another but at any angle to the parent particles, including large angles. These elementary particles must eventually hadronize to produce the high p_T hadrons. Intuitively, any inclusive single hadron production processes may be predicted by first calculating the equivalent partonic process (i.e., replacing the detected hadron by a parton and the inclusive sum over hadron final states by a sum over partonic ones), then allowing the "detected" parton to hadronize. This *parton model* is made more precise with the factorization theorem.

Our discussion is limited to inclusive single unpolarized hadron production, being better understood than its polarized counterpart. Final state partons will on average hadronize to hadrons of all species that are not kinematically forbidden by the particular reaction, but, of all the charged hadrons, partons will mostly hadronize to the three lightest ones, $\pi^\pm$, $K^\pm$, and $p/\bar{p}$, so their FFs are the most phenomenologically well constrained. The species of neutral meson and neutral baryon most likely to be produced in the hadronization process are π^0 and $n/\bar{n}$, respectively, but their FFs are accurately approximated by the FFs for $\pi^\pm$ and $p/\bar{p}$ due to SU(2) (nuclear) isospin symmetry between the u and d quark flavors. The next lightest species of meson and baryon are K_S^0 and $\Lambda/\bar{\Lambda}$, respectively, whose FFs have therefore also been greatly studied. (K_L^0 is not usually observed in experiment because it takes a long time to decay into charged particles.) Together with η, f_0, $\rho^\pm$, ρ^0, ω, $K^{*\pm}$, η', a_0, and ϕ mesons, whose FFs are unfortunately either unknown or rather poorly known at present, the particles mentioned here complete the list of known hadrons which have a mass less than or equal to the $\Lambda/\bar{\Lambda}$ mass and which are the most copiously produced in hadron production, and thus measurements of their production lead to a rather comprehensive picture of the hadronic final state. In this article we focus on the production of $\pi^\pm$, $K^\pm$, $p/\bar{p}$, K_S^0, and $\Lambda/\bar{\Lambda}$.

Much of the techniques for global fitting of PDFs can be carried over to global fitting of FFs, for example, the treatment of systematic errors on the experimental data and the propagation of experimental errors to the FFs, as well as the techniques used for the minimization of chi squared. On the theoretical side, much of the formalism of both the *fixed order* (FO) calculations and its improvement, via, e.g., large x resummation and incorporation of heavy quarks and their masses, is also very similar.

To date, the subject of fragmentation has been important in various areas of phenomenology (Albino *et al.*, 2008), and we give an incomplete list of examples: Phenomenological constraints on the nucleon PDFs for polarized quarks and antiquarks separately, which are important for the determination of the source of nucleon spin, can be obtained using the FFs for these particles to calculate measurements of semi-inclusive deeply inelastic scattering (DIS) with polarized initial state particles for the inclusive production of single unpolarized light charged hadrons (de Florian, Sampayo, and Sassot, 1998; Hasegawa, 1998; Airapetian *et al.*, 2004, 2005; de Florian, Navarro, and Sassot, 2005). Unpolarized valence quark PDFs can be similarly extracted but from data for which the initial state particles are unpolarized (Gronau, Ravndal, and Zarmi, 1973; Arneodo, 1989). In both cases, the differences between FFs for positively and negatively charged particles are required, which are

relatively poorly constrained by data from, e.g., pp reactions and are not constrained at all by accurate e^+e^- reaction data. Polarized $pp(\bar{p})$ reaction data for inclusive hadron production from, e.g., RHIC can also impose constraints on the nucleon PDF for the polarized gluon (de Florian, 2003; Jager, Schafer, Stratmann, and Vogelsang, 2003), and measurements of photoproduction in inclusive hadron production in polarized ep reactions at, e.g., the proposed electron-RHIC (eRHIC) (Deshpande, Milner, Venugopalan, and Vogelsang, 2005) or Large Hadron-Electron Collider (LHeC) (Dainton, Klein, Newman, Perez, and Willeke, 2006) colliders can impose constraints on the photon PDF for polarized partons (Jager, Stratmann, and Vogelsang, 2003, 2005). FFs provide a consistency check on transverse momentum dependent FFs, which replace FFs when the transverse momentum of the detected hadron is measured in addition to the longitudinal since formally the FFs are reproduced by integrating them over the transverse momentum. The suppression of π^0 production in heavy ion collisions relative to pp collisions (Adler *et al.*, 2003a; Adcox *et al.*, 2005) measured at RHIC and to be further investigated by the ALICE, ATLAS, and CMS Collaborations at the LHC provides information on the much anticipated scenario of a quark-gluon plasma that filled the Universe the first ten millionths of a second after the big bang and created the primordial matter. Such studies may therefore contribute to our understanding of both cosmology and the physics of nonperturbative QCD. Photons produced by partonic fragmentation (Koller, Walsh, and Zerwas, 1979; Gluck, Reya, and Vogt, 1993) contribute significantly to the photonic background of various direct photon signals in inclusive hadron production in general, such as the photon signal of the Higgs boson production from hadrons. Fragmentation of a quark to a lepton pair (Braaten and Lee, 2002) or, equivalently, to a virtual photon (Qiu and Zhang, 2001) is perturbatively calculable if the invariant mass is much greater than Λ_{QCD}, in contrast to FFs for hadrons and for the real photon, so measurement of the polarization of the virtual photon that decays to the lepton pair of the Drell-Yan cross section can be used to test models of the formation of J/ψ particles, whose production from fragmentation is otherwise similar to that of the virtual photon. Hirai, Kumano, Oka, and Sudoh (2008) proposed to identify exotic hadrons such as tetraquarks by identifying properties of the extracted FFs of a newly observed particle which are typical of FFs for quarks whose flavor is favored, i.e., that are of the same flavor as any of the detected hadron's valence quarks. Some fragmentation studies of squarks and gluinos into hadrons have been performed by Katsoufis and Vlassopulos (1985) and by Vlassopulos (1985) and recently into supersymmetric hadrons by Chang, Chen, Fang, Hu, and Wu (2007), which may be relevant at the LHC. The supersymmetric extension of the Dokshitzer-Gribov-Lipatov-Altarelli-Parisi (DGLAP) evolution of FFs for light charged hadrons has been studied by Fodor and Katz (2001), Coriano and Faraggi (2002), Aloisio, Berezinsky, and Kachelriess (2004), and Cafarella (2006) in the context of ultrahigh energy cosmic rays. FFs for light charged hadrons are required for the calculation of hadronic signatures of black hole production at the LHC (Mocioiu, Nara, and Sarcevic, 2003).

The rest of this article is structured as follows. The basic results of the QCD factorization theorem, which forms the starting point of all calculations of inclusive hadron production, are given in Sec. II, in particular the separation from the overall cross section of the process dependent parts, which can be calculated using the FO approach to perturbation theory. (The derivation of these results is outlined in Appendix A.) Then in Sec. III we discuss the extraction of FFs from accurate e^+e^- data and from various well motivated nonperturbative assumptions. The ability of using these calculations for fitted FFs to reproduce measurements is studied in Sec. IV. Then we turn to recent progress: Improvements to the standard FO approach that have not been incorporated into nearly all global fits are given in Sec. V, namely, hadron mass effects and large x resummation. The treatment of experimental errors and their propagation to fitted quantities, which has been rather comprehensively implemented in PDF fits but to a somewhat lesser degree in FF fits, is discussed in Sec. VI. The three most recent global fits, in which the implementation of these improvements can be found, are discussed and compared in Sec. VII. Finally, in Sec. VIII we examine the improvement of the standard FO approach at small x by resummation of *soft gluon logarithms*, which has so far been successfully tested at LO, and we consider what is needed for a full treatment of soft gluon logarithms to near-to-leading order (NLO). In Sec. IX we predict future experimental and theoretical progress of FF extraction and summarize the current progress in Sec. X. Definitions of various momentum fractions for the detected hadron, in particular the light-cone momentum fraction important in the factorization theorem, are given in Appendix B for general processes. The LO splitting functions are given in Appendix C for reference, the relevant Mellin space formulas in Appendix D, and a summary of all data that can be calculated and used to provide constraints on FFs in Appendix E. Some of these issues have recently been discussed by Arleo (2009), with an aim toward extending the formalism to describe fragmentation in QCD media.

II. RESULTS OF THE QCD FACTORIZATION THEOREM

Intuitively, the detected hadron h of inclusive single hadron production events is inclusively produced in the jet formed by a parton i produced at a short distance $1/\mu_f$ in the overall process and carries away a fraction z of the momentum of i, as shown by the amplitude in Fig. 1.

The probability density in z for this to take place is given by the FF $D_i^h(z,\mu_f^2)$. The hadronic cross section is then equal to the cross section with h replaced by i, hereafter referred to as the partonic cross section, weighted with the FF of i and summed and integrated

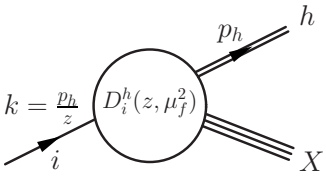

FIG. 1. Amplitude for the inclusive production of a hadron h from a parton i. After summing the modulus squared over X, the blob can be identified with the FF $D_i^h(z,\mu_f^2)$, where μ_f is the energy scale at which the parton is produced.

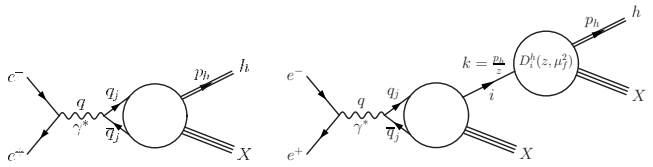

FIG. 2. Schematic illustration of factorization in inclusive hadron production. Amplitude for the process $e^+e^- \to \gamma^* \to q_j + \bar{q}_j \to h + X$ (left). Time flows from left to right. The virtual photon momentum q obeys $q^2 = s$, where $\sqrt{s}$ is the center of mass (c.m.) energy. The blob contains all QCD processes consistent with its external propagators and legs. Also shown is a schematic of the leading twist component of this process after factorization (right), involving an intermediate real parton i that fragments to the detected hadron h. The top right blob and its external lines represents the FF D_i^h, while the rest of the diagram is the equivalent partonic cross section, i.e., with h replaced by i. The lower label X refers to a sum over partons and their physical degrees of freedom, so is strictly speaking different to the upper label X.

over all degrees of freedom such as i and z, i.e., Eq. (1) below. According to the factorization theorem, which follows from QCD in a model independent way, the leading twist component of any inclusive single hadron production cross section takes this intuitive form, where the FFs are process independent or *universal* among different initial states. The factorization theorem also asserts that all processes in the partonic cross section that have energy scale below the factorization scale μ_f factor out of the partonic cross section and are accounted for by the FFs and that the resulting factorization scale dependence of these FFs may be calculated perturbatively. In this section, we highlight the results of the factorization theorem. An outline of the formal derivation of the factorization theorem is given in Appendix A.

Formally, the cross section is independent of the "probing scale" μ_f. However, the perturbative approximation to the factorized partonic cross section depends on μ_f through logarithms of the ratio of μ_f to the "energy scale" E_s of the process, which occur with higher powers at higher orders in α_s and spoil the accuracy of the series when large. Thus, the choice $\mu_f = O(E_s)$ should be made to ensure reliable results in practice. The precise choice of E_s in terms of the kinematic variables is somewhat arbitrary and conventional and will be chosen such that, for each process, the perturbative approximations of the partonic cross sections are reliable for the choice $\mu_f = E_s$ for all kinematic ranges to be studied. Note that E_s is a fixed physical quantity, in contrast to μ_f which should be allowed to vary in the range $\mu_f = O(E_s)$.

A. Factorized cross sections

In general, an inclusive single hadron production process depends on both E_s and the fraction x of the available light-cone momentum carried away by the detected hadron h (see Appendix B for more detailed discussion and definitions of momentum fractions such as x). For example, in $e^+e^- \to \gamma^* \to h + X$, whose kinematics are shown in Fig. 2 (left), $x \simeq 2|\mathbf{p}_h|/\sqrt{s}$ and $E_s = \sqrt{s}$. We assume for now that it is reasonable to neglect the effect of the hadron mass m_h, which is of $O(m_h^2/p_h^2)$ when $m_h \ll p_h$, where p_h is the momentum of the detected hadron. When the effect of hadron mass, to be discussed in Sec. V.A, is taken into account in the calculations, the scaling variable x of the factorization theorem and the ratios x_p and x_E (see Appendix B) must be distinguished from one another. Note that the cross section may depend on other variables in addition to x and E_s, but we will not indicate this explicitly unless necessary. The factorization theorem asserts that the cross section takes the form of a *convolution*,

$$d\sigma^h(x,E_s^2) = \sum_{i=-n_f}^{n_f} \int_x^1 dz\, d\sigma^j\left(\frac{x}{z}, \frac{E_s^2}{\mu_f^2}, \left\{\frac{m_k^2}{E_s^2}\right\}, a_s(\mu_f^2)\right) \times D_i^h(z,\mu_f^2), \tag{1}$$

up to higher twist terms, which are suppressed relative to the overall cross section by a factor $O(\Lambda_{\rm QCD}/E_s)$ or more. The parton label $i = 0$ for the gluon, while $i = (-)I$ for (anti)quarks, where $I = 1, \ldots, 6$ corresponds to the flavors d, u, s, c, b, and t, respectively. In other words, capitalized roman indices refer to (anti)quarks only, while uncapitalized roman indices refer to all partons including the gluon. The fact that $n_f \neq 6$ necessarily will be explained below. m_k is a renormalization scheme-dependent mass associated with parton k, which will be taken to be its pole mass, and $a_s = \alpha_s/(2\pi)$ is the expansion parameter in perturbative series. The $d\sigma^j$ are the equivalent partonic cross sections obtained by replacing the detected hadron h with a real on-shell parton i moving in the same direction but with momentum p_h/z and the sum over unobserved hadrons replaced with a sum over unobserved partons. Dividing Eq. (1) by dx and then performing the change of integration variable to $z' = x/z$ followed by the replacement $z' \to z$, which ensures that the partonic cross sections are now differential in z instead of x/z, we obtain the more familiar form,

$$\frac{d\sigma^h}{dx}(x,E_s^2) = \sum_{i=-n_f}^{n_f} \int_x^1 \frac{dz}{z} \frac{d\sigma^j}{dz}\left(z, \frac{E_s^2}{\mu_f^2}, \left\{\frac{m_k^2}{E_s^2}\right\}, a_s(\mu_f^2)\right) \times D_i^h\left(\frac{x}{z}, \mu_f^2\right). \tag{2}$$

For example, $e^+e^- \to h+X$ reactions can be factorized into the form of Eq. (1) [or Eq. (2)] as in Fig. 2 (right). In this case, $d\sigma^j$ is completely calculable in perturbation theory. For processes involving initial state hadrons, such as $ep \to e+h+X$ at HERA and $pp(\bar{p}) \to h+X$ at the LHC or RHIC, $d\sigma^j$ will be given by convolutions of perturbatively calculable quantities with PDFs for each initial state hadron, a result which also follows from the factorization theorem. The $d\sigma^j$ are otherwise perturbatively calculable if all subprocesses, with energy scale below some arbitrary factorization scale $\mu_f \gg \Lambda_{\rm QCD}$, are factored out of them and into the FFs D_i^h (and PDFs if applicable) according to the factorization theorem. While the $d\sigma^j$ differ from process to process, the FFs are universal and therefore, through them, measurements of one process impose constraints on others in which the same hadron is produced.

In more detail, the perturbative expansion of the unfactorized $d\sigma^j$ in the limit $E_s \gg m_i$ contains *potential mass singularities*, given by logarithms of the form $\ln(m_i/E_s)$ raised to powers of integers and, because the largest power in a given order in a_s grows with the order, they may spoil the convergence of the series even when $m_i \neq 0$. These potential mass singularities, which arise from energy processes much below E_s or, equivalently, μ_f, may be factored out of the $d\sigma^j$. There is clearly some freedom in choosing whether to place each process of energy scale around μ_f in $d\sigma^j$ or D_i^h, and this choice defines the *factorization scheme*. (In practice the scheme is fixed by the choice of subtraction terms in the factorization.) Although the leading twist component of $d\sigma^h$ is formally independent of the factorization scale and scheme choices, its perturbative approximation discussed above will depend on these choices, which therefore reflects the physics of the overall process. The theoretical error in the perturbative approximation can also be estimated by varying the arbitrary scale and scheme over the full range of physically reasonable choices. The potential mass singularities from (anti)quarks with mass $m_J \gg E_s$ are dampened by factors of E_s/m_J, i.e., they approximately decouple (Appelquist and Carazzone, 1975) and as such must not be factorized since doing so would introduce large uncanceled counterterms in $d\sigma^j$. Therefore, the *active partons*, those partons whose potential mass singularities are factored out of $d\sigma_i$ and into the FFs and to which the summation over i in Eq. (1) is restricted so that n_f labels the number of species of active quarks, should be limited to include only those partons whose masses $m_i \lesssim E_s$. This will always include the gluon and, since perturbative QCD is only valid in the region $E_s \gg \Lambda_{\rm QCD}$, the *light quarks*, defined to be those quarks whose masses are of $O(\Lambda_{\rm QCD})$ or less, i.e., the three lightest quarks d, u, and s or $I=1,2,3$. The intrinsic light hadron PDF of a quark is expected to be of $O(m_h/m_J)$ or less (Witten, 1976), but the same property may not necessarily hold for FFs. Therefore, it may also be necessary to always include some of the *heavy quarks*, defined to be those quarks whose mass $m_J \gg \Lambda_{\rm QCD}$, i.e., c, b, and t or $I=4,5,6$, in the list of active partons, in which case the cross section will not be perturbatively calculable if $m_J \ll E_s$. For example, it could happen that intrinsic charm quark fragmentation is deemed important in a cross section, but it cannot be incorporated into the calculation of the cross section if the only appropriate scheme is the three flavor one. This problem would be avoided if a method was known for correctly incorporating the intrinsic FF of quark J in a cross section when this quark is not active. This issue will be discussed further in Sec. II.C in the context of matching conditions between quantities defined with different numbers of active partons.

Note that there is another type of potential mass singularity appearing in the cross section, which behaves as a power of $\ln(E_s/m_J)$ as $m_J \to \infty$ for any heavy quark mass $m_J \gg E_s$. These can be absorbed into the strong coupling constant a_s using a renormalization scheme for which quark J is not active.

The n_fth scheme is a renormalization and factorization scheme for which the number of active quark flavors is n_f. Results are usually presented in the n_fth Collins-Wilczek-Zee (CWZ) scheme (Collins, Wilczek, and Zee, 1978), also known as the decoupling scheme, which reduces to the modified minimal subtraction ($\overline{\rm MS}$) scheme for only n_f massless quark flavors in the limit that n_f active quark masses vanish, and the remaining quarks' masses become infinite so that they completely decouple from the theory. The unsubtracted partonic cross sections, with heavy quarks and their masses included, as well as their subtraction terms in the CWZ schemes, have been calculated for e^+e^- reactions by Nason and Webber (1994) and Kneesch, Kniehl, Kramer, and Schienbein, (2008) and for ep reactions by Kretzer and Schienbein (1999). The inclusion of heavy quarks and their masses in the partonic cross sections for $pp(\bar{p})$ reactions have been calculated by Beenakker, Kuijf, van Neerven, and Smith (1989), Nason, Dawson, and Ellis (1989), and Beenakker, van Neerven, Meng, Schuler, and Smith (1991) and their subtraction terms by Kniehl, Kramer, Schienbein, and Spiesberger (2005a, 2005b, 2008).

B. DGLAP evolution

Roughly speaking, factorization replaces each logarithm $\ln(m_i/E_s)$, where $i=0,\ldots,n_f$, in the partonic cross section with $\ln(\mu_f/E_s)$. As mentioned at the beginning of this section, these artifacts of factorization may spoil the accuracy of the perturbation series in the same way that the potential mass singularities did unless we ensure that $\mu_f = O(E_s)$, in which case the μ_f dependence of $D_i^h(z,\mu_f^2)$ must also be known. Fortunately, unlike the z dependence, this μ_f dependence is perturbatively calculable, provided $\mu_f \gg \Lambda_{\rm QCD}$: writing the μ_f^2 dependence of the FFs in the form of the Dokshitzer-Gribov-Lipatov-Altarelli-Parisi (DGLAP) equation (Gribov and Lipatov, 1972; Lipatov, 1974; Altarelli and Parisi, 1977; Dokshitzer, 1977; Collins and Qiu, 1989),

$$\frac{d}{d\ln\mu_f^2}D_i^h(z,\mu_f^2)=\sum_{j=-n_f}^{n_f}\int_z^1\frac{dz'}{z'}P_{ij}(z',a_s(\mu_f^2))\times D_j^h\left(\frac{z}{z'},\mu_f^2\right),\tag{3}$$

with $i=-n_f,\ldots,n_f$, the splitting functions $P_{ij}(z,a_s)$ are each perturbatively calculable as a series in a_s. Specifically, denoting the square matrix with components P_{ij} by P, their expansion in a_s takes the form

$$P(z,a_s)=\sum_{n=1}^{\infty}P^{(n-1)}(z)a_s^n,\tag{4}$$

where $P^{(n-1)}(z)$ are nonsingular even in the limits for which any active parton mass vanishes. In general, P_{ij} can depend on parton masses. To ease calculations it is preferable to use schemes in which P_{ij} are mass independent, such as the commonly used CWZ (Collins, Wilczek, and Zee, 1978). Because of this mass independence, P in the n_fth CWZ scheme is equal to that of the $\overline{\text{MS}}$ scheme for n_f massless quarks only. Equations (3) and (4) serve similar purposes to the evolution of a_s,

$$\frac{d}{d\ln\mu^2}a_s(\mu^2)=\beta(a_s(\mu^2)),\tag{5}$$

where μ is the renormalization scale, and the perturbative expansion of the β function,

$$\beta(a_s)=-\sum_{n=2}^{\infty}\beta_{n-2}a_s^n,\tag{6}$$

respectively, which are used to resum powers of the logarithm $\ln(\mu/E_s)$ in perturbatively calculated quantities. In other words, the ultimate purpose of the DGLAP equation is to resum powers of the logarithm $\ln\mu_f$ in the partonic cross section. The physical interpretation of Eq. (3) is most easily made from its solution, which takes the form

$$D_i^h(z,\mu_f^2)=\sum_{j=-n_f}^{n_f}\int_z^1\frac{dz'}{z'}E_{ij}\left(\frac{z}{z'},a_s(\mu_f^2),a_s(\mu_{f0}^2)\right)\times D_j^h(z',\mu_{f0}^2).\tag{7}$$

Each quantity $E_{ij}(z,a_s(\mu_f^2),a_s(\mu_{f0}^2))$, which also obeys Eq. (3) on taking $D_i^h\to E_{ik}$, may be interpreted as the FF of parton i at resolution scale μ_f into parton j at resolution scale μ_{f0} carrying a fraction z of parton i's momentum. It is subject to the boundary condition $E_{ij}(z,a_s,a_s)=\delta_{ij}\delta(1-z)$ and depends only on $P^{(n-1)}(z)$ of Eq. (4). We will see in Sec. II.E that an analytic form for the perturbative calculation of E may be obtained in Mellin space.

C. Changing the number of active partons

So far, we have only considered the case where a fixed choice of parton species is active, i.e., whose mass logarithms are factored out of the partonic cross sections. Specifically, we have chosen the n_fth CWZ scheme (Collins, Wilczek, and Zee, 1978) in which the gluon and the n_f lightest quarks are active. This choice is necessary for reliable results when E_s is in the range $O(m_{n_f})<E_s<O(m_{n_f+1})$. However, this means that all quantities must be calculated in the (n_f+1)th CWZ scheme when E_s is in the range $O(m_{n_f+1})<E_s<O(m_{n_f+2})$. Consequently, this assignment of active quarks must be allowed to vary. Fortunately, the factorized partonic cross sections $d\sigma^i$ as a function of n_f are known, as are the necessary perturbative matching conditions between different schemes for a_s (Marciano, 1984) and for the FFs. Writing the FFs of the n_fth scheme as D_i^h with $i=-n_f,\ldots,n_f$ and the FFs of the (n_f+1)th scheme as $D_i^{h\prime}$ with $i=-(n_f+1),\ldots,n_f+1$, the matching conditions for the FFs take the form

$$D_i^{h\prime}(z,\mu_f^2)=\sum_{j=-n_f}^{n_f}\int_z^1\frac{dz'}{z'}A_{ij}\left(\frac{z}{z'},\left\{\frac{m_k^2}{\mu_f^2}\right\},a_s(\mu_f^2)\right)\times D_j^h(z',\mu_f^2),\tag{8}$$

where the matching matrix A is perturbatively calculable for $\mu_f=O(m_{n_f+1})$, where this matching should therefore be done. Otherwise, the precise choice of this matching threshold is arbitrary because it is nonphysical and should be distinguished from nonarbitrary physical thresholds such as that for the production of a charm quark. In the CWZ scheme (Collins, Wilczek, and Zee, 1978), A depends on m_{n_f+1} but not on m_k and is now known to NLO (Cacciari, Nason, and Oleari, 2005). The only nonzero components at NLO are A_{gg}, which vanishes if the matching is done at $\mu_f=m_{n_f+1}$ and $A_{n_f+1,g}$. The latter quantity is not needed if the full FF of the (n_f+1)th flavor heavy quark, both the intrinsic and extrinsic components, is treated as one single unknown function which must be fitted to data, which is usually the case. This is in contrast to the spacelike case: because the intrinsic component of a heavy quark PDF for the proton can normally be neglected, it can be treated as being completely extrinsic: i.e., the heavy quark is produced perturbatively from a light parton in the proton. In other words, heavy quark PDFs can be perturbatively calculated from the light parton PDFs, without the need for further unknown functions.

According to Eq. (8), a heavy quark FF with a negligible intrinsic component (i.e., its FF vanishes when it is not active) is fully determined from the other FFs. Therefore, if the intrinsic components of the heavy quarks' FFs are negligible, their FFs are perturbatively completely determined by only the gluon and the light quarks in the $n_f=3$ scheme: using Eq. (8) to convert to $n_f=4$ scheme gives the charm quark FF in terms of the gluon and light quark FFs: i.e., charm quark fragmentation proceeds via perturbative fragmentation to a gluon or light quark, which then fragments nonperturbatively to the detected hadron. Similarly the bottom quark FF for $n_f=5$ active quark flavors is fully determined from the gluon, light, and charm quark FFs.

It is not a good approximation, on the other hand, to neglect the intrinsic heavy quark FFs even for light hadrons. For example, processes such as $c\to D+X$ followed

by $D \to \pi + X$, where D refers to any D meson, contribute significantly to pion production. The intrinsic charm FF is certainly not negligible for charmed hadrons such as D mesons. In many calculations for light hadron production, the charm quark FF $D_4^{h\prime}(z,\mu_f^2)$ is treated as an unknown function at the matching scale where $\mu_f = O(m_4)$, just as the gluon and light quark flavor FFs at the initial scale $\mu_f = \mu_{f0}$ are, and the gluon and all four quark FFs are evolved from there according to the DGLAP equation of the $n_f=4$ scheme. A similar procedure is performed for the bottom quark FF. While this incorporation of intrinsic charm in the $n_f=4$ scheme is consistent with the factorization scheme, the conventional approach of setting the complete charm quark FF to zero in the cross section calculated in the $n_f=3$ scheme is not because intrinsic charm quark fragmentation effects should not depend on the choice of scheme (although the precise definition of the intrinsic charm quark FF itself is scheme dependent). Consequently, this approach contains an inconsistency: when E_s, and therefore μ_f, is close to the charm quark mass, both the three and four flavor number schemes will be valid but will lead to very different cross sections in the case that the intrinsic charm quark FF is large. In practice, this inconsistency of the three flavor scheme and four flavor scheme when one also considers a possibly important bottom quark FF does not matter since most cross sections of interest are of a sufficiently high energy scale that the five flavor scheme should suffice for all calculations.

D. Various treatments of quarks with non-negligible mass

In the above discussion, we have assumed that all quarks have non-negligible but finite masses. In practice, the energy scale is usually not close to any quark mass, so all perturbative results are usually approximated by the zero mass variable flavor number scheme (ZM-VFNS), where the masses m_J of quarks J above $\mu_f = O(E_s)$ are set to infinity so that these quarks decouple from the theory, which introduces a relative error of $O(E_s^2/m_J^2)$ to the cross section, while all quarks with masses below are treated as active and their masses m_i are set to zero, which introduces a relative error of $O(m_i^2/E_s^2)$. Such an approach therefore fails when the energy scale is of the order of a quark mass but is otherwise a reasonable approximation. However, the procedure discussed in the previous sections is more general and is called the general mass variable flavor number scheme (GM-VFNS), where both quarks and their masses are treated in a similar fashion to their treatment in the Aivazis-Collins-Olness-Tung (ACOT) scheme (Aivazis, Collins, Olness, and Tung, 1994; Collins, 1998b) of spacelike factorization. Such a procedure has, for example, been explicitly implemented for heavy flavor hadrons in photoproduction (Kramer and Spiesberger, 2001, 2003, 2004) and hadroproduction (Kniehl, Kramer, Schienbein, and Spiesberger, 2005a, 2005b, 2008) in $p\bar{p}$ reactions and more recently for e^+e^- reactions (Kneesch, Kniehl, Kramer, and Schienbein, 2008). The usual simplifications and improvements that have been made to the ACOT scheme since its inception may also be applied to fragmentation, at least in principle. For example, assuming that the intrinsic fragmentation of a heavy quark is negligible, the power suppressed terms in the NLO factorized cross section for the inclusive production of this heavy quark appearing in the overall hadronic cross section are in fact arbitrary since the only purpose of this heavy quark cross section is to complete the cancellation of all potential mass singularities in the overall hadronic cross section such that there are no singularities in the massless limit (Collins, 1998b). In the S-ACOT scheme (Krämer, Olness, and Soper, 2000), these power suppressed terms are set to zero for simplicity, while in the ACOT (χ) scheme (Tung, Kretzer, and Schmidt, 2002), the accuracy of the perturbative calculation relative to the original ACOT scheme is improved: The heavy quark production cross section is chosen again to be that for the production of a massless quark as in the S-ACOT scheme, but its LO part is also multiplied by a z dependent step function which is equal to that multiplying the gluon production cross section's potential mass singularity to ensure it and its counterterm only ever appear at the same values of z.

E. Analytic Mellin space solution of the DGLAP equation

The integrations over z on the right-hand sides of Eqs. (1), (3), and (7) are known as convolutions and are a typical feature of results of the factorization theorem. The Mellin transform, discussed in Appendix D, which does not destroy any information because this transform is invertible using the inverse Mellin transform of Eq. (D5), converts these convolutions into simple products, and therefore analytic work is usually performed in Mellin space. For example, Eq. (3) becomes

$$\frac{d}{d\ln\mu_f^2} D(N,\mu_f^2) = P(N,a_s(\mu_f^2)) D(N,\mu_f^2), \tag{9}$$

where for further simplification we are now also omitting parton labels i, j and the more trivial hadron label h: it is understood in Eq. (9) that the matrix P acts on the column vector D according to the usual matrix product definition. The elements of $P(N,a_s(\mu_f^2))$ for integer N are equal to the anomalous dimensions of the twist two spin N gauge invariant operators in D, which are needed in the operator product expansion (OPE). In the solution to Eq. (9),

$$D(N,\mu_f^2) = E(N,a_s(\mu_f^2),a_s(\mu_{f0}^2)) D(N,\mu_{f0}^2), \tag{10}$$

which is the Mellin transform of Eq. (7), the elements of E may be expressed analytically in terms of N, $a_s(\mu_f^2)$, and $a_s(\mu_{f0}^2)$ up to the same accuracy as P (Furmanski and Petronzio, 1982; Ellis, Kunszt, and Levin, 1994): since the LO result,

$$E_{\mathrm{LO}}(N,a_s,a_0) = \exp\left[-\frac{P^{(0)}(N)}{\beta_0}\ln\frac{a_s}{a_0}\right], \tag{11}$$

is an exact solution to Eq. (9) with $P=a_sP^{(0)}$, we are motivated to write the solution to any order in the form

$$E(N,a_s,a_0) = U(N,a_s)E_{\mathrm{LO}}(N,a_s,a_0)U^{-1}(N,a_0) \tag{12}$$

[note that the boundary condition $E(N,a,a)=\mathbf{1}$ is obeyed]. In the perturbative expansion of U,

$$U(N,a_s) = \mathbf{1} + \sum_{n=1}^{\infty} U^{(n)}(N)a_s^n, \tag{13}$$

the coefficients $U^{(n)}$ are constrained, via Eq. (9), in terms of $P^{(m)}$. These constraints are implemented by converting Eq. (9) via Eq. (12) to an evolution equation for U,

$$\frac{dU}{da_s} = -\frac{R}{\beta_0} + \frac{1}{\beta_0 a_s}[U,P^{(0)}], \tag{14}$$

where $R=\Sigma_{n=1}^{\infty}a_s^{n-1}R^{(n)}=-\beta_0[P/\beta+P^{(0)}/\beta_0 a_s]U$. The exponentiation in Eq. (11) and the commutator in Eq. (14) are handled by choosing a specific basis for the FFs in a factorization scheme in which the symmetries of QCD are obeyed. Such a basis will be given in Sec. II.F.

As a final remark, the Mellin space formalism makes clear the importance of the DGLAP equation in application of perturbation theory to cross-section calculations: any set of functions D_i of the variables $0<z<1$ and $0<\mu_f^2<\infty$ obeys the form of the DGLAP equation [Eq. (3)] by choosing $P(N,a_s(\mu_f^2)) = (dD(N,\mu_f^2)/d\ln\mu_f^2)D^{-1}(N,\mu_f^2)$, which follows from its Mellin transform [Eq. (9)]. (Here D can be regarded as a matrix whose columns consist of D_i for a given hadron species which varies from column to column; i.e., there is some freedom in the definition of P.) The importance of the formalism behind the DGLAP equation is that P is constrained in QCD to depend on purely partonic graphs and furthermore to be perturbatively calculable [these results follow from Eq. (A29)], and therefore the μ_f dependence of the FFs is completely and calculably constrained. In particular, when expanded in a_s it takes the form in Eq. (4) with nonsingular coefficients. However, Eq. (3) is not the only way to evolve the FFs in μ_f. Alternatives to Eq. (3) may be preferable for certain physical reasons, such as the double logarithmic approximation (DLA), discussed in Sec. VIII.C, which is more apt for the small x region, or the evolution proposed by Dokshitzer, Marchesini, and Salam (2006), whose equivalent splitting functions may exhibit certain physical properties not seen in the usual DGLAP splitting functions beyond LO, such as the Gribov-Lipatov relations and the expected large x behavior beyond leading order due to purely multiparton quantum fluctuations when the physical strong coupling constant is used as the expansion parameter. Such equations are similar to the DGLAP equation but with both occurrences of μ_f in Eq. (3) multiplied by (different) powers of z to ensure that the inverse of this modified scale represents the fluctuation lifetimes of successive virtual parton states pertinent to the kinematic region studied. However, if required, it is always possible to recast such alternative evolution equations back into the form of Eq. (3) and thereby use them to obtain an alternative expansion for P in the kinematic region of interest to that in Eq. (4). To put this in an alternative, but equivalent, way, Eq. (4) is not the only possibility for approximating P: In general, P in certain limits of N and a_s may be better approximated in the form $P(N,a_s)=\Sigma_r X^r R^{(r)}(Y)$, where X and Y are each in general a suitably chosen function of both N and a_s. We will see an example of such an alternative expansion in Sec. VIII.B, namely, Eq. (157) (where $\omega=N-1$).

F. Symmetries

Although FFs are not physical, the factorization scheme should be chosen such that they respect the symmetries of QCD in order to keep results as simple as possible, and we assume that this has been done. Indeed, the commonly used $\overline{\mathrm{MS}}$ scheme is such a scheme. Consider first the charge conjugation symmetry of QCD. Writing the cross section or FF for the production of h^+ (or h^-) as $O^{h^+(\text{or } h^-)}$, where $O=D_i$ or $d\sigma$, respectively, and then defining charge summed and charge asymmetry quantities as $O^{h^\pm}=O^{h^+}+O^{h^-}$ and $O^{\Delta_c h^\pm}=O^{h^+}-O^{h^-}$, respectively (or more generally as $O^{h/\bar{h}}=O^h+O^{\bar{h}}$ and $O^{\Delta_c h/\bar{h}}=O^h-O^{\bar{h}}$ which include also neutral hadrons), this symmetry implies that each of these two combinations of cross sections only depends on FFs that have been combined in the same way (or they vanish). The calculation of such cross sections is therefore simpler than that of the production of hadrons of a given charge, which depends on both charge summed and charge asymmetry FFs. The Lorentz invariance implies a similar feature for the polarization of the hadron and of the partons, assuming that there are only two possibilities for the hadron's polarization.

We now study the simplifications to the evolution of FFs when the charge conjugation symmetry is taken into account. Letting $D_{q_I}^h=D_I^h$ ($D_{\bar{q}_I}^h=D_{-I}^h$) denote the FF for the hadron h of the (anti)quark of flavor $I=1,\ldots,n_f$, this symmetry is accounted for by the results that follow from charge conjugation symmetry,

$$D_{q_I}^{h^+(\text{or } h^-)} = D_{\bar{q}_I}^{h^-(\text{or } h^+)}. \tag{15}$$

Equation (15) implies that charge summed FFs $D_{q_I}^{h^\pm} = D_{\bar{q}_I}^{h^\pm} = D_{q_I/\bar{q}_I}^{h^+} = D_{q_I/\bar{q}_I}^{h^-}$ where, for both h^+ and h^-,

$$D_{q_I/\bar{q}_I} = D_{q_I} + D_{\bar{q}_I}. \tag{16}$$

Due to charge conjugation symmetry, these FFs and the gluon FF mix only with each other on evolution but not with the valence quark FFs defined in Eq. (20) below. Furthermore, in a scheme for which P is explicitly independent of quark masses, such as the CWZ (Collins, Wilczek, and Zee, 1978), the SU(n_f) symmetry for n_f active quark flavors of equal mass that follows from QCD

implies that the gluon FF will mix via Eq. (3) with the quark FFs combined into one *singlet* quark FF,

$$D_\Sigma = \frac{1}{n_f}\sum_{I=1}^{n_f} D_{q_I/\bar{q}_I}. \tag{17}$$

In other words, Eq. (3) is obeyed with $D=(D_\Sigma, D_g)^T$ and

$$P = \begin{pmatrix} P_{\Sigma\Sigma} & P_{\Sigma g} \\ P_{g\Sigma} & P_{gg} \end{pmatrix}. \tag{18}$$

This SU(n_f) symmetry also implies that every *nonsinglet* quark FF, being any linear combination of the $D_{q_I/\bar{q}_I}$ that vanishes when they are all equal, will only mix with itself on evolution; i.e., it obeys Eq. (3) but with P reduced to the single quantity $P_{\rm NS}$ which is the same for all nonsinglets. The nonsinglets can be chosen such that they and the singlet form a linearly independent set of n_f FFs, so that after evolution the FFs of quarks of each flavor or any other alternative basis of FFs can be extracted by taking appropriate linear sums. A common choice for the set of nonsinglet FFs is

$$D_{q_I,\rm NS} = D_{q_I/\bar{q}_I} - D_\Sigma. \tag{19}$$

Equation (15) also implies that charge asymmetry FFs $D_{q_I}^{\Delta_c h^\pm} = -D_{\bar{q}_I}^{\Delta_c h^\pm} = D_{\Delta_c q_I/\bar{q}_I}^{h^+} = -D_{\Delta_c q_I/\bar{q}_I}^{h^-}$ where, for both h^+ and h^-,

$$D_{\Delta_c q_I/\bar{q}_I} = D_{q_I} - D_{\bar{q}_I}, \tag{20}$$

which we refer to as the *valence quark* FFs. Although valence quark FFs are the same as charge asymmetry FFs, we distinguish between them depending on the context—when working with the symmetries of quarks as we do in this section, we refer to them as valence quark FFs. Due to charge conjugation symmetry, valence quark FFs mix with each other on evolution but not with the summed FFs defined in Eq. (16) above. As for charge summed FFs, this mixing is further simplified by the SU(n_f) symmetry introduced above: The singlet valence quark FF,

$$D_{\Delta_c\Sigma} = \frac{1}{n_f}\sum_{I=1}^{n_f} D_{\Delta_c q_I/\bar{q}_I}, \tag{21}$$

and the nonsinglet valence quark FFs, which, similarly to the definition of nonsinglet quark FFs in Eq. (19), we take as

$$D_{I,\Delta_c\rm NS} = D_{\Delta_c q_I/\bar{q}_I} - D_{\Delta_c\Sigma}, \tag{22}$$

will obey Eq. (3) but with P reduced to the single quantity $P_{\Delta_c\Sigma}$ and $P_{\Delta_c\rm NS}$, respectively. As for $P_{\rm NS}$, $P_{\Delta_c\rm NS}$ is the same quantity for all nonsinglet valence quark FFs. At NLO, $P_{\Delta_c\Sigma}=P_{\Delta_c\rm NS}$, which leads to the simpler evolution in which each valence quark FF only mixes with itself: $D_{\Delta_c q_I/\bar{q}_I}$ obeys Eq. (3) with $P=P_{\Delta_c\Sigma}$ (or $P_{\Delta_c\rm NS}$).

The above decomposition into singlets, nonsinglets, and valence quarks allows us to explicitly determine $E_{\rm LO}$ from Eq. (11), as well as $U^{(n)}$ in terms of $P^{(m)}$ from Eq. (14), and thus to obtain a perturbative expression for E to any order via Eq. (12). In the nonsinglet and valence quark sectors, this is trivial since all quantities ($P^{(0)}$, U, etc.) are scalars, so $E_{\rm LO}$ can be calculated directly in the form given in Eq. (11) and because the commutator in Eq. (14) vanishes $U^{(n)}$ is straightforwardly determined by substitution of Eq. (13) into Eq. (14). In the singlet quark and gluon sectors, where $P^{(0)}$ is a 2×2 matrix that acts on the two component "vector" consisting of the quark singlet and the gluon, obtaining an explicit calculable form for $E_{\rm LO}$ from Eq. (11), as well as dealing with the commutator in Eq. (14) such that it can be solved for U, is more involved. Both these problems can be overcome by working in a basis in which the matrix $P^{(0)}$ is diagonal (Furmanski and Petronzio, 1982; Ellis, Kunszt, and Levin, 1994),

$$P^{(0)} = \lambda_+ M^+ + \lambda_- M^-, \tag{23}$$

where M^i are 2×2 projection matrices and λ_i are scalars, to be explicitly determined. (More generally, because of the projection operator property $\Sigma_i M^i = \mathbf{1}$, any nondiagonal matrix such as U can be written as a sum of its four ijth components $M^i U M^j$ in this basis.) Then, using the projection operator property $M^i M^j = M^i \delta_{ij}$, Eq. (11) diagonalizes to the directly calculable form

$$E_{\rm LO}(N,a_s,a_0) = \sum_i M^i(N)(a_s/a_0)^{-\lambda_i(N)/\beta_0}.$$

Furthermore, an order by order solution for U can be obtained by projecting out the ijth component of Eq. (14) in order to reduce the commutator to a matrix which is simply proportional to the ijth component of U: Matching the coefficient of a_s^{n-1} on both sides gives the relation between the ijth components of $U^{(n)}$ and $R^{(n)}$: $nM^iU^{(n)}M^j = -M^iR^{(n)}M^j/\beta_0 + (\lambda_j-\lambda_i)M^iU^{(n)}M^j/\beta_0$. Adding all four components of $U^{(n)}$ thus obtained gives

$$U^{(n)} = \sum_{ij} \frac{1}{\lambda_j - \lambda_i - \beta_0 n} M^i R^{(n)} M^j, \tag{24}$$

which can be substituted into Eq. (13) to give a perturbatively calculable form for U. Since $R^{(n)}$, defined immediately after Eq. (14), depends on the $U^{(m)}$ for $m=1,\ldots,n-1$, $U^{(n)}$ have to be obtained iteratively from Eq. (24), beginning with $U^{(1)}$.

It remains to determine λ_i and projection operators M^i satisfying Eq. (23). Using the property $\Sigma_i M^i = \mathbf{1}$, Eq. (23) implies that $M^\pm = (P^{(0)} - \lambda_\mp \mathbf{1})/(\lambda_\pm - \lambda_\mp)$. Using the property $M^iM^j = M^i\delta_{ij}$ implies that the determinant of $M^\pm$ vanishes, and therefore so does the determinant of $P^{(0)} - \lambda_\mp \mathbf{1}$. Consequently, $\lambda_\pm$ are the eigenvalues of $P^{(0)}$, i.e., $\lambda_\pm = [P_{qq}^{(0)} + P_{gg}^{(0)} \pm \sqrt{(P_{qq}^{(0)} - P_{gg}^{(0)})^2 - 4P_{qg}^{(0)}P_{gq}^{(0)}}]/2$.

In general, the zeros in the numerator of Eq. (24) lead to singularities in E for complex values of N. In the calculation of the cross section via the inverse Mellin transform defined by Eq. (D5), it is not necessary that the contour C should lie to the right of these singularities. Although this arbitrariness due to the dependence on the choice of C is of higher order than the order of the calculation, for numerical purposes it is preferable to

eliminate the singularities by choice of the spurious higher order terms. For example, at NLO, E is free of such singularities when Eq. (12) is calculated in the form $E=E_{\mathrm{LO}}+U^{(1)}E_{\mathrm{LO}}a_s-E_{\mathrm{LO}}U^{(1)}a_0$, which we note obeys the desired boundary condition $E(N,a,a)=\mathbf{1}$. Alternatively, the singularities can be made to cancel simply by choosing $U^{-1}(N,a_0)$ in Eq. (12) to be exactly equal to the inverse of $U(N,a_0)$ (Blümlein and Vogt, 1998) instead of expanding $U^{-1}(N,a_0)$ to finite order in a_0.

G. Sum rules

Intuitively, FFs as probability densities will be constrained by conservation laws. For example, from momentum conservation, the momentum of a parton i must equal the total momentum of all hadrons to which it fragments, giving the momentum sum rule

$$\sum_h \int_0^1 dz z D_i^h(z,\mu_f^2) = 1 \tag{25}$$

for every parton i. Similarly, charge conservation implies the charge sum rule

$$\sum_h \int_0^1 dz e_h D_i^h(z,\mu_f^2) = e_i, \tag{26}$$

where $e_{h(i)}$ is the electric charge of hadron h (parton i). In fact, although the probability density interpretation of FFs may not be correct for all schemes, Eqs. (25) and (26) hold in the $\overline{\mathrm{MS}}$ scheme (Collins and Soper, 1982): They are true for the bare FFs D_{Bi}^h of Appendix A, for which the probability density interpretation is valid, which is seen by applying the operation $\Sigma_h\int_0^1 dz(z)\times$ to the matrix element definition of the bare quark FFs in Eq. (A12) (and the similar definition for the bare gluon FF) and identifying the number operator for hadrons of species h in an infinitesimal region of momentum space, $dN_h=(2\pi)^{d-1}(dP^+/2P^+)d^{d-2}\boldsymbol{P}_T a_h^\dagger(P)a_h(P)$. Then Eqs. (25) and (26) follow for factorized FFs at all values of μ_f in schemes for which no subtraction is made on bare quantities that are free of divergences, such as the $\overline{\mathrm{MS}}$ scheme. Such intuitive but theoretically solid results may be regarded as "physical."

In practice, Eqs. (25) and (26) are not directly used to impose a precise constraint between FFs. First, the summation is over all hadron species h, so that they impose no constraint in global fits of FFs in the case of a specific hadron. Second, FFs at low z are poorly constrained because soft gluon logarithms render the FO approximation of the splitting functions inaccurate at small z. This is in contrast to the momentum sum rule for PDFs, which imposes a constraint between them for any given hadron because the summation is over parton species i instead of over hadron species, and PDFs are better understood at small momentum fraction. Instead, Eq. (25) may serve as an upper bound on FFs and therefore as a check on phenomenological extractions of them because, when the sum over h is limited to just a few hadrons and the lower bound for the integral over z is replaced by a value sufficiently greater than zero, it will be less than 1 if all FFs are positive. However, this positivity condition only follows from the probabilistic interpretation for FFs, which is not quite correct.

Equations (25) and (26) do impose constraints on partonic cross sections, examples are given in Sec. II.I, which give a useful check on their perturbative calculations.

H. Properties of splitting functions

The LO coefficients of the splitting functions [the $n=1$ coefficients $P^{(0)}$ in Eq. (4)] of the quark singlet and gluon sectors are given in Appendix C. Because of the Gribov-Lipatov relations (Gribov and Lipatov, 1972), they are equal to the spacelike ones after the interchange $P_{\Sigma g}^{(0)}\leftrightarrow P_{g\Sigma}^{(0)}$ is made. The LO coefficients of the splitting functions $P_{\Delta_c\mathrm{NS}}$, $P_{\Delta_c\Sigma}$, $P_{\Sigma\Sigma}$, and P_{NS} are equal to one another. The NLO coefficients [the $n=2$ coefficients $P^{(1)}$ in Eq. (4)] have been calculated by Curci, Furmanski, and Petronzio (1980) and Furmanski and Petronzio (1980) [see also Gluck, Reya, and Vogt (1993) and Ellis, Stirling, and Webber (1996) for the correction to a misprint therein]. Although the simple Gribov-Lipatov relation does not hold beyond LO, the timelike and spacelike splitting functions are related by analytic continuation of the form factor from the spacelike to the timelike case (Curci, Furmanski, and Petronzio, 1980; Furmanski and Petronzio, 1980; Stratmann and Vogelsang, 1997; Mitov, Moch, and Vogt, 2006; Moch and Vogt, 2008). Of the next-next-to-leading order (NNLO) coefficients $P^{(2)}$, the nonsinglet and singlet valences and the nonsinglet and the two diagonal singlet splitting functions have been calculated by Mitov, Moch, and Vogt (2006) and Moch and Vogt (2008) using this continuation. Only the off-diagonal splitting functions $P_{\Sigma g}^{(2)}$ and $P_{g\Sigma}^{(2)}$ need to be calculated before a full NNLO timelike evolution of all FFs will be possible. The resulting reduction in the theoretical error on all calculations when upgraded from NLO to NNLO should lead to a reduction on the total errors on FFs obtained in global fits, although this reduction will be generally somewhat smaller than the current experimental errors on FFs.

Using the momentum sum rule of Eq. (25) in Eq. (9) with $N=2$ and all hadron species h summed over gives a constraint on the splitting functions in the singlet and gluon sectors,

$$\int_0^1 dx x(2P_{\Sigma\Sigma}^{(n)}(x)+P_{\Sigma g}^{(n)}(x)) = \int_0^1 dx x(2P_{g\Sigma}^{(n)}(x)+P_{gg}^{(n)}(x)) = 0. \tag{27}$$

The factors of 2 account for the identical contributions of quarks and antiquarks. Similar momentum sum rule constraints exist for the spacelike splitting functions after the interchange $P_{\Sigma g}\leftrightarrow P_{g\Sigma}$ is made. Similarly, the charge sum rule of Eqs. (26) and (9) with $N=1$ implies that the valence quark splitting functions obey

$$\int_0^1 dx P^{(n)}_{\Delta_c \mathrm{NS}}(x) = \int_0^1 dx P^{(n)}_{\Delta_c \Sigma}(x) = 0, \tag{28}$$

which are similar to the valence sum rule constraints on the spacelike splitting functions.

I. The simplest case: $e^+e^- \to h+X$

We are now in a position to highlight the main features of the perturbative calculation of the above process, which serves as a simple illustration of the calculation of factorized cross sections in general. In this section we assume for simplicity that there are only n_f flavors of quarks, which are all massless. This process proceeds via $e^+e^- \to \gamma^*, Z \to q_J + \bar{q}_J \to \text{partons} \to h + X$, which is calculated by factorization of the modulus squared of the diagram in Fig. 2 (left), in which the resulting partonic kinematics are also shown (right). For clarity, we neglect the effects of the Z boson for now and discuss them later. The (anti)quark q_J ($\bar{q}_J$) at the electroweak vertex, called the *primary quark*, of specific flavor J is often identified or "tagged" in experiment, and we assume for generality that this is the case. Thus we make the replacements $d\sigma^i(z,\ldots) \to d\sigma^i_{q_J}(z,\ldots)$ and $d\sigma^h(x,E_s^2) \to d\sigma^h_{q_J}(x,s)$ in Eq. (2). Recall that x is the light-cone momentum fraction defined in Appendix B. In the case that the detected hadron is massless, which, however, we do not assume in this section, it is equal to $x_p = 2|\mathbf{p}_h|/\sqrt{s}$ (see Appendix B). We work to LO in electroweak theory. Expressed in terms of nonsinglets and pure singlets, the cross section in Eq. (2) can be written as

$$\frac{d\sigma^h_{q_J}}{dx}(x,s) = \int_x^1 \frac{dz}{z}\left[\frac{d\sigma^{\mathrm{NS}}_{q_J}}{dz}(z,s,\mu_f^2) D^h_{q_J/\bar{q}_J}\left(\frac{x}{z},\mu_f^2\right) + \frac{1}{n_f}\sum_{I=1}^{n_f}\frac{d\sigma^{\mathrm{PS}}_{q_J}}{dz}(z,s,\mu_f^2) D^h_{q_I/\bar{q}_I}\left(\frac{x}{z},\mu_f^2\right) + \frac{d\sigma^g_{q_J}}{dz}(z,s,\mu_f^2) D^h_g\left(\frac{x}{z},\mu_f^2\right)\right] \tag{29}$$

up to higher twist terms of $O(\Lambda_{\mathrm{QCD}}/\sqrt{s})$ or less. The nonsinglet partonic cross section $d\sigma^{\mathrm{NS}}_{q_J}/dz$ contains only those contributions in which the fragmenting quark $q_J/\bar{q}_J$ is part of the same quark line as that for the primary quark. The pure singlet partonic cross section $d\sigma^{\mathrm{PS}}_{q_J}/dz$ contains all other contributions, i.e., those for which the primary quark is not part of the same quark line as the quark which fragments. It is independent of the flavor of the fragmenting quark and gives the same result when this quark is replaced by an antiquark. Finally, $d\sigma^g_{q_J}/dz$ contains all contributions in which the fragmenting parton is a gluon.

Each partonic cross section may be written as

$$\frac{d\sigma^X_{q_J}}{dz}(z,s,\mu_f^2) = \sigma_0(s) N_c Q_{q_J}(s) C_X\left(z, a_s(s), \ln\frac{\mu_f^2}{s}\right) \quad \text{for} \quad X = \mathrm{NS},\ \mathrm{PS},\ \text{and}\ g. \tag{30}$$

The quantity $\sigma_0 = 4\pi\alpha^2/3s$ is the leading order (LO) cross section for the process $e^+e^- \to \mu^+ + \mu^-$, and the coupling of the primary quark q_J is accounted for by $Q_{q_J}(s) = e_e^2 e_{q_J}^2$, where e_f is the electric charge of a fermion f: $e_e = -1$ and $e_{q_J} = 2/3$ and $= -1/3$ for up and down type quarks q_J, respectively. Note that Q_{q_J} becomes dependent on s when the effects of the Z boson, which will be discussed later, are included. The C_X are the coefficient functions whose NLO (Altarelli, Ellis, Martinelli, and Pi, 1979; Baier and Fey, 1979) and NNLO (Rijken and van Neerven, 1996, 1997a, 1997b; Rijken, 1997; Mitov and Moch, 2006) terms are known. For the choice $\mu_f^2 = s$, the $C_X(z,a_s,0) = C_X(z,a_s)$ are given to NLO by

$$C_{\mathrm{NS}}(z,a_s) = \delta(1-z) + a_s C_F\left\{\left(\frac{2\pi^2}{3} - \frac{9}{2}\right)\delta(1-z) - \frac{3}{2}\left[\frac{1}{1-z}\right]_+ + (1+z^2)\left[\frac{\ln(1-z)}{1-z}\right]_+ + 1 + 2\frac{1+z^2}{1-z}\ln z + \frac{3}{2}(1-z)\right\},$$

$$C_{\mathrm{PS}}(z,a_s) = O(a_s^2),$$

$$C_g(z,a_s) = a_s C_F\left[2\frac{1+(1-z)^2}{z}[\ln(1-z) + 2\ln z]\right].$$

Note that the pure singlet contribution only enters at NNLO. The coefficient functions in the case where the masses of active heavy quarks are not neglected and the remaining heavy quarks are not decoupled (i.e., their masses are not set to infinity) are presented by Nason and Webber (1994).

In terms of singlets and nonsinglets,

$$\frac{d\sigma^h_{q_J}}{dx}(x,s) = \int_x^1 \frac{dz}{z}\left[\frac{d\sigma^{\mathrm{NS}}_{q_J}}{dz}(z,s,\mu_f^2) D^h_{q_J,\mathrm{NS}}\left(\frac{x}{z},\mu_f^2\right) + \frac{d\sigma^{\mathrm{S}}_{q_J}}{dz}(z,s,\mu_f^2) D^h_{\Sigma}\left(\frac{x}{z},\mu_f^2\right) + \frac{d\sigma^g_{q_J}}{dz}(z,s,\mu_f^2) D^h_g\left(\frac{x}{z},\mu_f^2\right)\right], \tag{31}$$

where the singlet D^h_Σ and nonsinglets $D^h_{q_J,\mathrm{NS}}$ are defined in Eqs. (17) and (19), respectively, and the singlet partonic cross sections is given by

$$\frac{d\sigma^{\mathrm{S}}_{q_J}}{dz} = \frac{d\sigma^{\mathrm{NS}}_{q_J}}{dz} + \frac{d\sigma^{\mathrm{PS}}_{q_J}}{dz}. \tag{32}$$

The full untagged cross section can always be obtained by summing the tagged quarks in Eq. (29) over all flavors,

$$\frac{d\sigma^h}{dx}(x,s) = \sum_{J=1}^{n_f} \frac{d\sigma^h_{q_J}}{dx}(x,s). \tag{33}$$

Conversely, Eq. (29) may be obtained from Eq. (33) simply by setting all $Q_{q_I}=0$ except Q_{q_J}. Thus the tagged cross sections $d\sigma^h_{q_J}/dx$ are physical at least in the sense that they are factorization scheme and scale independent.

We now include the effects of the Z boson, i.e., all processes $e^+e^- \to \gamma^*, Z \to q_J + \bar{q}_J \to h + X$. Under certain assumptions, discussed next, the Z boson couples to the primary quark in the same way as the virtual photon does. Thus its effect is incorporated purely by a modification to the electroweak coupling from the purely photonic one $Q_{q_J}(s) = e_e^2 e_{q_J}^2$ to (Schierholz and Schiller, 1980)

$$Q_{q_J} = e_e^2 e_{q_J}^2 + 2e_e v_e e_{q_J} v_{q_J} \frac{s(s-M_Z^2)}{(s-M_Z^2)^2 + M_Z^2\Gamma_Z^2} + (v_e^2 + a_e^2)(v_{q_J}^2 + a_{q_J}^2) \frac{s^2}{(s-M_Z^2)^2 + M_Z^2\Gamma_Z^2}, \tag{34}$$

where the vector and axial-vector couplings of a fermion f to the Z boson are given by

$$v_f = \frac{T_{3,f} - 2e_f \sin^2\theta_W}{2\sin\theta_W \cos\theta_W}, \qquad a_f = \frac{T_{3,f}}{2\sin\theta_W \cos\theta_W}, \tag{35}$$

respectively, with θ_W the electroweak mixing angle and $T_{3,f}$ the third component of weak isospin of the fermion's left-handed component: $T_{3,e}=-1/2$ and $T_{3,q_J}=1/2$ and $=-1/2$ for up and down type quarks q_J, respectively. The energy dependence of the decay width of the Z boson Γ_Z can be neglected in most applications (Consoli and Hollik, 1989), in which case it is equal to 2.4952 GeV (Amsler *et al.*, 2008).

The cross section obtained simply by choosing the effective electroweak coupling to be given by that in Eq. (34) excludes, however, certain contributions coming from the cross section involving a purely axial-vector coupling of the Z boson to the primary quark. For a detailed discussion of these contributions see Binnewies (1997), where they are referred to as class F contributions. These contributions cancel when at least one of the two couplings on either side of the cut of the boson (Z or γ) to the primary quark is a purely vector coupling, as a result of Furry's theorem (Furry, 1937). The total class F contribution to the cross section, being equal for particle and antiparticle production, will take the same form as $d\sigma^h_{q_J}/dx$ in Eq. (29) after factorization,

$$\frac{d\sigma^h_{q_J,F}}{dx}(x,s) = \int_x^1 \frac{dz}{z}\left[\frac{d\sigma^{\mathrm{NS}}_{q_J,F}}{dz}(z,s,\mu_f^2) D^h_{q_J/\bar{q}_J}\left(\frac{x}{z},\mu_f^2\right) + \frac{1}{n_f}\sum_{I=1}^{n_f} \frac{d\sigma^{\mathrm{PS}}_{q_J,F}}{dz}(z,s,\mu_f^2) D^h_{q_I/\bar{q}_I}\left(\frac{x}{z},\mu_f^2\right) + \frac{d\sigma^g_{q_J,F}}{dz}(z,s,\mu_f^2) D^h_g\left(\frac{x}{z},\mu_f^2\right)\right], \tag{36}$$

where

$$\frac{d\sigma^X_{q_J,F}}{dz}(z,s,\mu_f^2) = \sigma_0(s) N_c Q^F_{q_J}(s) C_{X,F}\left(z, a_s(s), \ln\frac{\mu_f^2}{s}\right) \tag{37}$$

with the effective electroweak coupling

$$Q^F_{q_J}(s) = (v_e^2 + a_e^2) a_{q_J}^2 \frac{s^2}{(s-M_Z^2)^2 + M_Z^2\Gamma_Z^2}. \tag{38}$$

In the untagged cross section, the replacement $a^2_{q_J} \to a_{q_J}\sum_{I=1}^{n_f} a_{q_I}$ must be made in Eq. (38) in order to account for interference effects between diagrams with different quark flavors at the Z boson vertex. Since $a_{\mathcal{Q}_u} = -a_{\mathcal{Q}_d}$, where $\mathcal{Q}_u$ and $\mathcal{Q}_d$ are any up and down type quarks, respectively, the class F contribution to the untagged cross section will vanish if every primary quark's partner in the same generation is also a primary quark and the masses of the two quarks in this generation are equal. Thus, for example, the class F contribution can be neglected when only the u, d, s, and c quarks are active and their masses can be neglected. In any case, the class F contribution can be neglected in NLO calculations since the series for $C_{F,X}$ begin at $O(a_s^2)$, where they are proportional to $C_F T_R$. We stress, however, that future NNLO calculations will be incomplete without the class F contribution.

In a single event in $e^+e^- \to \gamma^*, Z \to q_J + \bar{q}_J \to h + X$, the number of hadrons of species h produced with energy or momentum fraction between x and $x+dx$ is

$$N^h_{q_J}(x,s)dx = \frac{dx}{\sigma(s)} \frac{d\sigma^h_{q_J}}{dx}(x,s), \tag{39}$$

where, choosing $\mu = \sqrt{s}$, the total cross section $\sigma(s)$ at NLO is given by

$$\sigma(s) = \sum_I \sigma_0(s) N_c Q_{q_I}(s)\left(1 + \tfrac{3}{2} C_F a_s(s)\right). \tag{40}$$

From this result we can obtain two important sum rules. First, by energy or momentum conservation, the total energy of the final state $\Sigma_{h,J}\int_0^1 dx N^h_{q_J}(x,s) E_h$ must equal the energy of the initial state $\sqrt{s}$. Using $x = 2E_h/\sqrt{s}$, this equality of energies is equivalent to

$$\sigma_{q_J}(s) = \frac{1}{2}\sum_h \int_0^1 dx x \frac{d\sigma^h_{q_J}}{dx}(x,s), \tag{41}$$

where $\sigma_{q_J}(s)$ is the total cross section when quark q_J is tagged, given by Eq. (40) with all Q_{q_I} set to zero except that for $I=J$. In the $\overline{\text{MS}}$ scheme, the momentum sum rule of Eq. (25) and the nonsinglet, singlet, and gluon coefficient functions for $N=2$ also imply Eq. (41). The total electric charge of the final state when quark q_J is tagged is

$$\sum_h \int_0^1 dx e_h \frac{1}{\sigma(s)} \frac{d\sigma^h_{q_J}}{dx}(x,s) = 0, \tag{42}$$

which follows from Eq. (26).

A quantity which is often measured is the *multiplicity* of hadrons of species h, being the average total number of these hadrons produced in a single event. Using Eq. (39), the multiplicity is calculated from the cross section according to

$$\langle n^h_{q_J}(s)\rangle = \int_0^1 dx \frac{1}{\sigma(s)} \frac{d\sigma^h_{q_J}}{dx}(x,s). \tag{43}$$

This can be interpreted in a physically meaningful sense as the number of hadrons produced by fragmentation of quark J because, at LO,

$$\langle n^h_{q_J}(s)\rangle = \int_0^1 dx \frac{Q_{q_J}}{\sum_{I=1}^{n_f} Q_{q_I}} D^h_{q_J/\bar{q}_J}(x,s), \tag{44}$$

and because to all orders it is scheme and scale independent. The total (i.e., untagged) multiplicity is given by $\langle n^h(s)\rangle = \Sigma_J \langle n^h_{q_J}(s)\rangle$.

The cross section considered so far in this section can be decomposed into cross sections in which the vector boson is transversely and longitudinally polarized with respect to the direction of the detected hadron, denoted by the subscripts T and L, respectively,

$$\frac{d\sigma^h_{q_J}}{dx} = \frac{d\sigma^h_{q_J,T}}{dx} + \frac{d\sigma^h_{q_J,L}}{dx}. \tag{45}$$

As usual, $d\sigma^h_{q_J,T}/dx$ and $d\sigma^h_{q_J,L}/dx$ are factorized in the same way as $d\sigma^h_{q_J}/dx$ in Eq. (29). The corresponding coefficient functions are defined as before via

$$\frac{d\sigma^X_{q_J,\eta}}{dz}(z,s,\mu_f^2) = \sigma_0(s) Q_{q_J}(s) C_{\eta,X}\left(z, a_s(s), \ln\frac{\mu_f^2}{s}\right) \tag{46}$$

for $X=\text{NS},\text{PS}$, and g and for $\eta=T$ and L To $O(a_s)$,

$$C_{L,\text{NS}}(z,a_s) = a_s C_F,$$

$$C_{L,\text{PS}}(z,a_s) = O(a_s^2), \tag{47}$$

$$C_{L,g}(z,a_s) = a_s C_F\left[4\frac{1-z}{z}\right].$$

Therefore, these coefficient functions up to and including the $O(a_s^2)$ terms are required for a NLO calculation of $d\sigma^h_{q_J,L}/dx$, as is the LO part of the longitudinal component of $d\sigma^h_{q_J,F}/dx$, being of $O(a_s^2)$. Note that the transverse coefficient functions are given by $C_{T,X}=C_X-C_{L,X}$.

From a standard tensor analysis, the dependence of the differential cross section on the scattering angle θ of the detected hadron is (Mele and Nason, 1991; Nason and Webber, 1994; Rijken and van Neerven, 1996, 1997a, 1997b; Rijken, 1997; Mitov and Moch, 2006)

$$\frac{d^2\sigma^h_{q_J}}{dx\, d\cos\theta} = \frac{3}{8}(1+\cos^2\theta)\frac{d\sigma^h_{q_J,T}}{dx} + \frac{3}{4}\sin^2\theta\frac{d\sigma^h_{q_J,L}}{dx} + \frac{3}{4}\cos\theta\frac{d\sigma^h_{q_J,A}}{dx}. \tag{48}$$

Equation (48) is in fact the most general form for the inclusive production of a single hadron from a vector boson and reduces to Eq. (45) on integrating over $\cos\theta$. The coefficient of $\cos\theta$, the asymmetric cross section $d\sigma^h_{q_J,A}/dx$, is due to parity-violating effects of the Z boson. Unlike $d\sigma^h_{q_J,T}/dx$, $d\sigma^h_{q_J,L}/dx$, and $d\sigma^h_{q_J,F}/dx$, the factorized $d\sigma^h_{q_J,A}/dx$ depends only on the valence quark FFs,

$$\frac{d\sigma^h_{q_J,A}}{dx}(x,s) = \int_x^1 \frac{dz}{z}\frac{d\sigma_{q_J,A}}{dz}(z,s,\mu_f^2) D^h_{\Delta_c q_J/\bar{q}_J}\left(\frac{x}{z},\mu_f^2\right). \tag{49}$$

Here the partonic cross sections are given by

$$\frac{d\sigma_{q_J,A}}{dz}(z,s,\mu_f^2) = \sigma_0(s) Q^A_{q_J}(s) C_A\left(z, a_s(s), \ln\frac{\mu_f^2}{s}\right), \tag{50}$$

where the electroweak coupling is given by

$$Q^A_{q_J}(s) = 2a_e a_{q_J}\left(e_e e_{q_J}\frac{s(s-M_Z^2)}{(s-M_Z^2)^2+M_Z^2\Gamma_Z^2} + 2v_e v_{q_J}\frac{s^2}{(s-M_Z^2)^2+M_Z^2\Gamma_Z^2}\right) \tag{51}$$

and, to NLO,

$$C_A(z,a_s) = C_{T,\text{NS}}(z,a_s) - a_s C_F(1-z). \tag{52}$$

III. GLOBAL FITTING OF FRAGMENTATION FUNCTIONS FROM e^+e^- REACTION DATA

A comprehensive review of measurements of inclusive single hadron production in e^+e^- reactions, $e^+e^- \to \gamma^*, Z \to h+X$, up to the year 1995 is given by Lafferty, Reeves, and Whalley (1995), and all data to the present day can be obtained in numerical form from http://durpdg.dur.ac.uk/HEPDATA/. Usually, the normalized cross section

$$F_{S_A}^h(x,s) = \frac{\sum_{q_J \in S_A} d\sigma_{q_J}^h(x,s)/dx}{\sum_{q_J \in S_A} \sigma_{q_J}(s)} \tag{53}$$

is measured, where S_A is the set of all tagged quarks. Equation (41) requires the normalization of this cross section to be such that

$$\int_0^1 dx \frac{x}{2} \sum_h F_{S_A}^h(x,s) = 1. \tag{54}$$

As for Eq. (41), the factor $1/2$ in Eq. (54) arises from the fact that only half the c.m. energy is available to the detected hadron. At LO, the results of Sec. II.A give

$$F_{S_A}^h(x,s) = \frac{\sum_{q_J \in S_A} Q_{q_J} D_{q_J/\bar{q}_J}^h(x,s)}{\sum_{q_J \in S_A} Q_{q_J}}, \tag{55}$$

i.e., the measured cross section is essentially an FF or a charge weighted sum of FFs. In practice, cross sections are measured in an x bin of finite width. Setting the range of the bin as $x_l < x < x_h$, such cross sections must be calculated as

$$\langle F_{S_A}^h \rangle (x_l,x_h,s) = \frac{1}{x_h - x_l} \int_{x_l}^{x_h} dx F_{S_A}^h(x,s). \tag{56}$$

Fortunately, by working in Mellin space this bin averaging can be calculated analytically: from Eq. (D5)

$$\langle F_{S_A}^h \rangle (x_l,x_h,s) = \frac{1}{x_h - x_l} \frac{1}{2\pi i} \int_C dN \frac{x_h^{1-N} - x_l^{1-N}}{1-N} \times F_{S_A}^h(N,s). \tag{57}$$

The large amount of accurate data for inclusive single light charged and neutral hadron production from these reactions, in particular from LEP, has been used to accurately constrain many of the degrees of freedom for unpolarized charge summed FFs for light hadrons through global fits. The experimental data sets from e^+e^- reactions relevant for present global fits of FFs for $\pi^\pm$, $K^\pm$, $p/\bar{p}$, K_S^0, and $\Lambda/\bar{\Lambda}$ particles are summarized in Tables III–VII. The normalization uncertainty common to all data points is also given and therefore, in order to be correctly implemented, should be treated separately from the statistical uncertainty which varies from data point to data point. This method will be discussed in Sec. VI.B. Measurements in which the quark at the electroweak boson vertex is tagged as either a light b or c flavor quark have been performed by the TPC (Lu, 1986; Aihara *et al.*, 1987), DELPHI (Abreu *et al.*, 1998), and SLD (Abe *et al.*, 1999) Collaborations and as either a d, u, s, b, or c flavor quark by the OPAL Collaboration (Abbiendi *et al.*, 2000c), which allows FFs of quarks with the same electroweak couplings to be separately constrained, namely, u and c quark FFs can be separated from one another and d, s, and b quark FFs can be separated from one another (Kretzer, Leader, and Christova, 2001). The tagging probabilities

$$\eta_{q_J}^h(x,s) = \int_x^1 dx F_{q_J}^h(x,s) = (1-x)\langle F_{q_J}^{h^\pm} \rangle (x,1,s) \tag{58}$$

have been measured (Abbiendi *et al.*, 2000c) by the OPAL Collaboration for $q_J = u$, d, s, c, and b individually, which in particular are the only data from e^+e^- reactions that give phenomenological separate constraints on the d and s quark FFs. However, they are rather limited in number and/or accuracy and in particular only exist for $x > 0.2$. In addition, the experimental definition of these measurements may not coincide with the theoretical definition in Eq. (58) (de Florian, Sassot, and Stratmann, 2007b).

Global fits to data from e^+e^- reactions have been performed by Chiappetta, Greco, Guillet, Rolli, and Werlen (1994), Cowan (1994), Binnewies, Kniehl, and Kramer (1995a, 1995b, 1996), de Florian, Stratmann, and Vogelsang (1998), Kniehl, Kramer, and Pötter (2000), Kretzer (2000), Bourhis, Fontannaz, Guillet, and Werlen (2001), Bourrely and Soffer (2003), Albino, Kniehl, and Kramer (2005, 2006, 2008b), Hirai, Kumano, Nagai, and Sudoh (2007), and de Florian, Sassot, and Stratmann (2007a, 2007b) via minimization of χ^2, which is typically achieved through the minimization program MINUIT (James, 1998; James and Roos, 1975). Currently, all calculations are performed to NLO accuracy, and competitive phenomenological extractions of $\alpha_s(M_Z)$ have simultaneously been performed in some of these fits. Other determinations of FFs (Baier, Engels, and Petersson, 1979; Anselmino, Kroll, and Leader, 1983; Greco and Rolli, 1993, 1995; Greco, Rolli, and Vicini, 1995) using theoretical constraints such as dimensional-counting rules for the large z behavior (Baier, Engels, and Petersson, 1979; Jones and Gunion, 1979) or Monte Carlo (Greco and Rolli, 1993, 1995; Greco, Rolli, and Vicini, 1995) have used such data to motivate the values of the parameters used in these approaches. Data for which the energy scale E_s is less than a few GeV are excluded to avoid higher twist effects, detected hadron mass effects, the unreliability of truncated perturbative series, and other effects beyond the standard FO approach that may be relevant at low E_s. Usually, data for which $x < 0.1$ or even $x < 0.05$ are excluded from fits because small x logarithms in the FO calculation may prevent this region from being described and because of other possible small x effects not accounted for in the calculations. Improvements to the theoretical description of this region will be discussed in Sec. VIII. Measurements of $p/\bar{p}$ production in e^+e^- reactions are rather inaccurate, and therefore more accurate measurements of production of unidentified particles, when used together with measurements of $\pi^\pm$ and $K^\pm$ production and/or FFs for these two particles, would make a signifi-

cant improvement to the constraints on FFs for $p/\bar{p}$. However, the amount of contamination by charged particles other than the light charged hadrons in unidentified particle data is unknown but may be significant: As noted by Kniehl, Kramer, and Pötter (2000), particle unidentified data from the ALEPH (Aranda, 1995; Buskulic *et al.*, 1995a, 1995b) and OPAL (Ackerstaff *et al.*, 1999) Collaborations are inconsistent with similar data from DELPHI (Abreu *et al.*, 1998) and SLD (Abe *et al.*, 1999). Furthermore, including such data would require uniting the fits for each hadron species into a single fit, which is a greater computational challenge than performing these fits separately [although the fits for different hadron species may have to be united if $\alpha_s(M_Z)$ is included in the list of parameters to be fitted].

Longitudinal and transverse cross section measurements for hadron production in e^+e^- reactions have provided accurate constraints on the summed FFs $D^h_{q_I/\bar{q}_I}$. Measurements of the longitudinal cross section could significantly improve the current constraints on the gluon FF because it appears at LO according to Eq. (47). However, for all such data (Akers *et al.*, 1995; Aranda, 1995; Buskulic *et al.*, 1995b; Abreu *et al.*, 1999b) the particle has not been unidentified. The differences between the FFs, namely, the valence quark FFs $D^h_{\Delta_c q_I/\bar{q}_I}$, could be constrained by measurements of the asymmetry cross section $d\sigma^h_{q_I,A}/dx$, which has been performed at LEP (Akers *et al.*, 1995; Abreu *et al.*, 1999b). Unfortunately, no identification of the detected charged particle's species has been made in these asymmetry measurements, so that, as mentioned in Sec. I, the only constraints on the valence quark FFs are provided by data from pp reactions at RHIC which are rather poor, and also by HERMES data for which low $E_s=Q$ effects may be important.

In global fits, the FFs are extracted at some "initial" or "starting" scale $\mu_f=\mu_{f0}$. The FFs D_i, which are usually taken to be $D_i^{h/\bar{h}}$, and the charge asymmetry $D_i^{\Delta_c h/\bar{h}}$ (which in the case that i is a quark are equal to the summed and valence quark FFs, respectively) or D_i^h $D_i^{\bar{h}}$ are typically parametrized in the form

$$D_i(z,\mu_{f0}^2) = N_i z^{a_i}(1-z)^{b_i} f_i(z), \tag{59}$$

and the parameters $N_i, a_i, b_i, \ldots$ are freed in the fit. The function $f_i(z)$, which was set to 1 in early fits, depends on further free parameters and is used to extend the function space available to D_i. The $(1-z)^b$ behavior is motivated by dimensional-counting rules (Jones and Gunion, 1979) and is expected to set in at large enough μ_f due to the large z behavior of the splitting functions (Albino and Ball, 2001). The z^a behavior is chosen because of the evolution behavior at small (but not too small) z, to be discussed in Sec. VIII. However, these physical arguments do not precisely follow from QCD and, furthermore, the choice of parametrization used in a fit only needs to provide a sufficient region of function space to the FFs for the data to be as well described as the high energy theory approximation allows. Usually, μ_{f0} is chosen to be below the lowest value of E_s of the data, but such that $\mu_{f0} \gg \Lambda_{\mathrm{QCD}}$ in order for the perturbative calculation of the DGLAP evolution to still be valid. Typically $\mu_{f0}=O(1)$ GeV. In principle, any value may be chosen. Even the choice $\mu_{f0}=O(\Lambda_{\mathrm{QCD}})$ may be justified since the resulting large theoretical errors in the evolution around this scale would effectively be absorbed into the parameters on fitting, i.e., these low scale effects essentially just modify the choice of parametrization, although then the choice of parametrization in Eq. (59) may not be suitable.

These choices of parametrization for each FF are usually the strongest nonperturbative theoretical constraint if other nonperturbative constraints are exact or at least good approximations in the framework of current experimental and theoretical information. An example of such a reliable constraint is Eq. (15), which is exact in the standard model (in a physical scheme such as $\overline{\mathrm{MS}}$). On the other hand, as noted for the generation of the asymmetry between strange quark and antiquark PDFs of the proton of Catani, de Florian, Rodrigo, and Vogelsang (2004), because $P_{\Delta_c\Sigma} \neq P_{\Delta_c\mathrm{NS}}$ beyond NLO [see the discussion following Eq. (22)], the condition for FFs of unfavored quarks q_J to obey $D^h_{q_I}=D^h_{\bar{q}_I}$ for all μ_f is only possible in certain cases. For example, neglecting electroweak effects, suppose we impose the constraint $D_u^{\pi^+} - D_{\bar{u}}^{\pi^+} = D_{\bar{d}}^{\pi^+} - D_d^{\pi^+}$ at $\mu_f=\mu_{f0}$, which follows from SU(2) isospin symmetry between u and d. This symmetry is exact in the limit that the masses of these quarks are equal (and electroweak effects can be ignored), which is a reasonable assumption given that their masses are 1.5–4 and 4–8 MeV, respectively. Then, if the charge symmetry constraint $D^{\pi^+}_{q_I}=D^{\pi^+}_{\bar{q}_I}$ for $q_I=s,c,b,\ldots$ is also chosen to hold at $\mu_f=\mu_{f0}$, it will hold for all μ_f, as will the isospin symmetry constraint above, because $D_{\Delta_c\Sigma}$ and $D_{I,\Delta_c\mathrm{NS}}$, which do not mix with any other FFs on evolution, vanish at $\mu_f=\mu_{f0}$ and therefore all μ_f. In other words, the small violation of SU(2) isospin is responsible for the asymmetry between the fragmentation to π^+ from an unfavored quark such as s and that from its antiquark. Therefore, these unfavored asymmetries to π^+ are expected to be smaller than the unfavored asymmetries to, e.g., $h=K^+$ because the differences in masses between u and s imply that $D_u^{K^+}-D_{\bar{u}}^{K^+}$ and $D_{\bar{s}}^{K^+}-D_s^{K^+}$ cannot be expected to be similar for all z. Note that electroweak effects only predict nonzero unfavored asymmetries for π^+ and K^+ but do not predict which of these two asymmetries is the largest. Similarly as for Eqs. (25) and (26), the μ_f independence of the isospin and charge symmetry constraints implies that these constraints may be regarded as physical but only when taken together. Other than the constraints mentioned above, insufficient phenomenological constraints in global fits may require imposing yet further theoretical constraints between FFs which have no real physical justifications and which may not hold for all μ_f. We consider some examples below.

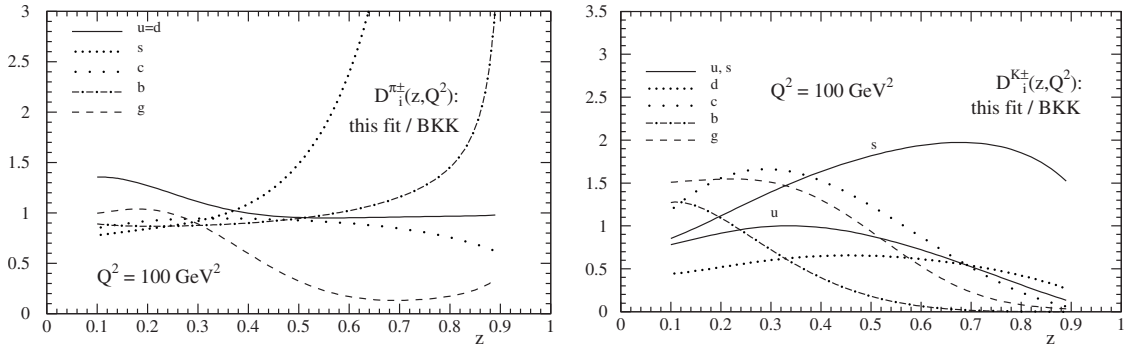

FIG. 3. Comparison of FFs from different global fits. Ratios of Kretzer (labeled "this fit") FFs to BKK FFs for $\pi^{\pm}$ (left) and $K^{\pm}$ (right) at μ_f^2=100 GeV^2 (where μ_f is written as Q). From Kretzer, 2000.

If FFs for different hadron species are related by symmetry, FFs for one of these hadron species can be used to make predictions for, or can be constrained by, processes in which another of these hadrons is detected. For example, SU(2) isospin symmetry implies that

$$D_i^{\pi^0} = \tfrac{1}{2} D_i^{\pi^{\pm}}, \quad D_{u,d,s,c,b,g}^{K_S^0} = \tfrac{1}{2} D_{d,u,s,c,b,g}^{K^{\pm}},$$
$$D_{u,d,s,c,b,g}^{n/\bar{n}} = D_{d,u,s,c,b,g}^{p/\bar{p}}. \tag{60}$$

However, we note that some hadrons are not produced by direct partonic fragmentation but rather by decay from another hadron, which itself may have been produced by either partonic fragmentation or hadronic decay. If the decay channels involved in the production of, e.g., π^0 and $\pi^{\pm}$ do not respect SU(2) isospin symmetry, the relation between their FFs above will be violated even if it is true for direct fragmentation.

A valuable consequence of the second result in Eq. (60) arises (Christova and Leader, 2007, 2009): For any initial state, the difference between $d\sigma^{K^{\pm}}/2$ and $d\sigma^{K_S^0}$ depends only on the FF $(D_d - D_u)^{K^{\pm}}/2 = (D_u - D_d)^{K_S^0}$, which is a nonsinglet. Therefore, this FF is rather well constrained relative to the other FF components. This is similar to the consequence from charge conjugation symmetry that the difference between $d\sigma^{h^+}$ and $d\sigma^{h^-}$ depends only on the charge asymmetry FFs. The assumption $D_{s,c,b,g}^{K_S^0} = \frac{1}{2} D_{s,c,b,g}^{K^{\pm}}$ may be violated by those $K^{\pm}$ and K_S^0 arising from complicated decay channels involving other hadrons instead of from direct partonic fragmentation, which may differ between $K^{\pm}$ and K_S^0. However, SU(2) isospin suggests that these hadronic decay processes for $K^{\pm}$ should be similar to those for K_S^0. An indication of this is found in the AKK08 (Albino-Kniehl-Kramer, 2008b) fit because the fitted masses of $K^{\pm}$ and K_S^0 differ from their true masses by the same amount, as discussed in Sec. VII.C. Since the nonsinglet splitting functions and coefficient functions for e^+e^- reactions are known to NNLO, the nonsinglet $(D_u - D_d)^{K_S^0}$ can also be extracted (Albino and Christova, 2010; Christova, Leader, and Albino, 2010) and through it $\alpha_s(M_Z)$ to NNLO. Such a procedure would be similar to the NNLO extraction of the nonsinglet PDF $f_u^p - f_d^p$ and $\alpha_s(M_Z)$ using data from proton and deuteron targets (Blümlein, Böttcher, and Guffanti, 2004, 2007) and would allow for a further test of perturbative stability in the timelike case. Note in particular that because soft gluon logarithms at small x are absent in nonsinglet splitting functions and coefficient functions, fits of $(D_u - D_d)^{K_S^0}$ to measurements on the difference between $K^{\pm}$ production and twice the K_S^0 production at much lower x values than those of the data used in global fits should be possible.

Aside from the rather limited measurements of tagging probabilities from OPAL (Abbiendi *et al.*, 2000c), defined in Eq. (58), measurements at LEP, taken at c.m. energies at the Z pole mass, have not implemented tagging of individual flavors of light quarks. Consequently, global fits to LEP data will not significantly constrain the differences between the individual light quark flavor FFs. If the OPAL tagging probabilities are not included in the fit, these differences will be completely unconstrained, leading to significant discrepancies between each of the light quark FFs from different sets such as Binnewies-Kniehl-Kramer (BKK) and Kretzer, as shown in Fig. 3.

These discrepancies are constrained solely by theoretical constraints, which differ from one set to another. However, LEP data do constrain the sum of these FFs weighted with the respective electroweak couplings given by Eq. (34) (neglecting effects beyond LO). In fact, because these electroweak couplings are approximately equal at the Z pole mass according Eq. (34) this sum is approximately proportional to the three flavor singlet quark FF (Kretzer, Leader, and Christova, 2001). This may explain why, despite the different theoretical constraints on the Kniehl-Kramer-Pötter (KKP) (Kniehl, Kramer, and Pötter, 2000) and Kretzer (2000) sets, the values for this FF from these sets are similar in the fit range of x (see Fig. 4) except at large z because the data at large x are scarce.

Some data for $\sqrt{s} < M_Z$ were also used in the extraction of these FF sets, although they are much lower in accuracy and value compared to the LEP data. Data over a range of c.m. energies will provide some constraints on the difference between the u quark FF and

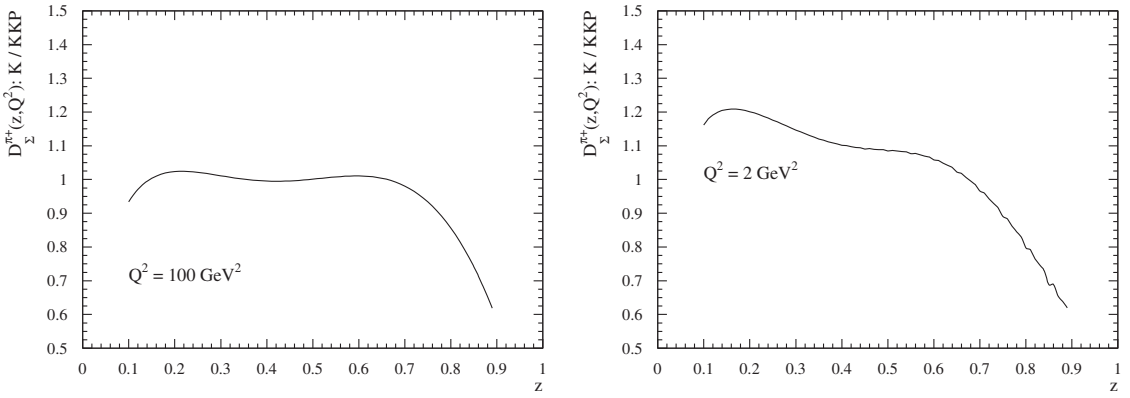

FIG. 4. As in Fig. 3 for the ratios of the Kretzer (labeled "K") to the KKP values for the singlet $D_\Sigma^{\pi^+}=D_u^{\pi^+}+D_{\bar{u}}^{\pi^+}+D_d^{\pi^+}+D_{\bar{d}}^{\pi^+}+D_s^{\pi^+}+D_{\bar{s}}^{\pi^+}$ at $\mu_f^2=100$ GeV^2 (left) and 2 GeV^2 (right). From Kretzer, Leader, and Christova, 2001.

the sum of the d and s quark FFs. This may explain why, in Fig. 3, the u quark FFs from BKK and Kretzer are similar, at least relative to the s quark FF for $\pi^\pm$ and $K^\pm$, and also relative to the d quark FF for $K^\pm$. However, because the electroweak couplings of the d and s quarks are equal at all energies, no untagged e^+e^- reaction data can constrain the difference between their FFs. Therefore, since the OPAL tagging probabilities were not available at the time that these analyses were carried out, the difference between d and s quark FFs were constrained by fixing one of these two FFs in the fit. For example, in the KKP fit, the d quark FF for $\pi^\pm$ is fixed to the u quark one, which according to SU(2) isospin symmetry is a good approximation. For $K^\pm$, the s quark FF is fixed to the u quark FF, which would be a valid approximation if the s and u quark masses were similar. This is clearly not the case—the s quark FF should be somewhat larger because the u ($\bar{u}$) quark must form a bound state with a heavier $\bar{s}$ (s) quark from the vacuum (Field and Feynman, 1977). This strangeness suppression, measured by the strangeness suppression factor γ_s, being the ratio of the production probability from the hadronization sea of s quarks to that of u and d quarks, is indeed observed in the OPAL tagging probabilities (Abbiendi *et al.*, 2000c), where it is found to be in the range $0.5>\gamma_s>0.35$. For $p/\bar{p}$, the d quark FF is fixed to half the u quark FF merely to reflect the fact that there are more u than d quarks in the proton. This condition is chosen to hold at $\mu_f=\mu_{f0}$ but cannot hold for all μ_f and is therefore not physical.

To illustrate the reliability of the theoretical approach used in global fits [including the choice of FF parametrization and SU(2) isospin symmetry], we show in Fig. 5 the description, over a large range of c.m. energies and using the KKP FF set, of $\pi^\pm$ data from e^+e^- reactions, which provide stronger constraints on FFs for $\pi^\pm$ than other data do on other FFs. The description of all data except the oldest data, from DASP, is good in the range $x>0.1$. Data below this range were excluded in the fit, which hence the deviation there from the data is no cause for concern. The fact that this deviation is so large may be due to neglected theoretical effects at small x such as unresummed logarithms or mass effects of the detected hadron.

IV. PREDICTIONS FROM GLOBALLY FITTED FRAGMENTATION FUNCTIONS

The universality of FFs between processes with different initial states as implied by the factorization theorem allows data from one process to be described using FFs sufficiently constrained by data from another process,

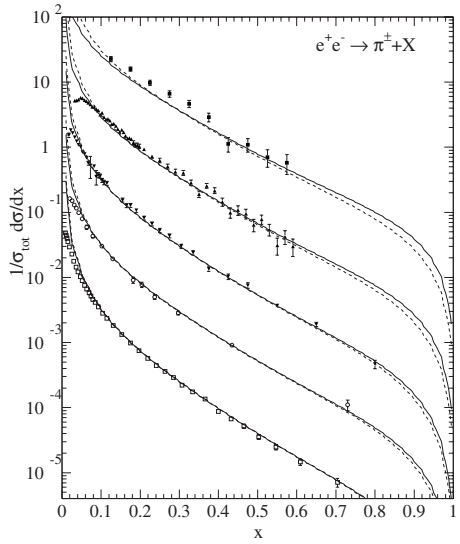

FIG. 5. NLO (solid) and LO (dashed) predictions using the KKP FF set for inclusive $\pi^\pm$ production at (from top to bottom) DASP (Brandelik *et al.*, 1979), ARGUS (Albrecht *et al.*, 1989), TPC (Aihara *et al.*, 1988a, 1988b), TASSO (Braunschweig *et al.*, 1989a, 1989b), and SLD (Abe *et al.*, 1999) at $\sqrt{s}=5.2$, 9.98, 29, 34, and 91.2 GeV, respectively. Each pair of curves is rescaled relative to the nearest pair above by a factor of 1/10. From Kniehl, Kramer, and Pötter, 2000.

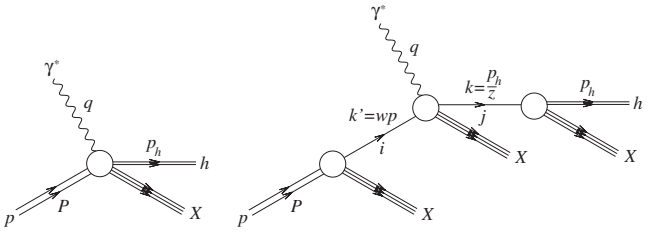

FIG. 6. Schematic of factorization in the current fragmentation region for inclusive single hadron production in neutral current DIS $ep \to e+h+X$, giving all relevant kinematics including that of the initial (k') and final (k) state real partons involved in the hard interaction. The blob on the left is the PDF $f_i^{\text{proton}}(w,\mu_f^2)$, on the right the FF $D_j^h(z,\mu_f^2)$, and in the center the hard interaction $d\sigma^{ij}(x_B/w, x/z, Q^2/\mu_f^2, a_s(\mu_f^2))$, where x_B is the Bjorken x defined in Eq. (63), Q^2 is the photon's negative virtual mass squared [see Eq. (61)], and x is the light-cone momentum fraction defined in Appendix B. As mentioned in Fig. 2, each label X does not refer to the same final state.

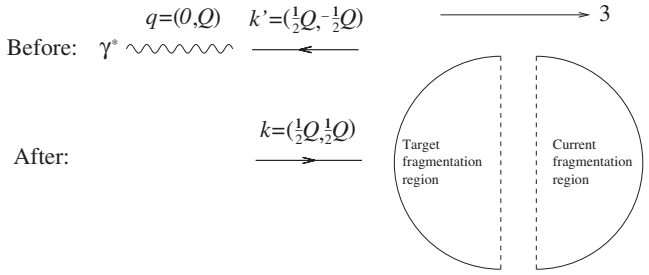

FIG. 7. Kinematics of the virtual photon and quark in the proton which it strikes, before and after this happens, in the Breit frame. Only the time and three components of momenta are given, in that order, the one and two components vanishing in all cases. At LO, all proton remnants move in the negative 3-direction, while the struck quark will fragment into a hadron moving in the positive three direction. At any order, most hadrons produced by fragmentation of a hard parton will go into the current fragmentation region, i.e., will have a positive three component of momentum.

giving a test of theoretical and/or experimental results. Essentially, such a universality test involving predictions that have been measured would really be a test of whether all relevant physics effects have been accounted for in the calculations used in the global fits and in the calculations for the predictions, assuming experimental errors on FFs, to be discussed in Sec. VI, have been propagated to these predictions. In other words, such fits will give a handle on the importance of contributions of supposedly negligible effects such as higher twist. In this section we discuss such programs, focusing mainly on descriptions of data from ep and pp reactions.

A. *ep* reactions from HERA

In this section we discuss inclusive single hadron production in neutral current DIS, $ep \to e+h+X$ or, omitting the purely leptonic subprocess and assuming that the contribution from Z boson exchange is negligible, $\gamma^* p \to h+X$, whose relevant kinematics are shown in Fig. 6 (left).

The hard scale E_s of the process is provided by the real positive number Q, where

$$Q^2 = -q^2 > 0 \tag{61}$$

is the negative virtuality of the spacelike virtual photon γ^*. Unlike e^+e^- reactions, ep reactions are complicated by the initial state hadron, which at leading twist contributes partons with densities given by PDFs to the hard interaction with the virtual photon and contributes hadronic remnants to the final state. Because of the hardness of the collision, the hadronic final state separates into two clusters which are kinematically fairly distinguishable: those produced by fragmentation of a hard parton which must therefore be assigned to h and those which are proton remnants contained in X. However, some hadrons cannot be unambiguously assigned to h or the proton remnants, which at the theoretical level translates into the need for fracture functions (Graudenz, 1994; Trentadue and Veneziano, 1994; Graudenz, 1997; Collins, 1998a) in the cross section to absorb those additional potential mass singularities which are not absorbed by the FFs and PDFs. These fracture functions describe the process

$$p \to h + i + X \tag{62}$$

and are complementary, but different, to FFs, which describe the process $i \to h+X$ and to PDFs, which describe the process $p \to i+X$. Fracture functions may be represented mathematically as $M_{p,i}^h(\xi,x,\mu_f^2)$, where x is the fraction of available light-cone momentum taken from the detected hadron, as defined in Appendix B, and $0 < \xi < 1-x$ is the fraction of the initial proton p's light-cone momentum taken from the parton i. The factorization scale μ_f represents the energy scale of the parton i as usual. The detected hadron h in Eq. (62) is a remnant of the initial proton and the parton i in Eq. (62) is required to connect the process in Eq. (62) with the hard interaction. In other words, fracture functions describe the partonic structure of the initial hadron after it has produced the detected hadron. In this sense, a fracture function is both an FF and a PDF, which explains why it depends on two momentum fractions. Fracture functions are nonperturbative and therefore, like FFs and PDFs, contribute unknown degrees of freedom to the cross section. Since on evolution they mix with both FFs and PDFs but not vice versa, one anticipates the existence of a scheme and scale independent cross section which does not depend on them. Indeed, fracture functions do not contribute to the cross section when the direction of the detected hadron's momentum is within the *current fragmentation region*: In the Breit frame, which is the frame in which the virtual photon's energy vanishes and its spatial momentum is antiparallel with the initial protons (see Fig. 7), this region is defined by $\theta < \pi/2$, where θ is the angle between the spatial momentum of the detected hadron and that of the virtual photon.

This region, consequently, is essentially devoid of proton remnants: i.e., hadrons in this region are assigned to h and not X, which results in all nonperturbative information in the calculation of the corresponding leading twist cross section provided by the FFs and PDFs only. The scaling variable for the initial proton is the Bjorken scaling variable

$$x_B = Q^2/2Pq, \tag{63}$$

where Q^2 was defined in Eq. (61). The light-cone momentum fraction x of Appendix B is defined in the class of frames in which the virtual photon's and initial proton's spatial momenta are parallel and in opposite directions. Note that the Breit frame belongs to such a class. Aligning the three axes with the virtual photon's direction, its momentum in light-cone coordinates (defined at the beginning of Appendix B) is given by

$$q = (q^+, -Q^2/2q^+, \mathbf{0}) \tag{64}$$

and the initial proton's momentum by

$$P = (0, P^-, \mathbf{0}). \tag{65}$$

Then $x = p_h^+/q^+$, which has the same value in all frames of this class since the + component is invariant under boosts in the 3-direction. It is easily verified by direct calculation that the fully Lorentz invariant definition of x is

$$x = Pp_h/Pq. \tag{66}$$

The Breit frame is obtained by setting $q^+ = Q/\sqrt{2}$ in Eq. (64), i.e., by choosing

$$q = (Q/\sqrt{2}, -Q/\sqrt{2}, \mathbf{0}). \tag{67}$$

At LO, the detected hadron will have a momentum

$$p_h = (xq^+, 0, \mathbf{0}), \tag{68}$$

in which case $x = x_p$, where

$$x_p = 2p_h q/q^2, \tag{69}$$

which is an alternative scaling variable also used in theoretical calculations (Sakai, 1979) and in experiment [see, e.g., Breitweg *et al.* (1997)]. In the Breit frame, this variable coincides with the definition of x_p defined in Appendix B because $x_p = 2|\mathbf{p}_h|/Q$.

From Fig. 6 (right) the cross section $d\sigma^h_{\text{proton}}(x, x_B, Q^2)$ is given by the equivalent partonic cross section $d\sigma^{ij}(x/z, x_B/w, Q^2)$ weighted by the probability $dw f_j^{\text{proton}}(w, \mu_f^2)$ for the proton to produce a parton i carrying away a momentum fraction in the range w to $w+dw$ and weighted by the probability $dz D_i^h(z, \mu_f^2)$ for the parton j to fragment to a hadron h carrying away a momentum fraction in the range z to $z+dz$ summed over all partons i, j and all kinematically allowed (infinitesimal) ranges dw and dz,

$$d\sigma^h_{\text{proton}}(x, x_B, Q^2) = \sum_{ij} \int_x^1 dz \int_{x_B}^1 dw \times d\sigma^{ij}\left(\frac{x_B}{w}, \frac{x}{z}, \frac{Q^2}{\mu_f^2}, a_s(\mu_f^2)\right) \times f_j^{\text{proton}}(w, \mu_f^2) D_i^h(z, \mu_f^2). \tag{70}$$

For simplicity, we used the same value μ_f for the factorization scale of the PDFs as that for the FFs. The PDF of parton i in a hadron h is written as f_i^h, and $d\sigma^{ij}$ is the cross section for the equivalent purely partonic processes $\gamma^* i \to j + X$, which is known to NLO (Altarelli, Ellis, Martinelli, and Pi, 1979; Baier and Fey, 1979). Note that, by comparing with Eq. (1), the cross section for the production of a parton i is given by

$$d\sigma^i\left(\frac{x}{z}, \frac{E_s^2}{\mu_f^2}, a_s(\mu_f^2)\right) = \sum_j \int_{x_B}^1 dw d\sigma^{ij}\left(\frac{x_B}{w}, \frac{x}{z}, \frac{Q^2}{\mu_f^2}, a_s(\mu_f^2)\right) \times f_j^{\text{proton}}(w, \mu_f^2). \tag{71}$$

After the change of integration variables $z \to x/z$ [as performed in Eq. (1) in order to obtain Eq. (2)] and $w \to x_B/w$ in Eq. (70), we find that

$$\frac{d\sigma^h_{\text{proton}}}{dx dx_B dQ^2}(x, x_B, Q^2) = \sum_{ij} \int_x^1 \frac{dz}{z} \int_{x_B}^1 \frac{dw}{w} \times \frac{d\sigma^{ij}}{dz dw dQ^2}\left(w, z, \frac{Q^2}{\mu_f^2}, a_s(\mu_f^2)\right) \times f_i^{\text{proton}}\left(\frac{x_B}{w}, \mu_f^2\right) D_j^h\left(\frac{x}{z}, \mu_f^2\right). \tag{72}$$

At LO, the purely partonic cross section is given by

$$\frac{d\sigma^{ij}}{dz dw dQ^2}\left(w, z, \frac{Q^2}{\mu^2}, a_s(\mu^2)\right) = \frac{d\sigma_0}{dQ^2}(Q^2) \sum_I \delta_{ij} \delta_{iI} e_{q_I}^2 \delta(1-w) \delta(1-z), \tag{73}$$

where σ_0 is the cross section for the elastic process $e\mu \to e\mu$ involving one photon exchange in the t channel.

The normalized cross section,

$$G^h_{\text{proton}}(x, \text{cuts}) = \frac{\int_{\text{cuts}} dx_B dQ^2 d\sigma^h_{\text{proton}}(x, x_B, Q^2)/dx dx_B dQ^2}{\int_{\text{cuts}} dx_B dQ^2 d\sigma_{\text{proton}}(x_B, Q^2)/dx_B dQ^2}, \tag{74}$$

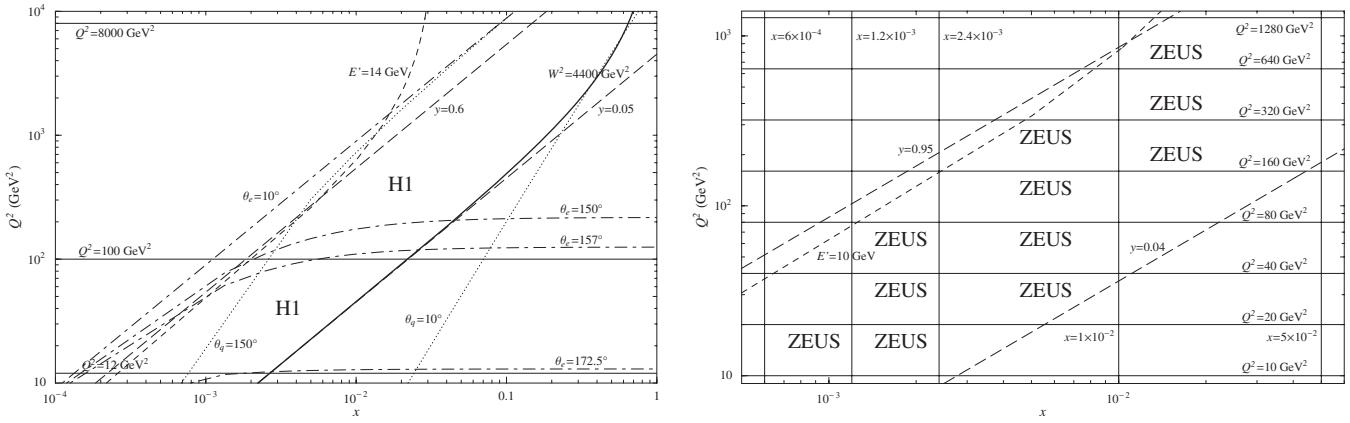

FIG. 8. Cuts in the (x_B,Q^2) plane (where x_B is written x) used in the H1 analysis of Adloff *et al.* (1997) (top), with $E=27.5$ GeV and $\sqrt{s}=300.3$ GeV, and in the ZEUS analysis of Derrick *et al.* (1996) (bottom), with $E=26.7$ GeV and $\sqrt{s}=296$ GeV. The low and high Q^2 regions used by H1 are each indicated by the label "H1" and the region used by ZEUS by the label "ZEUS," being bound in each case by the nearest cut to the label. From Albino, Kniehl, Kramer, and Sandoval, 2007.

is measured in practice, where $d\sigma_{\text{proton}}$ is the DIS ($ep\rightarrow e+X$) cross section. Some cancellation of PDF uncertainties between the numerator and denominator of Eq. (74) should occur. In any case, these uncertainties are expected to be lower than the FF ones. The normalization of G^h_{proton} may be obtained by following similar steps to those that lead to Eq. (54): Similar to Eq. (39), the number of hadrons of species h produced with energy or momentum fraction between x and $x+dx$ is $N^h(x,Q^2)dx=\{dx/[d\sigma_{\text{proton}}/dx_BdQ^2]\}d\sigma^h_{\text{proton}}/dxdx_BdQ^2$. The total momentum in the 3-direction of the hadrons in the current fragmentation region is $\Sigma_h\int_0^1 dxN^h(x,Q^2)p_h$, where p_h is the three component of the detected hadron's momentum. This must equal that of the struck quark, which according to Fig. 7 is $Q/2$ in the Breit frame. Therefore, since Eq. (69) implies that $x=2p_h/Q$ in this frame, $G^h_{\text{proton}}(x,\text{cuts})$ has the normalization

$$\int_0^1 dxxG^h_{\text{proton}}(x,\text{cuts})=1. \tag{75}$$

From the momentum sum rule [Eq. (25)], this implies that the denominator in Eq. (74) is calculated from

$$\frac{d\sigma_{\text{proton}}}{dx_BdQ^2}(x_B,Q^2)=\sum_i\int_{x_B}^1\frac{dw}{w}\frac{d\sigma^i}{dwdQ^2}\left(w,\frac{Q^2}{\mu^2},a_s(\mu^2)\right)\times f_i^{\text{proton}}\left(\frac{x_B}{w},\mu^2\right), \tag{76}$$

where

$$\frac{d\sigma^i}{dwdQ^2}=\sum_j\int_0^1 dz\frac{d\sigma^{ij}}{dzdwdQ^2}, \tag{77}$$

which at LO is therefore

$$\frac{d\sigma^i}{dwdQ^2}=\frac{d\sigma_0}{dQ^2}(Q^2)\sum_I\delta_{iI}e^2_{q_I}\delta(1-w). \tag{78}$$

As shown by Sandoval (2009), the contribution from Z boson exchange can be as much as 15% in the region $Q\simeq 100$ GeV. However, this effect approximately cancels between the numerator and denominator of the normalized cross section in Eq. (74), which is why we choose to neglect the effect of the Z boson.

The region of the (x_B,Q^2) plane, written "cuts" in Eq. (74), is usually specified by experimentalists as cuts on the squared c.m. energy of the virtual photon-proton system,

$$W^2=(P+q)^2=Q^2(1/x_B-1), \tag{79}$$

on the fraction of the energy of the initial electron or positron which is lost in the rest frame of the proton,

$$y_B=Pq/Pk=Q^2/x_Bs, \tag{80}$$

where $\sqrt{s}$ is the c.m. energy of the initial ep system and on the scattered electron or positron's energy E' in the laboratory frame,

$$E'=E-Q^2(E/x_Bs-1/4E), \tag{81}$$

where E is the initial electron or positron energy, also in the laboratory frame. A lower bound on E' prevents the scattered electron or positron being falsely identified with isolated low energy deposits in the calorimeter while the true scattered electron or positron passes undetected down the beam pipe. The H1 Collaboration imposed additional cuts (Kant, 1995; Adloff *et al.*, 1997; Dixon, 1997) on the angle of deflection of the electron or positron and struck parton in the laboratory frame, θ_e and θ_p, respectively, to maintain good detector acceptance. These are given in terms of x_B and Q^2 by

$$\cos\theta_e=\frac{x_Bs(4E^2-Q^2)-4E^2Q^2}{x_Bs(4E^2+Q^2)-4E^2Q^2} \tag{82}$$

and

$$\cos\theta_p=\frac{x_Bs(x_Bs-Q^2)-4E^2Q^2}{x_Bs(x_Bs-Q^2)+4E^2Q^2}. \tag{83}$$

The regions in the (x_B,Q^2) plane used by the H1 Collaboration of Adloff *et al.* (1997) and by the ZEUS Col-

laboration of Derrick *et al.* (1996) are shown in Fig. 8.

As for $F_{S_A}^h$ in e^+e^-, G_{proton}^h is usually averaged over a finite bin width in x. Conservation of energy and momentum implies that, after being struck by the virtual photon, the quark's spatial momentum changes in sign only, as shown in Fig. 7. Therefore, at LO, all hadrons produced in the current fragmentation region originate from fragmentation of the struck quark. [We note in passing that, at LO, hadrons produced in the remaining region $\theta > \pi/2$, the target fragmentation region (see Fig. 7), can only be proton remnants, which theoretically means that fracture functions play a more important role than FFs (or PDFs) in this region, making this a region for extracting fracture functions.] Therefore, measurements in the current fragmentation region can provide good constraints on the FFs. The distribution of hadrons in this region is similar to that in any one of the two event hemispheres in e^+e^- reactions with $\sqrt{s}=Q$, where a hemisphere is defined to be the union of all directions that make an angle less than $\pi/2$ with the thrust axis of the hadron distribution of the event, which at LO is aligned with either the primary quark or antiquark. In mathematical terms, if the range in Q^2 is negligible, which is usually a good approximation since G_{proton}^h is independent of Q up to $O(1/\ln Q)$ corrections, the LO calculation

$$G_{\text{proton}}^h(x,\text{cuts}) = \frac{\sum_{J=1}^{n_f} e_{q_J}^2 (g_{q_J}(Q^2) D_{q_J}^h(x,Q^2) + g_{\bar{q}_J}(Q^2) D_{\bar{q}_J}^h(x,Q^2))}{\sum_{J=1}^{n_f} e_{q_J}^2 (g_{q_J}(Q^2) + g_{\bar{q}_J}(Q^2))} \tag{84}$$

is similar to that for e^+e^- in Eq. (55) with $\sqrt{s}=Q$ and tagged quarks summed over all flavors (and with $Q_{q_J} \to e_{q_J}^2$ because the contribution to the ep reaction cross section from Z boson exchange has not yet been calculated) except for the presence of the PDF dependent factors

$$g_{q_J}(Q^2) = \int_{\text{cuts}} dx_B f_{q_J}^{\text{proton}}(x_B, Q^2).$$

Such factors drop out of single flavor quark tagged ep reactions, i.e., quark tagged ep and e^+e^- reactions are even more physically similar. Because of the variation among g_{q_J} and assuming that SU(2) isospin symmetry and charge symmetry of the initial proton's sea are poor approximations, the separation of the different quark flavor FFs and the valence quark FFs if the charge of the detected hadron in ep reactions is identified can be constrained by suitable data from both e^+e^- and ep reaction data or even by ep data alone by choosing different regions in the (x_B, Q^2) plane for cuts. Recall that untagged data from e^+e^- reactions alone can constrain neither the separation between FFs of quarks of the same electroweak couplings nor in the case of transverse and longitudinal cross sections, the valence quark FFs.

The ratios of the various tagged cross sections to the total cross section, for both ep and e^+e^- reactions, are shown in Fig. 9 using the AKK (Albino, Kniehl, and Kramer, 2005) FF set.

Calculations for ep reactions are also performed using the KKP and Kretzer FF sets. As for e^+e^- reactions, quark tagging for ep reactions is performed by setting the electroweak coupling to zero for all quark flavors except that of the tagged quark flavor and is therefore "physical" in the sense of being scheme and scale independent. However, quark tagging in ep reactions may not be possible at least in the near future. The purpose of Fig. 9 is only to highlight the relative differences in importance of the contributions to the overall production from the fragmentations of the various quarks in both reactions. In particular, u quark fragmentation proves to be more important in ep reactions while b quark fragmentation is more important in e^+e^- reactions, as expected from the relative magnitudes of the proton PDFs for these quarks. According to Fig. 10, the relative yields of the various hadron species are similar. Thus the complementary information on fragmentation between e^+e^- and ep reactions should also apply at the level of hadron identification, which is of primary interest at present.

Data from ep reactions are no better than data from e^+e^- reactions at constraining the gluon FF since it again only enters at NLO and not at LO according to Eq. (84). The most significant constraints on gluon fragmentation come at present from $pp(\bar{p})$ reactions, discussed in Sec. IV.B.

Comparisons have been made by Albino, Kniehl, Kramer, and Sandoval (2007), with data from the H1 (Adloff *et al.*, 1997) and ZEUS (Derrick *et al.*, 1996; Breitweg *et al.*, 1997) experiments using the CYCLOPS program (Graudenz, 1997), the CTEQ6M PDF set (Pumplin, Stump, Huston, Lai, Nadolsky, and Tung, 2002), and the AKK, Kretzer, and KKP FF sets. The comparison with the H1 data at low and high Q^2 ranges is shown in Fig. 11.

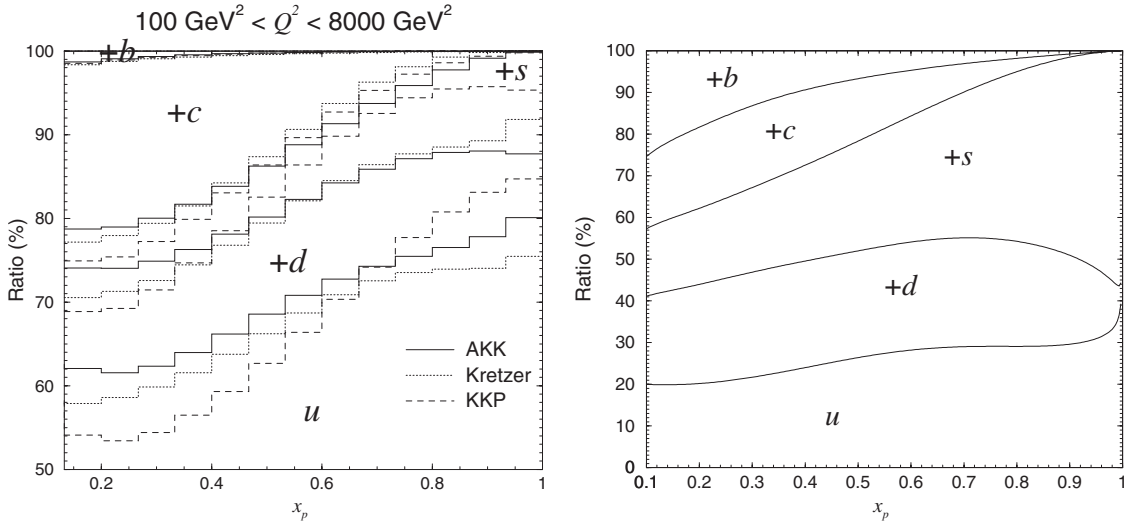

FIG. 9. The relative contributions to hadron production from fragmentation of the various quark flavors. Left: The ratios of the quark tagged components of the cross section to the untagged cross section for the high Q H1 data using the AKK, KKP, and Kretzer FF sets. The lowest three curves show the contribution from the u quark tagged component only, the next three curves above the sum of the u and d components, the next three u, d, and s, etc. Right: The ratios of the quark tagged components of the $e^+e^- \to h^\pm + X$ cross section, where $h^\pm$ is any light charged hadron, to the untagged cross section, at $\sqrt{s} = 91.2$ GeV and using the AKK FF set. Both plots, as well as the plots in Figs. 10–13, x is written as x_p. From Albino, Kniehl, Kramer, and Sandoval, 2007.

The strong disagreement between the calculations from the different FF sets at large x most likely arises from large experimental errors on the FFs due to poor constraints from e^+e^- reaction data at large momentum fraction. Otherwise, the calculations are fairly independent of the FF set used despite different theoretical constraints on the FFs among the different sets. In other words, any dependence of the cross section on those FF components not well constrained by e^+e^- reaction data which may arise as a consequence of the differences among the g_{q_J} factors in Eq. (84) is in fact negligible and/or the theoretical constraints on the FFs in the case of the KKP and Kretzer sets and the OPAL tagging probabilities in the case of the AKK set are sufficiently reliable. At high Q^2, the calculation for all three FF sets agrees well with the data, which may be due to reliable constraints on the charged pion production [note in particular that light quark flavor OPAL tagging probabilities were used in the extraction of the AKK set and SU(2) isospin in the extraction of the Kretzer and KKP sets], which dominates the cross section. Therefore, the disagreements at small x values and, perhaps, at large x values found with the lower Q^2 data may be due to neglected effects beyond the FO approach at leading twist.

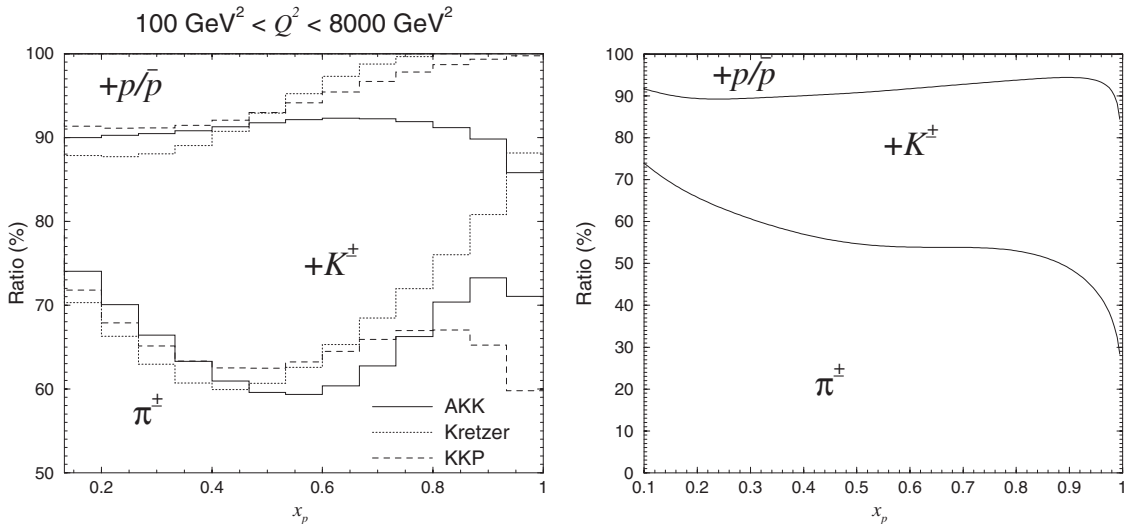

FIG. 10. The ratios of the individual hadron species constituting the sample for the high Q H1 data using the AKK, Kretzer, and KKP FF sets (left), and the ratios of the individual hadron species constituting the sample for the $e^+e^- \to h^\pm + X$ cross section (right), where $h^\pm$ is any light charged hadron, to the cross section for the full sample at $\sqrt{s} = 91.2$ GeV and using the AKK FF set. From Albino, Kniehl, Kramer, and Sandoval, 2007.

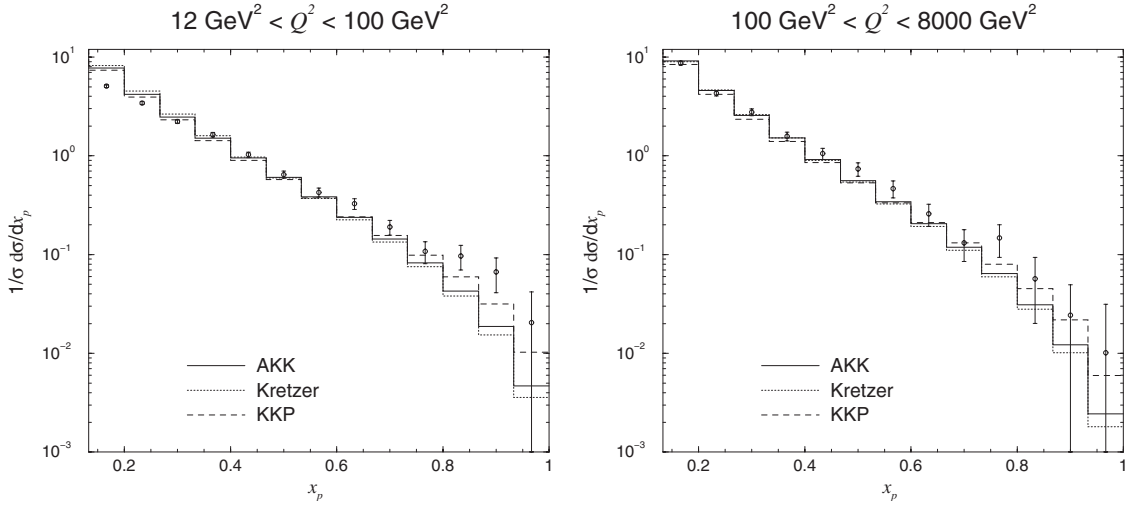

FIG. 11. Comparisons of theoretical predictions using the AKK, Kretzer, and KKP FF sets with the x distributions from H1 (Adloff *et al.*, 1997).

For example, resummation of soft gluon emission logarithms that become large at small and large x may be necessary to improve the calculation here. This is shown in Fig. 12 by the effect of renormalization and factorization scale variation on the calculation, being largest at small and large x and for the lower Q^2 range.

These observations are found to some degree in the comparison with the ZEUS data of Derrick *et al.* (1996), in Fig. 13, although disagreement of the predictions with one another is largest around $x=0.3$. The description of the data in the range $0.3<x<0.5$ is generally good, but above this range it fails for $Q^2<100$ GeV^2, which again may be due to neglected effects at large x in the calculation. However, this is unlikely because the scale variation in this region is small, suggesting that the perturbative series is stable here.

Finally, we show comparisons with the new data from the H1 (Aaron *et al.*, 2007) and ZEUS (Brzozowska, 2007) Collaborations in Fig. 14.

The H1 Collaboration reported using a sample which is a factor of 10 larger than that for the older H1 data of Adloff *et al.*, 1997, discussed above to extract these data, as well as a to better understand the experimental uncertainties, while the ZEUS Collaboration reported an integrated luminosity of 0.5 fb^{-1} to be compared with 0.55 pb^{-1} in the older ZEUS data of Derrick *et al.* (1996) considered above. The description of these much more accurate data is much worse compared to that of the previous HERA data discussed above and thus may require better constrained FFs and/or further improvements in the theory. One possible improvement for the description of the ZEUS data at large Q^2 may be the inclusion of Z boson effects.

In general, various low Q^2 effects that have been neglected in these calculations may be important, particularly higher twist, heavy quarks, and the mass of the hadron. The effect of the latter will be considered in Sec. V.A. Such effects may not be important when Q

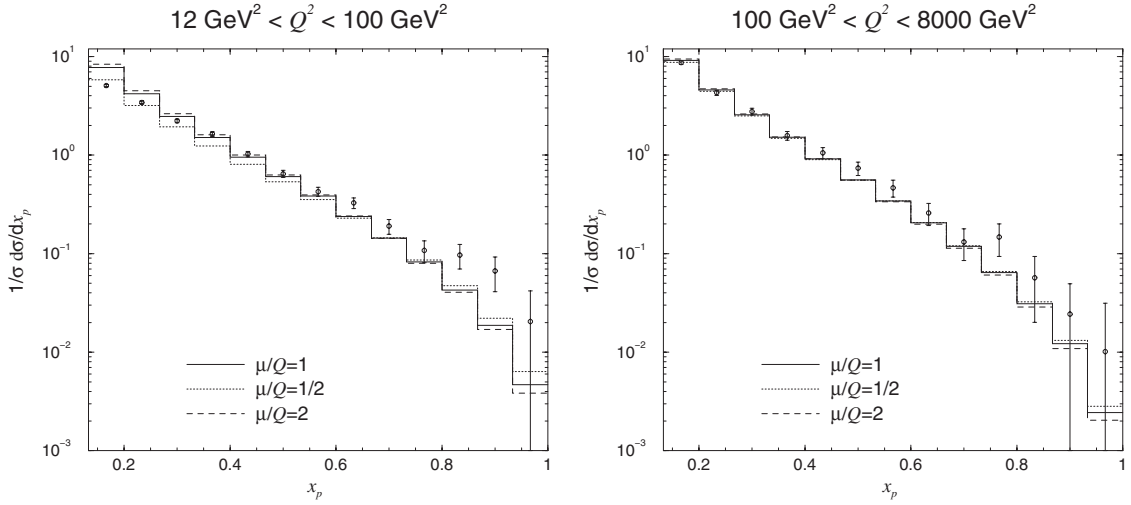

FIG. 12. As in Fig. 11, using only the AKK FF set and showing the modifications arising from scale variation. From Albino, Kniehl, Kramer, and Sandoval, 2007.

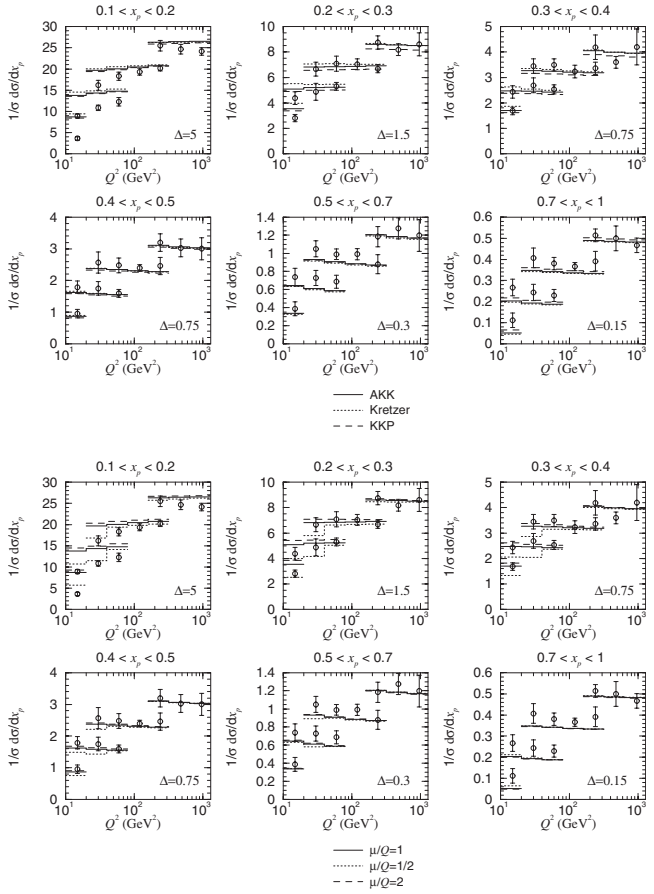

FIG. 13. Comparisons of theoretical predictions using the AKK, Kretzer and KKP FF sets with the ZEUS data (Breitweg *et al.*, 1997) (top) and showing the modifications arising from scale variation using only the AKK FF set (bottom). Each data set is measured in a specific x bin and, together with its predictions, is shifted upward relative to the one below by the indicated value for Δ. From Albino, Kniehl, Kramer, and Sandoval, 2007.

$=O(1)$ GeV because, as Fig. 15 shows, the de Florian–Sassot–Stratmann (DSS) Collaboration (de Florian, Sassot, and Stratmann, 2007a) used the standard FO approach to successfully fit π^+ and π^- FFs to accurate π^+ and π^- production measurements from ep reactions at HERMES obtained mostly in the range $1 \lesssim Q \lesssim 2$ GeV. However, it is possible that low Q effects not accounted for in the standard FO approach were in fact absorbed by the FFs as a consequence of the fitting. That such data can truly be described by the standard FO approach could be tested by, for example, performing a simultaneous fit both to these ep reaction data and to accurate π^+ and π^- production measurements from e^+e^- reactions for which $1 \lesssim \sqrt{s} \lesssim 2$ GeV.

We note that measurements of charged particle production from ep reactions have been performed at the European Muon Collaboration (Ashman, 1991). Since the particle species is not identified, these data have not been used in fits due to their possible contamination by particles other than light charged hadrons, such as electrons.

B. Hadron-hadron reactions

The inclusive production of single hadrons in hadron-hadron reactions are important because they can verify and improve constraints on the charge and flavor separation of quark FFs provided by ep and e^+e^- reactions. Perhaps most importantly, data from pp reactions at RHIC should constrain gluon FFs significantly better than data from ep and e^+e^- reactions can, owing to the occurrence of the gluon FF at LO in the calculation.

The dimensionless quantity describing the inclusive single hadron production in the collision of two hadrons h_1 and h_2, $h_1h_2 \to h+X$, which is measured in experiment, is

$$H^h_{h_1h_2}(x,y,s) = s^2 E \frac{d^3\sigma^h_{h_1h_2}}{d\boldsymbol{p}^3}(p_T,y,s) = s^2 \frac{1}{2\pi p_T}\frac{d^2\sigma^h_{h_1h_2}}{dp_T dy}(p_T,y,s) \tag{85}$$

(exploiting azimuthal symmetry in the second equality), where $\sqrt{s}$ is the c.m. energy, E and $\boldsymbol{p}$ are the energy and spatial momentum, respectively, of the detected hadron h, p_T is its transverse momentum relative to the spatial momenta of h_1 and h_2, which are antiparallel, and the rapidity

$$y = \frac{1}{2}\ln\frac{E+p_L}{E-p_L}, \tag{86}$$

with p_L as the longitudinal momentum (in the direction of the spatial momentum of h_1) of h and x is the scaling variable defined in Appendix B, i.e., in the c.m. frame and for h massless it is given by

$$x = \frac{2p_T}{\sqrt{s}}\cosh y = \frac{2E}{\sqrt{s}}. \tag{87}$$

We may also write

$$x = 1 - V + VW, \tag{88}$$

where V and W are the variables typically used in perturbative calculations, related to the usual Mandelstam variables s, t, and u of h through

$$V = 1 + t/s, \qquad W = -u/(s+t). \tag{89}$$

According to Eq. (1), the cross section at leading twist factorizes according to

$$H^h_{h_1h_2}(x,y,s) = \sum_i \int_x^1 dz H^i_{h_1h_2}\left(\frac{x}{z},y,\frac{s}{\mu_f^2},a_s(\mu_f^2)\right) D^h_i(z,\mu_f^2), \tag{90}$$

where $H^i_{h_1h_2}$ is the equivalent partonic production cross section. This equation has the following physical interpretation: In any frame related to the c.m. frame via a boost (anti)parallel to the beam direction (for massless hadrons the precise choice of frame is irrelevant—later

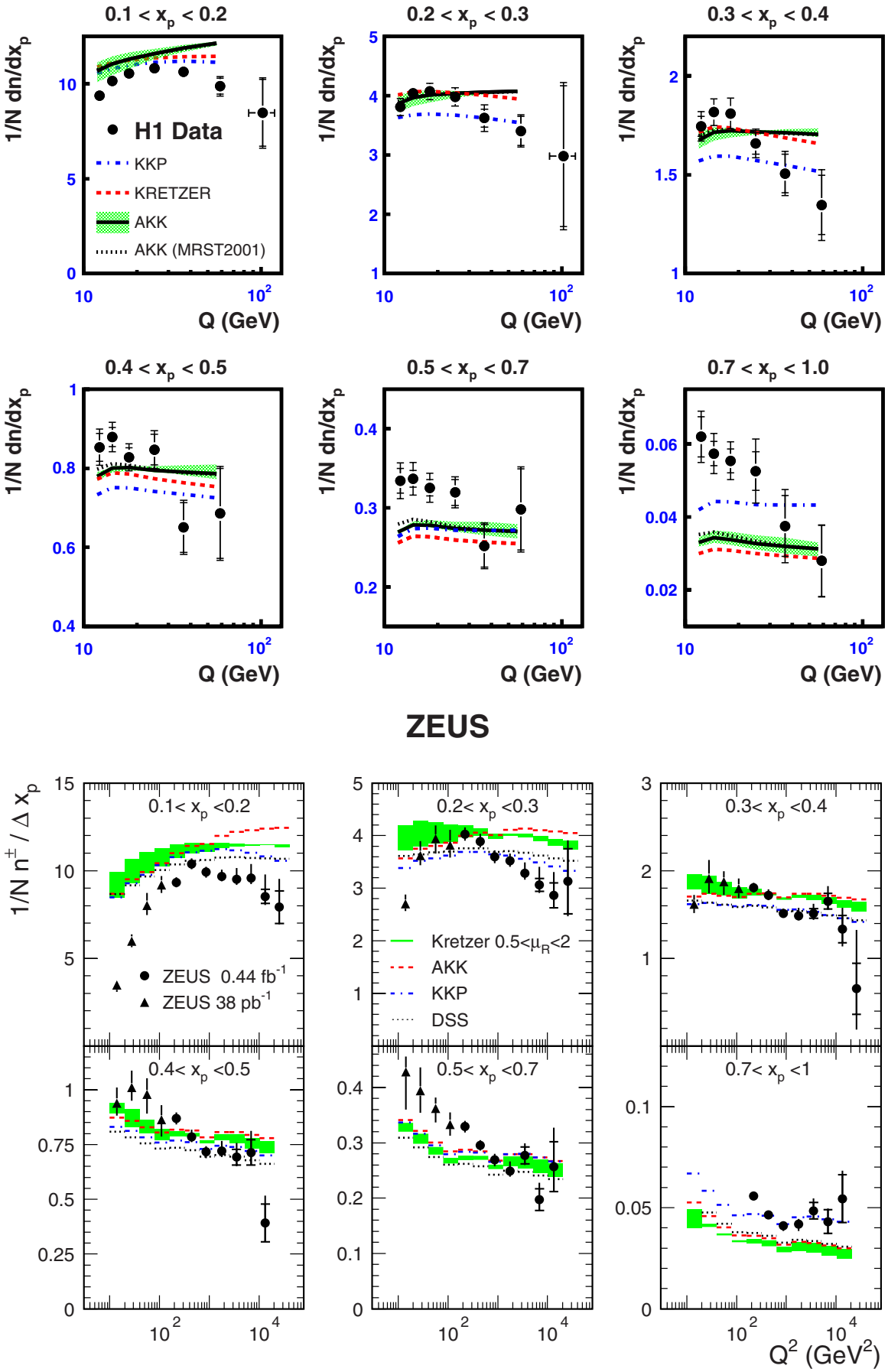

FIG. 14. (Color online) Comparisons of theoretical predictions using the AKK, Kretzer, and KKP FF sets with the new data from the H1 (Aaron *et al.*, 2007) (top) and ZEUS (Brzozowska, 2007) (bottom) Collaborations.

when we treat the mass effects of the detected hadron, we need to specify a frame), the reaction of h_1 with h_2 results in the inclusive production of a parton i, which subsequently fragments to a hadron moving in the same direction and carrying away a fraction z of the parton's momentum. Note that the partonic rapidity is the same as the hadronic rapidity since for massless hadrons y can be approximated by the *pseudorapidity*

$$\eta = -\ln(\tan\theta/2), \tag{91}$$

where θ is the angle which both the detected hadron and the massless fragmenting parton make with the beam in the c.m. frame.

The quantity $H^i_{h_1h_2}$ in Eq. (90) depends on the nonperturbative initial state hadrons h_i, $i=1,2$ through their PDFs according to

$$H^i_{h_1h_2}\left(x,y,\frac{s}{\mu_f^2},a_s(\mu_f^2)\right) = \sum_{i_1i_2}\int_x^1 dx_1\int_{x/x_1}^1 dx_2 H^i_{i_1i_2}\left(\frac{x}{x_1x_2},y,\frac{x_2}{x_1},\frac{x_1x_2s}{\mu_f^2},\frac{x_1x_2s}{M_1^2},\frac{x_1x_2s}{M_2^2},a_s(\mu_f^2),a_s(M_1^2),a_s(M_2^2)\right)$$
$$\times f^{i_1}_{h_1}(x_1,M_1^2) f^{i_2}_{h_2}(x_2,M_2^2), \tag{92}$$

where M_k, of which $H^i_{h_1h_2}$ is formally independent, is the factorization scale associated with the initial hadron h_k. This result, which also follows from the factorization theorem, can be interpreted as the inclusive production of parton i from the interaction of a parton i_k from one initial state hadron h_k, where $k=1,2$, moving parallel to it and carrying away a momentum fraction x_k, with a parton from the other. The perturbatively calculable cross section $H^i_{i_1i_2}$ describes the purely partonic process $i_1i_2 \to i+X$ and has been calculated to NLO (Ellis, Furman, Haber, and Hinchliffe, 1980; Ellis and Sexton, 1986; Aversa, Chiappetta, Greco, and Guillet, 1988a, 1988b, 1989). It depends on the c.m. energy of the partonic system i_1i_2, given by the square root of x_1x_2s. Since it is not evaluated in the c.m. frame of this partonic process, in order to make connection with the c.m. frame of the overall hadronic process it must therefore also depend on the ratio x_1/x_2, which determines the Lorentz transformations between the hadronic and partonic c.m. frames [see Eq. (116) and the discussion preceding].

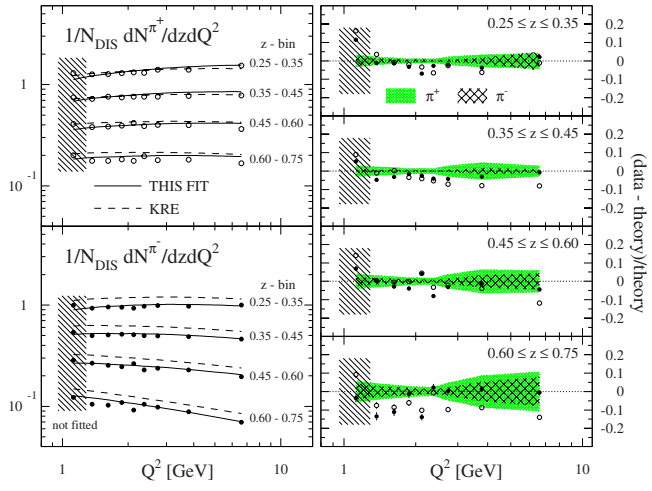

FIG. 15. (Color online) Comparison of the calculations using the NLO DSS (labeled "THIS FIT") and Kretzer (labeled "KRE") FF sets of the multiplicities for the production of positively (open circles) and negatively (full) $\pi^{\pm}$ measured by HERMES. The shaded bands in the plots on the right indicate estimates of theoretical uncertainties due to finite bin-size effects. From de Florian, Sassot and Stratmann, 2007a.

The components of $H^i_{i_1i_2}$ with $i=g$ are of $O(a_s^2)$, while the rest are either of this order or higher. Therefore the gluon FF appears at LO in this cross section, in contrast to ep and e^+e^- reactions, and therefore pp reactions can provide NLO constraints on the gluon. However, large NLO corrections (Ellis, Furman, Haber, and Hinchliffe, 1980) suggest that perturbative instability is a large source of error. Indeed, the NLO cross section suffers a large scale variation, as can be seen for instance in Fig. 22. This theoretical error is much greater than that coming from the propagated PDF uncertainty.

As for ep reactions, the detected hadron h in, e.g., h_1h_2 reactions will sometimes be a soft remnant from one of the initial state hadrons instead of being produced by the hard partonic processes $i_1i_2 \to i+X$ followed by $i \to h+X$. As for ep reactions, these production channels are accounted for by fracture functions for each initial state hadron (Trentadue and Veneziano, 1994). No further nonperturbative input is required since it is clear from which initial hadron a remnant hadron was produced. Mathematically, all potential mass singularities which cannot be absorbed into PDFs and FFs can be absorbed into fracture functions. As a result of universality, they are process independent [apart from the initial state hadron(s)], so that the factorized fracture functions in h_1h_2 reactions are identical to those in ep reactions when the same factorization scheme is used, as are the potential mass singularities that they absorb. As for ep reactions, one anticipates the existence of a scheme and scale independent cross section for $h_1h_2 \to h+X$ which does not depend on fracture functions since the evolution of FFs and PDFs does not depend on them, i.e., a current fragmentation region analogous to that in ep reactions which is free of initial hadron remnants. Certainly, contributions from target fragmenta-

tion to the cross section $H^h_{h_1h_2}$ considered will decrease with increasing p_T and decreasing y (Blokzijl, 1975) because the detected hadron moves further away from the beam. Removal of these target fragmentation effects altogether may be possible by placing kinematic restrictions on processes with alternative final states for inclusive single hadron production, such as the semi-inclusive Drell-Yan process $h_1h_2 \to \gamma^* + h + X$ (Ceccopieri and Trentadue, 2008).

As discussed in Sec. II.F, charge summed cross sections $H^{h^\pm} = H^{h^+} + H^{h^-}$ [omitting the h_1h_2 subscript appearing in, e.g., Eq. (85)] depend only on charge summed FFs, and charge asymmetry cross sections $H^{\Delta_c h^\pm} = H^{h^+} - H^{h^-}$ depend only on charge asymmetry FFs. In both types of observable, the contributions to the production from the fragmentations of the various partons in the proton can be studied, imposing tests on FFs through expectations for these contributions: Now restoring the h_1h_2 subscript and omitting the $h^\pm$ superscript, we decompose the charge summed cross section into three terms,

$$H^{h^\pm} = \hat{H}^{u_v} D_u^{h^\pm} + \hat{H}^{d_v} D_d^{h^\pm} + \sum_{i=g,q_s} \hat{H}^i D_i^{h^\pm}, \tag{93}$$

where we omit arguments, integral symbols, etc. define $\hat{H}^{q_v} = \hat{H}^q - \hat{H}^{\bar{q}}$, and use the label q_s to refer to sea quarks. The first and second terms in Eq. (94) quantify the contribution to the overall production from fragmentations of the initial proton's u and d valence quarks, respectively. These quarks are the source of the charge asymmetry, to be discussed below. Since there are more valence u than d quarks in the initial protons, the ratio of the first term to the second is expected to be greater than unity in the production of $\pi^\pm$ particles, which are equally likely to be produced from u quark fragmentation as they are from d (see Fig. 16). This ratio is expected to be larger for $p/\bar{p}$ production (see third plot in Fig. 16), where u quark fragmentation is larger than d and even larger for $K^\pm$ production (see second plot in Fig. 16), where d quark fragmentation is unfavored.

The third term in Eq. (93) corresponds to the charge symmetric contribution. It can be regarded as the contribution to the production from the fragmentation of the collective sea of initial protons. This type of fragmentation does not contribute to the charge asymmetry production because it is charge conjugation invariant. Therefore, the larger the third term is relative to the first two, the smaller the charge asymmetry cross section is expected to be relative to the charge summed cross section. In the case of hadron production with nonzero strangeness, such as $K^\pm\Lambda/\bar{\Lambda}$ and K^0_S, the third term in Eq. (93), which contains the contributions from the favored fragmentation of s quarks in the protons' sea, is expected to dominate over the first two terms because fragmentation from the protons' valence u and/or d quarks necessarily involves the unlikely production of a heavier s quark from an extrinsic gluon. This behavior is seen in the third plot of Fig. 16. In the case of $\pi^\pm$ and $p/\bar{p}$ production, it is not clear whether the first two terms are the most important terms due to favored u and d quark fragmentation or the third term which accounts for fragmentation from the protons' abundant

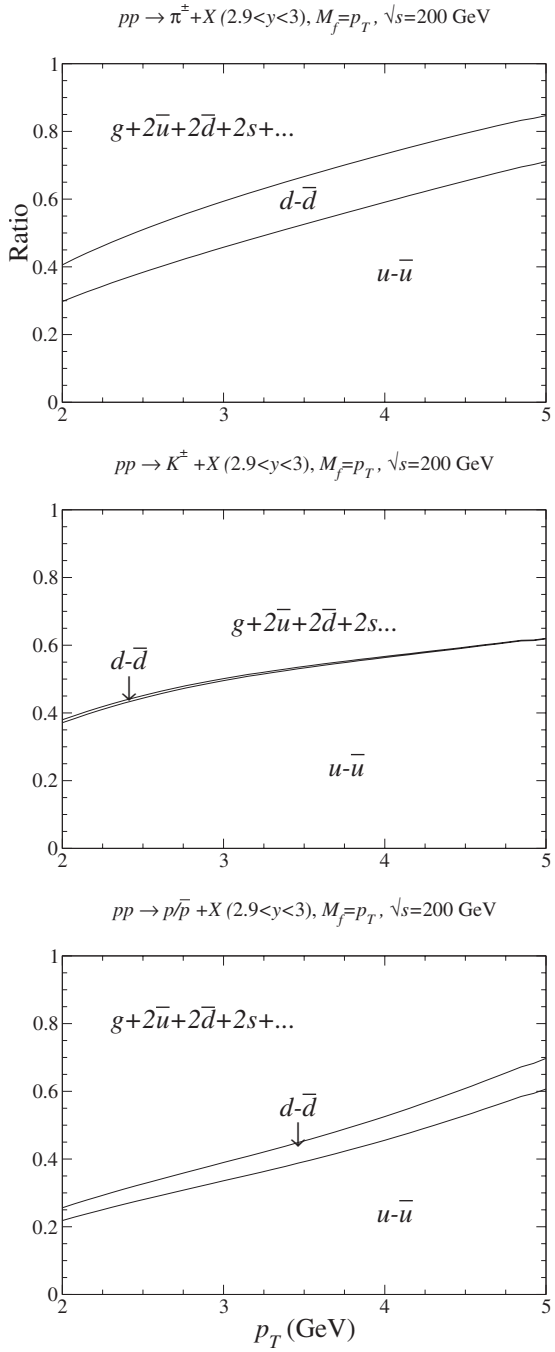

FIG. 16. Contributions, as fractional ratios, to the production from fragmentation of the initial state protons' valence quarks and sea partons for BRAHMS kinematics with $2.9 < y < 3$ using the AKK08 FF sets. The notation $u-\bar{u}$ refers to the contribution from u valence fragmentation $\hat{H}_u D_u^{h^\pm} - \hat{H}_{\bar{u}} D_{\bar{u}}^{h^\pm} = \hat{H}^{u_v} D_u^{h^\pm}$ [see Eq. (93)]. The ratios are stacked, i.e., for a given p_T value, the distance on the y axis from zero to the first curve gives the $u-\bar{u}$ contribution, from the first to the second curve the $d-\bar{d}$ contribution, and from the second curve to 1 the sea parton contribution. From Albino, Kniehl, and Kramer, 2008b.

partonic sea. It turns out that the third term always dominates.

The individual terms in Eq. (93) are factorization scheme and scale dependent and are therefore unphysical. Fortunately, their above physical interpretations can also be given to each term in the equivalent physical decomposition at NLO,

$$H_{pp} = (H_{p\bar{p}} - H_{pp})|_{u_v} + (H_{p\bar{p}} - H_{pp})|_{d_v} + (2H_{pp} - H_{p\bar{p}}), \tag{94}$$

where $|_{u_v}$ ($|_{d_v}$) means that the valence d (u) quark PDF is set to zero. Note that there is no contribution to the first two terms from the protons' sea parton PDFs. Interactions between valence u quarks from one proton and valence d quarks from the other do not contribute here because the cross sections for the processes $q_I q_J \to h^\pm + X$ and $q_I \bar{q}_J \to h^\pm + X$ with $I \neq J$ are identical at NLO. Although the third term in Eq. (93) is much smaller than the third term in Eq. (94), the relative sizes of the terms in both equations (Fig. 16) are qualitatively similar.

The charge asymmetry is determined from the FFs according to

$$H^{\Delta_c h^\pm} = \hat{H}^{u_v} D_u^{\Delta_c h^\pm} + \hat{H}^{d_v} D_d^{\Delta_c h^\pm}. \tag{95}$$

Both terms are factorization scheme and scale independent. Note that from the quark composition of $\pi^\pm$ that $D_d^{\Delta_c \pi^\pm}$ is expected to be negative and $D_u^{\Delta_c \pi^\pm}$ positive (this should at least be true for their first moments). In addition, the quark composition of the proton suggests that the production of u over $\bar{u}$ is greater than the production of d over $\bar{d}$, i.e., $\hat{H}^{u_v} > \hat{H}^{d_v} > 0$. The first plot in Fig. 17 is consistent with these expectations. This allows for the excess of π^+ over π^-, but it should be noted that this excess is not guaranteed unless $\hat{H}^{u_v}$ is sufficiently greater than $\hat{H}^{d_v}$ or the magnitude of $D_d^{\Delta_c \pi^\pm}$ is sufficiently smaller than $D_u^{\Delta_c \pi^\pm}$. For $h^\pm = p/\bar{p}$, all four quantities in Eq. (95) are expected to be positive so that a definite excess of p over $\bar{p}$ is predicted. Because of the expectations $\hat{H}^{u_v} > \hat{H}^{d_v}$ and, from the quark composition of $p/\bar{p}$, $D_u^{\Delta_c p/\bar{p}} > D_d^{\Delta_c p/\bar{p}}$, the first term in Eq. (95) is expected to dominate over the second. These expectations are observed in the second plot of Fig. 17.

Likewise, an excess of K^+ over K^- is predicted, although in this case the second term in Eq. (95) vanishes due to the physically reasonable assumption $D_d^{\Delta_c K^\pm} = 0$ at NLO. Note that there is no dependence on $D_s^{\Delta_c K^\pm}$, so that this FF is not constrained by $pp(\bar{p})$ reaction measurements.

C. Other processes

Further tests of universality have been performed by Kniehl, Kramer, and Pötter (2001) by comparing calculations using the KKP FF set obtained with measurements of unidentified hadron production from $p\bar{p}$ reactions at the Super Proton Synchrotron by the UA1 and

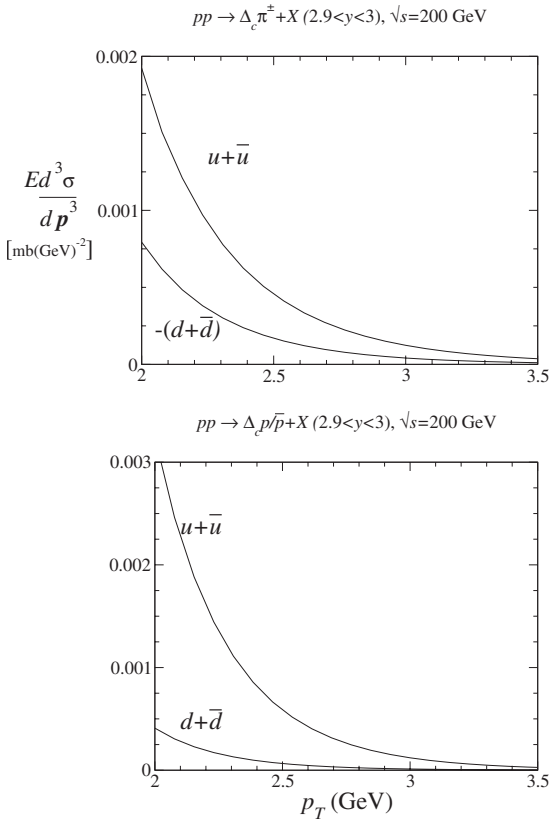

FIG. 17. Contributions to the charge asymmetry $\Delta_c h^\pm$ from fragmentation of the initial state protons' valence quarks for BRAHMS kinematics for which $2.9 < y < 3$ using the AKK08 FF sets. The notation $u+\bar{u}$ means $\hat{H}_u D_u^{\Delta_c \pi^\pm} + \hat{H}_{\bar{u}} D_{\bar{u}}^{\Delta_c \pi^\pm} = \hat{H}^{u_v} D_u^{\Delta_c h^\pm}$ [see Eq. (95)]. The cross section is given by the difference between the two curves. From Albino, Kniehl, and Kramer, 2008b.

UA2 Collaborations and at the Fermilab Tevatron by the CDF Collaboration and from photoproduction (requiring photon PDFs) in γp reactions from H1 and ZEUS at HERA and in $\gamma\gamma$ reactions from OPAL at LEP2. The data overall were measured over a wide range of p_T and y. Good agreement with all data was found provided that the theoretical error was produced in the cross section when μ_f / E_s is allowed to vary from 1/2 to 2. This cross section variation is rather large, and the experimental errors are unfortunately largest at large p_T where additional nonperturbative information such as higher twist is expected to be the important. The photoproduction calculations also acquire large errors from the rather badly constrained parton distribution functions (PDFs) of the photon. Distributions in y generally have even larger theoretical errors. More stringent tests of universality were performed by Aurenche, Basu, Fontannaz, and Godbole (2004), Daleo, de Florian, and Sassot (2005), and Kniehl, Kramer, and Maniatis (2005) through analysis of pseudorapidity and p_T distributions from H1 for the process $ep \to e + \pi^0 + X$ and by Kniehl, Kramer, and Maniatis (2005) through analysis of p_T distributions from ZEUS for the process $ep \to e + h + X$, which did not require the use of photon PDFs [ex-

cept in the low Q region (Fontannaz, 2004)]. The disagreement found with the ZEUS data was reduced by Nadolsky, Stump, and Yuan (2001) through resummation of multiple parton radiation at low p_T.

V. IMPROVEMENTS TO THE STANDARD APPROACH

The standard FO calculation discussed so far describes much of the data well but is incomplete. The FO approximation of the high energy parts of the factorized cross section is only applicable to the kinematic regions for which $E_s \gg \Lambda_{\rm QCD}$ and x is not too close to 0 or 1. The boundaries of this acceptable region are otherwise unknown. Terms originating from the emission of soft gluons become large for large and small x and low E_s and must be summed to all orders with a procedure known as *resummation*. We now discuss the well-known procedure of large x resummation in DGLAP evolution and in e^+e^- reactions in Sec. V.B and leave the resummation of soft gluon logarithms at small x to Sec. VIII. Only the ZM-VFNS has been implemented in global fits so far, whose error of $O(1)$ whenever $E_s = O(m_J)$ can be removed using instead the GM-VFNS. Even with these improvements to the perturbative approximation, the definition of the cross section considered so far itself requires various formal modifications, which become increasingly important with decreasing E_s. The effects of the detected hadron's mass, of $O(m_h^2/E_s^2)$, will be discussed in Sec. V.A. Higher twist effects, of $O(\Lambda_{\rm QCD}/E_s)$ or less, remain unknown at present.

A. Hadron mass effects

At sufficiently high energy scales, the standard FO approach describes data from various reactions well. In particular, the same AKK FF set (Albino, Kniehl, and Kramer, 2005) describes simultaneously the accurate pion production data from pp and e^+e^- reactions. This suggests that low E_s and small x effects in general are not important for these data. The strongest caveat to this argument is the possible importance of hadron mass effects, which are not so important for $\pi^\pm$, being the lightest hadrons, but which may be relevant for other particles. Therefore, for the other particles it may be necessary to account for hadron mass effects in the theory. In fact, as discussed in Sec. VII, the fitted hadron masses for $\pi^\pm$, $p/\bar{p}$, and $\Lambda/\bar{\Lambda}$ occurring in the calculation for the e^+e^- reactions in global fits are approximately equal to their true values (Albino, Kniehl, and Kramer, 2008b), suggesting that it is the first effect beyond the standard FO approach to become relevant as x and the energy scale E_s of the process decreases.

In this section, we calculate the effects of hadron mass in e^+e^-, ep, and hadron-hadron reactions. Our approach is analogous to the collinear factorization framework approach of Aivazis, Olness, and Tung (1994) for incorporating target mass effects in fully inclusive DIS cross sections rather than the OPE approach of Georgi and Politzer (1976). A detailed review and study of the various approaches to target mass corrections can be found in Schienbein *et al.* (2008), which also contains a collection of useful references. Our approach is not unique since the ambiguity in the definition of the leading twist contribution to the cross section is up to $O(\Lambda/E_s)$.

We begin with Eq. (1) [or Eq. (2)], whose perturbative quantities are explicitly independent of the hadron mass (and therefore given by their results calculated with the hadron mass set to zero), provided that z is the ratio of the light-cone momentum fraction of the detected hadron to that of the fragmenting parton as dictated by the factorization theorem. The light-cone momentum fraction x of the factorization theorem and any experimentally measured momentum fractions x_e, such as x_p and x_E (see Appendix B for the definitions of x, x_p, and x_E), are unequal when the detected hadron's mass m_h cannot be neglected. It is therefore necessary to determine explicitly the functional dependence $x = x(x_e, m_h^2/E_s^2)$ and to multiply the result calculated from the factorization theorem, $d\sigma/dx(x(x_e, m_h^2/E_s^2), E_s^2)$, by the factor dx/dx_e in order to obtain the measured result $d\sigma/dx_e(x_e, E_s^2)$. Note that dx/dx_e can depend on the momentum of the parton from any initial state hadron that occurs in the hard interaction. We assume that all quarks are massless, although the generalization to massive quarks is conceptually straightforward.

1. e^+e^- reactions (Albino, Kniehl, Kramer, and Ochs, 2006)

We now obtain the relations between x, the light-cone momentum fraction defined in Appendix B, and the experimentally measured fractions $x_p = 2|\boldsymbol{p}_h|/\sqrt{s}$ and $x_E = 2E_h/\sqrt{s}$. See Fig. 2 for the definitions of the various kinematical quantities in this reaction, although we note that the definition of z via $k = p_h/z$, which holds when the hadron is massless, will be generalized to Eq. (98) below. Using the light-cone coordinates defined in Appendix B, we work in a frame for which the virtual boson's momentum is given by

$$q = (\sqrt{s}/\sqrt{2}, \sqrt{s}/\sqrt{2}, \mathbf{0}) \tag{96}$$

and the hadron's momentum by

$$p_h = (x\sqrt{s}/\sqrt{2}, m_h^2/\sqrt{2}x\sqrt{s}, \mathbf{0}), \tag{97}$$

which also serves as an implicit definition of x, the light-cone momentum fraction defined explicitly in Appendix B. The momentum fraction z is defined by the relation to p_h of the + component of each parton's momentum k which contribute at leading twist,

$$k^+ = p_h^+/z. \tag{98}$$

Note that for massless partons, $k^- = 0$. The condition $\boldsymbol{k}_T = 0$ is always true. Using $|\boldsymbol{p}_h| = (p_h^+ - p_h^-)/\sqrt{2}$, we find

$$x_p = x(1 - m_h^2/sx^2). \tag{99}$$

Note that x and s appear in the combination $x\sqrt{s}$, which is twice the minimum value of k^+. Inverting Eq. (99) gives

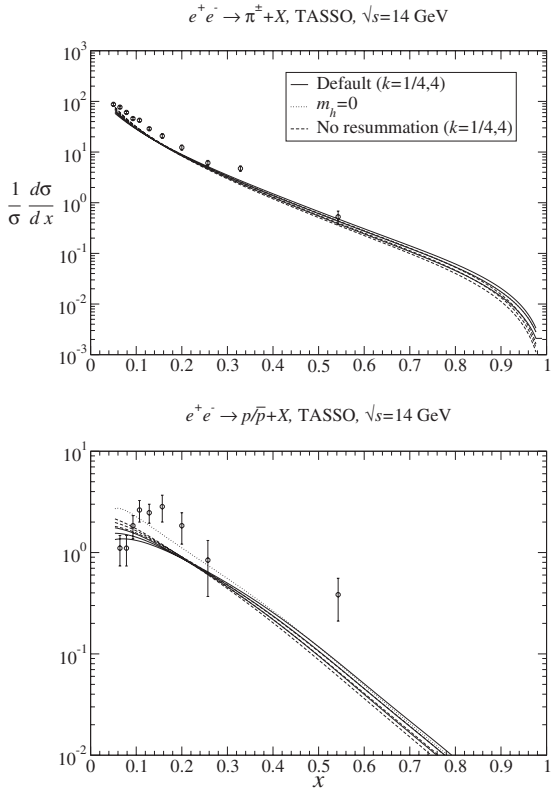

FIG. 18. Comparison of the calculation using the AKK08 FF sets with measurements of the invariant differential cross sections for inclusive production in e^+e^- reactions at $\sqrt{s}$=14 GeV from TASSO (Althoff *et al.*, 1983) (labeled "Default"). Large x resummation, discussed in Sec. V.B, has been implemented. Also shown is the calculation when mass effects are neglected (the dotted curve labeled m_h=0) and when the ratio $k=\mu_f^2/s$ is increased to 4 (lower solid curve) and decreased to 1/4 (upper solid curve). In the case of $\pi^\pm$, the m_h=0 curve cannot be seen because it overlaps with the default curve. From Albino, Kniehl, and Kramer, 2008b.

$$x = x_p\left(\frac{1}{2} + \frac{1}{2}\sqrt{1 + 4m_h^2/sx_p^2}\right). \tag{100}$$

Consequently, the experimental cross section $d\sigma^h/dx_p$, for example, can be calculated according to

$$\begin{aligned}\frac{d\sigma^h}{dx_p}(x_p,s) &= \frac{dx}{dx_p}(x_p,m_h^2/s)\frac{d\sigma^h}{dx}(x(x_p,m_h^2/s),m_h^2/s)\\ &= \left(\frac{1}{2} + \frac{1}{2}\left[1 + \frac{4m_h^2}{sx_p^2}\right]^{-1/2}\right)\\ &\quad\times\frac{d\sigma^h}{dx}(x(x_p,m_h^2/s),s),\end{aligned} \tag{101}$$

where $d\sigma^h/dx$ is calculated in Eq. (2), which is explicitly hadron mass independent. The above formulas with x_E in place of x_p are the same but with $m_h^2 \to -m_h^2$.

As Fig. 18 shows, hadron mass effects become more important with decreasing x and decreasing $\sqrt{s}$. Furthermore, the effect of hadron mass for $\pi^\pm$ is much less than that for the heavier $p/\bar{p}$, for which the shift at small x in the cross section created by hadron mass effects is significantly larger than the theoretical error on the standard FO calculation.

2. *ep* reactions (Albino, Kniehl, Kramer, and Sandoval, 2007)

When the detected hadron's mass is nonzero, Eq. (68) is modified to

$$p_h = (xq^+, m_h^2/2xq^+, \mathbf{0}). \tag{102}$$

The relation between x_p defined in Eq. (69) and the light-cone momentum fraction x is

$$x_p = x(1 - m_h^2/Q^2x^2) \tag{103}$$

or

$$x = x_p\left(\frac{1}{2} + \frac{1}{2}\sqrt{1 + 4m_h^2/Q^2x_p^2}\right). \tag{104}$$

As in Eq. (98) for e^+e^- reactions above, the parton's + component of momentum in the c.m. frame is given by $k^+=p_h^+/z$, where k is the momentum of the fragmenting partons at leading twist. For massless partons, $k^-=0$ and $\boldsymbol{k}_T=0$ is always true. The measured cross section is given by

$$\begin{aligned}&\frac{d\sigma^h}{dx_p dx_B dQ^2}(x_p,x_B,Q^2)\\ &\quad= \left(\frac{1}{2} + \frac{1}{2}\left[1 + \frac{4m_h^2}{Q^2x_p^2}\right]^{-1/2}\right)\\ &\qquad\times\frac{d\sigma^h}{dx dx_B dQ^2}(x(x_p,m_h^2/Q^2),x_B,Q^2),\end{aligned} \tag{105}$$

where $d\sigma^h/dxdx_BdQ^2$ is the usual explicitly hadron mass independent calculation, given in Eq. (72). This modification to the normalization is similar to that of Dokshitzer and Webber (1998), Dixon, Kant, and Thompson (1999), and Breitweg *et al.* (1999) up to terms of $O([m_h^2/(x^2Q^2)]^2)$.

As Fig. 19 shows, hadron mass effects become important with decreasing x (left) and increasing hadron mass (right). Hadron mass effects are also found to become less important with increasing Q (right) as expected.

Note that the effect of the initial proton's mass in HERA data is expected to approximately cancel between the numerator and denominator in Eq. (74) and thus is not accounted for. Furthermore, it is only important at large x_B, while according to Fig. 8 the HERA data are taken at relatively small x_B values.

3. Hadron-hadron reactions (Albino, Kniehl, and Kramer, 2008b)

The cross section is related to its partonic equivalent by

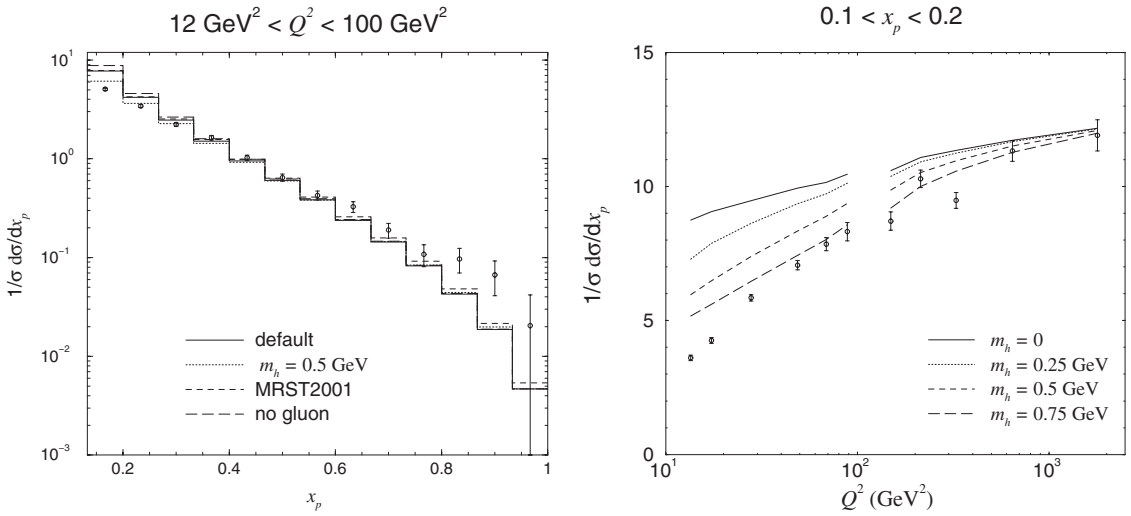

FIG. 19. Variations in the cross section calculation. Left: Comparisons of theoretical predictions using the AKK FF sets with the distribution in x (written x_p here) of unidentified hadrons from ZEUS (Derrick *et al.*, 1996). The modifications to the default predictions (solid line), calculated with $m_h=0$, arising from the replacement of the CTEQ6M PDF set of Pumplin, Stump, Huston, Lai, Nadolsky, and Tung (2002) by the MRST2001 (Martin-Roberts-Stirling-Thorne 2001) PDF set of Martin, Roberts, Stirling, and Thorne (2002) from the removal of the evolved gluon and from the incorporation of the hadron mass effect are shown. Right: Comparisons of theoretical predictions using the AKK FF set with the ZEUS data (Breitweg *et al.*, 1997) measured in the interval $0.1<x_p<0.2$ and for different values of m_h. The four curves on the left (and the data they are to be compared with) are calculated (and measured) with different kinematical cuts to the four curves and the data on the right. From Albino, Kniehl, Kramer, and Sandoval, 2007.

$$d\sigma^h_{i_1i_2} = \sum_{ii_1i_2} \int dx_1 \int dx_2 f^{h_1}_{i_1}(x_1,\mu_f^2) f^{h_2}_{i_2}(x_2,\mu_f^2) \times \int_x^1 dz\, d\sigma^i_{i_1i_2} D^h_i(z,\mu_f^2), \tag{106}$$

where z is defined by

$$k^+ = p^+/z \tag{107}$$

in the partonic c.m. frame, namely, the c.m. frame of the two initial partons i_1 and i_2 if the 3-axis is taken to be parallel with the parton's and hadron's spatial momenta. The measured cross section $F^h_{h_1h_2}$ of Eq. (85) is differential in the Lorentz invariant element $d^3\boldsymbol{p}/E$. Equation (90) is produced by dividing the left-hand side of Eq. (106) by this element, and its relation to the equivalent partonic element $d^3\boldsymbol{k}/k^0$ that appear explicitly on the right-hand side must be found. Working in the partonic c.m. frame and assuming massless partons for simplicity, the relations $k^0=|\boldsymbol{k}|$ and $E=\sqrt{\boldsymbol{p}^2+m_h^2}$ and the fact that the detected hadron and fragmenting parton are spatially parallel imply first that

$$\frac{d\boldsymbol{p}^3}{E} = \frac{|\boldsymbol{p}|^2}{\sqrt{|\boldsymbol{p}|^2+m_h^2}} d|\boldsymbol{p}|d\Omega, \qquad \frac{d\boldsymbol{k}^3}{k^0} = |\boldsymbol{k}|d|\boldsymbol{k}|d\Omega, \tag{108}$$

where Ω is the solid angle, and second that, from Eq. (107) and using $k^+=(k^0+|\boldsymbol{k}|)/\sqrt{2}$ and $p^+=(p^0+|\boldsymbol{p}|)/\sqrt{2}$,

$$2z|\boldsymbol{k}| = |\boldsymbol{p}| + \sqrt{|\boldsymbol{p}|^2+m_h^2}. \tag{109}$$

From these last two results we obtain

$$\frac{d\boldsymbol{p}^3}{E} = \frac{1}{z^2R^2}\frac{d\boldsymbol{k}^3}{k^0}, \tag{110}$$

where

$$R = 1 - m_h^2/(|\boldsymbol{p}| + \sqrt{|\boldsymbol{p}|^2+m_h^2})^2. \tag{111}$$

[We note a couple of misprints in the explicit result for R Albino, Kniehl, and Kramer (2008b): the right-hand side should not have been raised to the power of 2 and the "−" in front of m_h^2 in the denominator should have read "+."] Equation (106) then becomes

$$E\frac{d^3\sigma^h_{h_1h_2}}{d\boldsymbol{p}^3} = \sum_{ii_1i_2} \int dx_1 \int dx_2 f^{h_1}_{i_1}(x_1,\mu_f^2) f^{h_2}_{i_2}(x_2,\mu_f^2) \times \int dz \frac{1}{z^2R^2}|\boldsymbol{k}| \frac{d^3\sigma^i_{i_1i_2}}{d\boldsymbol{k}^3} D^h_i(z,\mu_f^2). \tag{112}$$

Before Eq. (112) can be calculated, the explicit dependence of R on x_1 and x_2 needs to be found. According to Eq. (111), this dependence will be known once we determine $|\boldsymbol{p}|=|\boldsymbol{p}|(p_T,y,x_1,x_2)$, where recall that $\boldsymbol{p}$ is the detected hadron's momentum in the partonic c.m. frame. In this frame, where the rapidity is written y' and the transverse momentum is the same as that in the hadronic c.m. frame, we find that

$$|\boldsymbol{p}| = \sqrt{m_T^2\cosh^2 y' - m_h^2}, \tag{113}$$

where

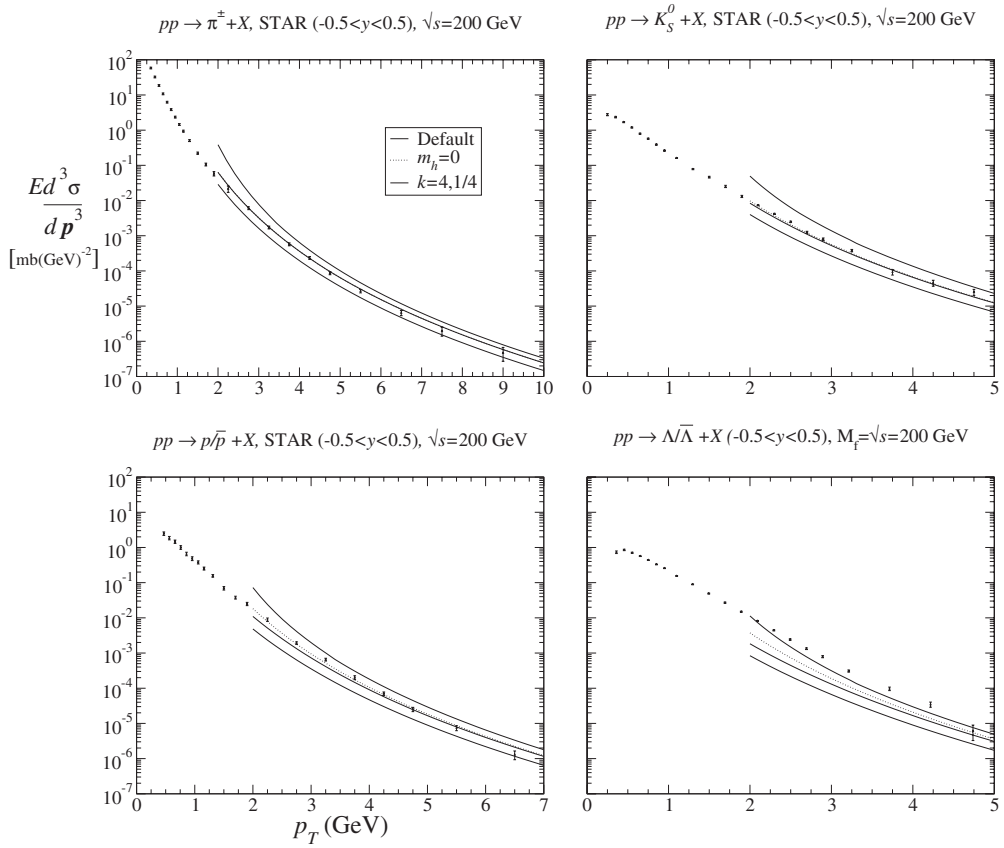

FIG. 20. Comparison of the calculation using the AKK08 FF sets with measurements of the invariant differential cross sections for inclusive production in pp collisions at $\sqrt{s}$=200 GeV data from STAR (Adams *et al.*, 2006a, 2006b; Abelev *et al.*, 2007) for which $-0.5<y<0.5$ (labeled default). Also shown is the calculation when mass effects are neglected (the dotted curve labeled $m_h=0$) and when the ratio $k=\mu_f^2/p_T^2$ is increased to 4 (lower solid curve) and decreased to 1/4 (upper solid curve). In the case of $\pi^{\pm}$, the $m_h=0$ curve cannot be seen because it overlaps with the default curve. From Albino, Kniehl, and Kramer, 2008b.

$$m_T=\sqrt{p_T^2+m_h^2}. \tag{114}$$

According to Eq. (113), the dependence of $|\boldsymbol{p}|$ on x_1 and x_2 will be determined once we find $y'=y'(y,x_1,x_2)$. Letting $e^{\phi(x_1,x_2)}$ denote the boost factor which transforms the sum of the energy and longitudinal component of momentum between the partonic and hadronic c.m. frames, the relation between y' and y is

$$y'=y+\phi(x_1,x_2), \tag{115}$$

To obtain $\phi=\phi(x_1,x_2)$, we align the 3-axis with the beams. The + (−) component of the parton from h_1 (h_2) in the hadronic c.m. frame is $k_1^+=x_1P_1^+(k_2^-=x_2P_1^+)$, where P_1^+ is the + component of momentum of h_1, equal to the − component of momentum of h_2. All other components of these partons' momenta vanish. In the partonic c.m. frame, the + component of the parton from h_1 and the − component of the parton from h_2 are equal and given by $k_1^+e^{\phi}=k_2^-e^{-\phi}$, so that $x_1e^{\phi}=x_2e^{-\phi}$, or, finally,

$$\phi=\ln\sqrt{x_2/x_1}, \tag{116}$$

respectively.

In Fig. 20 hadron mass effects become more important as the mass of the detected hadron increases and as p_T decreases but remain smaller than the theoretical error calculated in the standard approach. Similar results are obtained in the whole range $|y|\lesssim 3$; i.e., the size of hadron mass effects is fairly independent of rapidity in this range.

B. Large x resummation

When x is sufficiently large, the accuracy of the FO perturbative calculations for the equivalent hard partonic cross section and the DGLAP evolution is worsened by unresummed divergences occurring in the formal limit $x\to 1$. Here the "large x" region refers to where these logarithms are important but is otherwise not more precisely defined and could even include rather small x values. The possible importance of large x resummation effects for available experimental data was discussed by Bourhis, Fontannaz, Guillet, and Werlen (2001), where uncertainties due to unresummed large x logarithms were minimized by scale optimization. Resummation of these logarithms should reduce this theoretical error. The effects of these unresummed logarithms should become more significant with decreasing E_s, where errors due to perturbative truncation are largest. Resummation of all large x logarithms that occur up to NLO in e^+e^- reactions is now possible using recent

results (Cacciari and Catani, 2001). Resummation makes a significant improvement to current global fits (Albino, Kniehl, and Kramer, 2008b), discussed in Sec. VII.

In general, in the series expansion of the hard part $\mathcal{W}(x,a_s)$, these large x divergences take the form $a_s^n[\ln^{n-r}(1-x)/(1-x)]_+$, where $r=0,\ldots,n$ labels the class of divergence. In Mellin space, these divergences therefore take the form $a_s^n \ln^{n+1-r} N$ at large N; i.e., they spoil the convergence of the series at large N. They may be factored out, which results in the calculation of $\mathcal{W}$ taking the form

$$\mathcal{W}(N,a_s) = \mathcal{W}_{\rm res}(N,a_s)\left(\sum_n a_s^n \mathcal{W}_{\rm FO}^{(n)}(N)\right), \tag{117}$$

where the FO series in parenthesis on the right-hand side is free of these divergences since they are all contained in $\mathcal{W}_{\rm res}$. $\mathcal{W}$ at large N is approximated by $\mathcal{W}_{\rm res}$ when the divergences in $\mathcal{W}_{\rm res}$ are resummed, which involves writing $\mathcal{W}_{\rm res}$ as an exponential and expanding the exponent in a_s keeping $a_s \ln N$ fixed [i.e., in the language in Sec. II.E the series is of the form $\ln \mathcal{W}_{\rm res}(N,a_s) = \Sigma_r X^r R^{(r)}(Y)$ with $X=a_s$ and $Y=a_s \ln N$]. The perturbative series for the NLO quark coefficient function $C_q = C_{\rm NS} = C_{\rm S}$ for inclusive quark production in e^+e^- reactions contains leading (class $r=0$) and next-to-leading (class $r=1$) divergences, which can be replaced in the manner of Eq. (117) by all such divergences of these two classes. These divergences are all contained in (Cacciari and Catani, 2001)

$$\ln C_q(N,a_s(s)) = \int_0^1 dz \frac{z^{N-1}-1}{1-z}\left[\int_s^{(1-z)s} \frac{dq^2}{q^2} A(a_s(s)) + B(a_s((1-z)s))\right] + O(1), \tag{118}$$

where

$$(A,B)(a_s) = \sum_{n=1}^{\infty} (A,B)^{(n)} a_s^n. \tag{119}$$

To determine them explicitly requires the following results:

$$A^{(1)} = 2C_F,$$

$$A^{(2)} = -C_F\left[C_A\left(\frac{\pi^2}{3}-\frac{67}{9}\right)+\frac{20}{9}T_R n_f\right], \tag{120}$$

$$B^{(1)} = -\tfrac{3}{2}C_F.$$

Since Eq. (118) is algebraically similar to the resummed quark coefficient function of DIS (Catani and Trentadue, 1989), we obtain all the divergences of classes $r=0$ and $r=1$, known as leading logarithms (LLs) and next-to-leading logarithms (NLLs), respectively, directly from the $\overline{\rm MS}$ result of Albino and Ball (2001),

$$\ln C_q^{r=0,1}(N,a_s) = \frac{A^{(1)}}{a_s\beta_0^2}[(1-\lambda_s)\ln(1-\lambda_s)+\lambda_s] + \frac{A^{(1)}\beta_1}{2\beta_0^3}\ln^2(1-\lambda_s) + \left(\frac{B^{(1)}}{\beta_0}-\frac{A^{(1)}\gamma_E}{\beta_0} + \frac{A^{(1)}\beta_1}{\beta_0^3}-\frac{A^{(2)}}{\beta_0^2}\right)\ln(1-\lambda_s) - \left(\frac{A^{(2)}}{\beta_0^2}-\frac{A^{(1)}\beta_1}{\beta_0^3}\right)\lambda_s, \tag{121}$$

where $\lambda_s = a_s\beta_0 \ln N$. The first term in Eq. (121) accounts for all LLs and the remaining terms for all NLLs. According to the general form of Eq. (117), the resulting resummed quark coefficient function that we seek is

$$C_q = C_q^{r=0,1}[1 + a_s(C_q^{(1)} - C_q^{r=0,1(1)})], \tag{122}$$

where

$$C_q^{r=0,1(1)} = \frac{A^{(1)}}{2}\ln^2 N + (A^{(1)}\gamma_E - B^{(1)})\ln N \tag{123}$$

is the coefficient of the $O(a_s)$ term in the expansion of $C_q^{r=0,1}$ in a_s. The form of Eq. (122) ensures that the original NLO result is obtained when the right-hand side is expanded in a_s, i.e., when the resummation is "undone," up to $O(a_s)$ because it prevents double counting of the divergences. Note that there are an infinite number of other schemes which are consistent with these criteria and give the large N behavior of Eq. (121), a typical feature of perturbation theory. For example, Eq. (122) is still correct up to NLO and up to NLL after the modification $N \to N+a$ in Eq. (121) [and, therefore, in Eq. (123) but not in $C_q^{(1)}$], where a is a finite, possibly complex, constant, so for not too large a Eq. (122) is expected to be suitable in calculations of the cross section for both large and intermediate x's.

Equation (121) contains a Landau pole when $\lambda_s=1$, where N is real and $\gg 1$. However, in the inverse Mellin transform it is not necessary for the contour in the complex N plane to run to the right of this pole, as it should for the other poles, because it is unphysical, created by the ambiguity of the asymptotic series. In x space it gives essentially a higher twist contribution and is therefore negligible. Asymptotic convergence of the series occurs when the contour is chosen to be to the left of this pole, known as the *minimal prescription* (Catani, Mangano, Nason, and Trentadue, 1996), which is also more efficient for the numerical evaluation of the inverse Mellin transform than running the contour to the right of the pole.

According to Fig. 21, the effect of the resummation is to increase the cross section for e^+e^- reactions (at the standard choice $\mu_f/\sqrt{s}=1$) and more so with increasing x. This behavior is also shown in Fig. 18. This is a typical feature of soft gluon resummation in both timelike and spacelike processes. Figure 21 also shows that resummation lowers the scale variation if the resummed result is compared with the unresummed result at the same val-

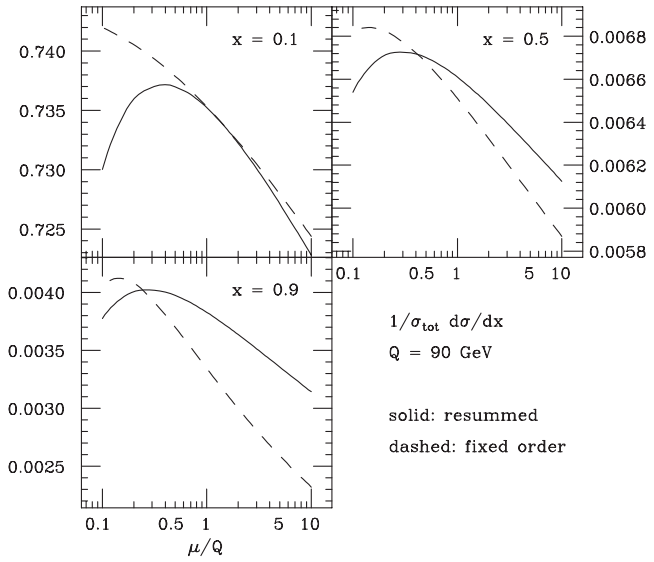

FIG. 21. Dependence of the unresummed (fixed order) and resummed cross section on the ratio $\mu_f/\sqrt{s}$, written here as μ/Q. The renormalization scale is fixed to the factorization scale. From Cacciari and Catani, 2001.

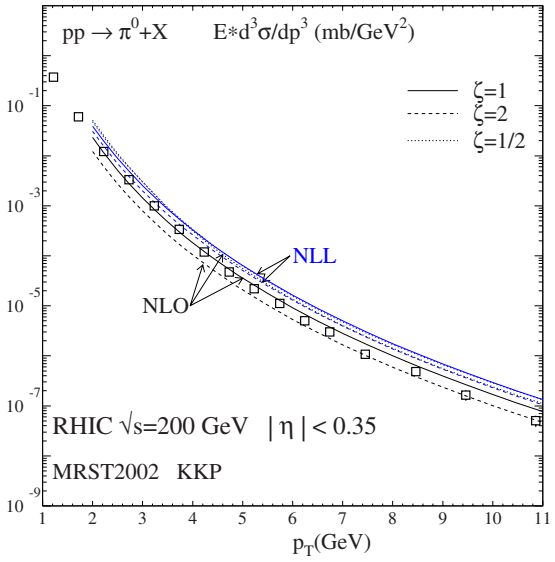

FIG. 22. (Color online) Dependence of the unresummed (NLO) and resummed (NLL) cross sections on the factorization scale μ_f, where $\xi=\mu_f/p_T$. The renormalization scale is fixed to the factorization scale. From de Florian and Vogelsang, 2005.

ues for $\mu_f=\mu$. From this we can infer that resummation lowers the theoretical error, assuming that the factorization scale in the resummed case can be given the same interpretation as the factorization scale in the unresummed case. However, caution is advised here because resummation within a FO calculation is not a systematic improvement to the original, unresummed, FO calculation in the same way that extending the original FO calculation to higher orders is.

Explicit results for the resummation of large x logarithms in ep reactions do not exist at present but, in the current fragmentation region, are likely to be similar to the results for e^+e^- reactions above due to the physical similarities between these two processes.

Large x resummation is particularly valuable for $pp(\bar{p})$ reactions where the scale variation is large, as shown in Fig. 22. Note again the reduction in theoretical error due to the resummation. Unfortunately, in this case formal results only exist for the case that rapidity is integrated over all values, the results for a given finite rapidity range having to be determined approximately (de Florian and Vogelsang, 2005). Note that for a given p_T the effect of the resummation is expected to increase with decreasing $\sqrt{s}$ because $x=2p_T\cosh y/\sqrt{s}$ (neglecting the detected hadron's mass).

For consistency, the large x logarithms in the DGLAP evolution of the FFs must also be resummed. These logarithms occur in the diagonal parts of the splitting function (i.e., in $P_{\Delta_c\Sigma}$, $P_{\Delta_c\mathrm{NS}}$, P_{NS}, $P_{\Sigma\Sigma}$, and P_{gg} of Sec. II.F). The FO result for P is already resummed because these divergences approach $1/(1-z)$ as $z\to 1$ or $\ln N$ as $N\to N$ in Mellin space at every order (Korchemsky, 1989; Albino and Ball, 2001). This is because they originate from soft radiation which is classical in nature and therefore can be arranged to appear at LO only by choosing a physical strong coupling (Kalinowski, Konishi, Scharbach, and Taylor, 1981). In other words, there are no $r=0$ divergences (i.e., LLs), while the divergence at LO, proportional to $a_s\ln N$, is the only $r=1$ divergence (NLL), the divergence at NLO, proportional to $a_s^2\ln N$, is the only $r=2$ divergence, etc. However, this means that the FO expansion of the matrix U in Eq. (13) is unresummed. Resumming the NLLs gives an improved approximation of U at large N (Albino, Kniehl, and Kramer, 2008b),

$$U(N,a_s)=\sum_i \exp\{u^{[1]}_{\alpha_i\alpha_i}a_s\ln N+O(a_s(a_s\ln N)^n)\}M^i, \tag{124}$$

where $\alpha_+=\Sigma$ and $\alpha_-=g$ and

$$u^{[1]}_{\alpha_i\alpha_i}=\lim_{N\to\infty}\left(\frac{\beta_1}{\beta_0^2}P^{(0)}_{\alpha_i\alpha_i}(N)-\frac{1}{\beta_0}P^{(1)}_{\alpha_i\alpha_i}(N)\right)\Big/\ln N. \tag{125}$$

A method for resumming these logarithms in the analytic Mellin space solution to the DGLAP equation of Furmanski and Petronzio (1982) and Ellis, Kunszt, and Levin (1994), discussed in Sec. II.E is given by Albino, Kniehl, and Kramer (2008b). As shown in Fig. 23, the effect of this resummation at $\mu/\mu_f=1$ is much smaller than that in the coefficient functions, although the modification to the theoretical error obtained by scale variation is substantial.

VI. THE TREATMENT OF EXPERIMENTAL ERRORS

One of the main purposes of fitting FFs to experimental data is to make predictions for other observables that depend on them through the universality of FFs implied by the factorization theorem. For example, FFs fitted to

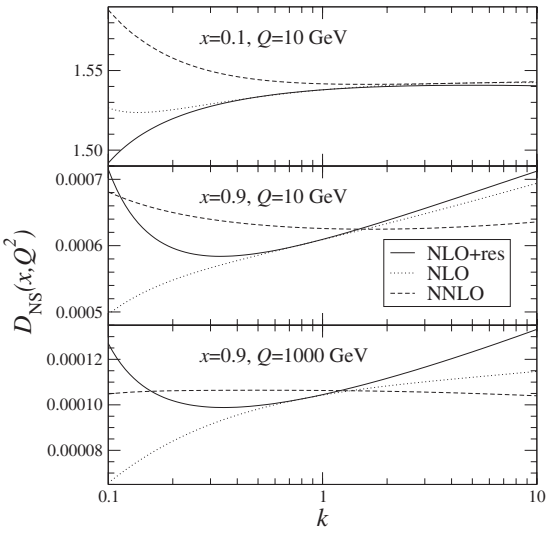

FIG. 23. Dependence of the unresummed (NLO) and resummed (NLO+res) nonsinglet FF on the renormalization scale μ. The factorization scale μ_f is written Q and $k=\mu/Q$. From Albino, Kniehl, and Kramer, 2008b.

e^+e^- reaction data might be used to theoretically predict future measurements from pp reactions. The more that a prediction depends on components of the FFs which were not well constrained by the experimental data used in the fit, the greater the difference between a prediction's calculation and its measurement can be. For example, the importance of the gluon FF relative to the quark FFs in e^+e^- reactions is much less than in pp reactions, so that a pp reaction prediction could deviate significantly from measurement when calculated using FFs that were fitted only to e^+e^- reaction data. A fit performed with the prediction's measurement added to the set of data to be fitted to is the optimal way to test whether all relevant physics effects have been taken into account in the theoretical calculations of all data. If a large χ^2 is obtained then effects omitted from the calculation such as higher twist or even new physics beyond the standard model are relevant. We assume of course that the data and calculation are reliable. If it is not possible to include the prediction's measurement in the fit, then this test can be performed by propagating the calculated prediction's error from the data used in the fit and comparing with the measurement's error. In this case, relevant effects have been omitted in the calculation if these two errors do not overlap. For example, the experimental error on the gluon FF fitted to e^+e^- reaction data will be large, leading to a wide range of allowed values for the pp reaction prediction. The propagated error on a prediction is best determined by adding a fictitious measurement of the prediction to the set of data used in the fit and then repeating the fit multiple times for a range of measurement values. Once done, the acceptable values of this measurement are taken to be those for which a good fit is obtained, i.e., for which χ^2 is less than some value. This is precisely what is achieved by the Lagrange multiplier method discussed in Sec. VI.C. A less reliable but more practical alternative to constraining predictions is to perform the error propagation in two steps (Pumplin, Stump, and Tung, 2002; Pumplin *et al.*, 2002; Stump *et al.*, 2002; Hirai, Kumano, Nagai, and Sudoh, 2007): the errors on the FFs propagated from the data used in the fit are determined, and then those FF errors are propagated to the prediction. This method is more practical because a fit does not need to be performed each time constraints on a prediction are to be determined. However, the Lagrange multiplier method avoids explicitly determining a large number of propagated errors on the FFs.

In the above discussion, we assumed that the constraints provided by the experimental data used in a fit are complete in the sense that all systematic effects in the experiment are available. In practice it can happen that some important systematic effects are unknown, resulting in a failure to fit or to describe a measurement even though all relevant physics effects are accounted for in the calculation. In this case it must be determined whether this measurement is consistent with other similar measurements from other experiments.

Recently a method has been developed and applied by the NNPDF Collaboration which uses neural networks as unbiased interpolants (Ball, 2009; Honkanen, 2009; Ubiali, 2009). This method solves a number of statistical issues in global fits.

In the rest of this section we discuss these issues in more detail. We first discuss the meaning of χ^2 and the interpretation of the parameter values at its minimum. The current method of presenting PDF errors such that they can be easily propagated to predictions is then discussed because this procedure is applicable to FFs. Finally, we discuss the Lagrange multiplier method already applied in FF fits since this is perhaps the most reliable method of propagating errors to predictions.

A. Relation between χ^2 and probability densities

In this section we define χ^2 for a given set of measurements and explain why the location of its minimum in the space of parameters of the theory corresponds to the most likely parameters values according to these measurements. Our starting point is Bayes' theorem (Giele and Keller, 1998; Amsler *et al.*, 2008), which states that the probability, as a quantification of the present degree of confidence from experience, for the vector f^e of experimental values f_i^e to take values between f^e and f^e+df^e and for the vector f^t of "true" values f_i^t to take values between f^t and f^t+df^t is given by

$$P(f^e,f^t)df^e df^t = P(f^t|f^e)df^t P(f^e)df^e = P(f^e|f^t)df^e P(f^t)df^t. \tag{126}$$

The probability densities $P(f^t|f^e)$, $P(f^t)$, $P(f^e)$, and $P(f^e|f^t)$ appearing in Eq. (126) will now be defined. $P(f^e|f^t)df^e$ is the probability that measurements give results between f^e and f^e+df^e given true values f^t, and its dependence on f^e is determined from experiment. The quantity $\chi^2(f^e,f^t)$ is defined through

$$P(f^e|f^t) \propto e^{-(1/2)\chi^2(f^e,f^t)}. \tag{127}$$

For example, in the case that the experimental uncertainties are purely statistical and are Gaussian distributed,

$$\chi^2 = \sum_i \left(\frac{f_i^t - f_i^e}{\sigma_i}\right)^2. \tag{128}$$

We defer to Sec. VI.B the form of χ^2 when systematic errors are present. $P(f^t)df^t$ is the probability that the true results lie between f^t and f^t+df^t, which reflects the knowledge of these observables prior to the $f_i^e \pm \sigma_i$ measurements. $P(f^e)df^e$ is the probability that measurements will give results between f^e and f^e+df^e prior to the experiment taking place and may be determined from $P(f^e|f^t)$ and $P(f^t)$ by performing the integration in the first and second equalities in Eq. (126) over f^t using $\int P(f^t|f^e)df^t=1$ and dividing out the factor df^e,

$$P(f^e) = \int P(f^e|f^t)P(f^t)df^t. \tag{129}$$

Finally, $P(f^t|f^e)df^t$ quantifies the "degree of belief" for the true observables to take values between f^t and f^t+df^t as a result of the experimental results f^e and is the quantity through which the test theoretical calculations are constrained by the experimental data by identifying these calculations with the test true values f^t. From Eqs. (126) and (129),

$$P(f^t|f^e) = \frac{P(f^e|f^t)P(f^t)}{\int P(f^e|f^t)P(f^t)df^t}. \tag{130}$$

If the experimental errors are sufficiently small, $P(f^t)$ will be approximately constant in f^t in the region of most statistical relevance, $f_i^t \pm \sigma_i$, and so approximately divides out of this expression. Then also using Eq. (127), we have finally

$$P(f^t|f^e) \propto e^{-(1/2)\chi^2(f^e,f^t)}. \tag{131}$$

Consequently, the values of f^t in which we are most confident are those for which χ^2 is a minimum since then the likelihood $P(f^t|f^e)$ is maximal. In the absence of a model, this would imply that the most likely values of f^t are $f^t=f^e$. Such a condition cannot be satisfied if the f^t is believed to be described by a theory involving a vector a of unknown parameters a_i, whose number should be much less than the number of data points or components of f^t in order to justify tests in which theory is compared with data. In that case, we should be considering probability densities in a instead of in f^t. Now, any probability distribution $p(f^t)$ in f^t and the equivalent $p(a)$ in a are related via $p(f^t)df^t=p(a)da$, i.e., $p(a)=p(f^t)J_{f^t}(a)$, where $J_{f^t}(a)$ is the Jacobian of f^t in a. Again, if the experimental errors are sufficiently small such that $J_{f^t}(a)$ is approximately constant in a in the region of most statistical relevance, $P(a|f^e) \propto P(f^t|f^e)$ and Eq. (131) becomes

$$P(a|f^e) \propto e^{-(1/2)\chi^2(f^e,f^t(a))}. \tag{132}$$

Thus the minimization of χ^2 with respect to a gives the most likely parameters values for these experimental data.

If the theoretical model and experimental data are reliable, the expected value of the minimized χ^2 is $\chi^2_{\min} = N_{\mathrm{DF}} \pm \sqrt{2N_{\mathrm{DF}}}$ (Soper and Collins, 1994; Collins and Pumplin, 2001), where N_{DF} is the number of degrees of freedom, i.e., the difference between the number of data points and the number of parameters fitted. Often the value of the reduced $\chi^2_{\min}$, $\chi^2_{\mathrm{DF}}=\chi^2_{\min}/N_{\mathrm{DF}}$, is quoted since this value is always expected to be around unity, with an error $\sqrt{2/N_{\mathrm{DF}}}$.

B. Incorporation of systematic errors in χ^2

An experimental systematic effect is a physical effect arising from a single experiment dependent source (which does not include physical effects common to all experiments measuring similar observables), and therefore the modification to the central value of any data point f_i^e due to this systematic effect is correlated with its modification to any other from the same experiment. Thus, the Kth source of systematic uncertainty will cause f_i^e to be shifted to $f_i^e+\lambda_K\sigma_i^K$, where λ_K, which is statistically distributed, measures the importance of the systematic effect itself and as a result is independent of the measurements, and σ_i^K measures the influence of this systematic effect on each measurement. While $\lambda_K\sigma_i^K$ is fixed, the relative normalization between λ_K and σ_i^K is not. It can be fixed by choosing the probability density in λ_K to be proportional to $\exp(-\lambda_K^2/2)$, assuming Gaussian systematic errors. Therefore, χ^2 for Gaussian statistical errors in Eq. (128) is modified to

$$\chi^2 = \sum_i \left(\frac{f_i^t - f_i^e - \sum_K \lambda_K\sigma_i^K}{\sigma_i}\right)^2 + \sum_K \lambda_K^2. \tag{133}$$

For the specific theory used to calculate the data, minimization of Eq. (133) with respect to λ_K gives an estimate of the Kth systematic effect on each data point $\lambda_K\sigma_i^K$ knowing only the statistically acceptable maximum size of this systematic effect on each data point $|\sigma_i^K|$ and its direction relative to the other data points (the sign of σ_i^K). Performing such a minimization numerically delays termination of the minimization routine used to perform the global fits. Therefore, this minimization should be done analytically (Pumplin, Stump, Huston, Lai, Nadolsky, and Tung, 2002; Albino, Kniehl, and Kramer, 2008b): the most likely values of the λ_K occur where

$$\partial\chi^2/\partial\lambda_K = 0. \tag{134}$$

Solving these equations for λ_K gives

$$\lambda_K = \sum_i \frac{f_i^t - f_i^e}{\sigma_i^2}\left(\sigma_i^K - \sum_{jkL} \sigma_i^L \sigma_j^L (C^{-1})_{jk} \sigma_k^K\right), \tag{135}$$

where the covariance matrix is given by

$$C_{ij} = \sigma_i^2 \delta_{ij} + \sum_K \sigma_i^K \sigma_j^K. \tag{136}$$

Substituting the best fit results for the λ_K in Eq. (135) into Eq. (133) gives the more familiar expression for χ^2 when systematic errors are accounted for,

$$\chi^2 = \sum_{ij} (f_i^t - f_i^e)(C^{-1})_{ij}(f_j^t - f_j^e). \tag{137}$$

In practice, not all information on the systematic effects in an experiment is available. For example, the analysis often provides only the "total" systematic error on a data point equal to all systematic errors of the data point from all sources added in quadrature. In this case, Eq. (128) is typically used in global fits with the statistical error modified to be the statistical error and this total systematic error added in quadrature. This corresponds to setting the off-diagonal components of the covariance matrix in Eq. (136) to zero, i.e., neglecting correlation effects between data points. More serious is the presence of unknown systematic effects. Such effects have to be neglected even though they could be important, but as the number of data sets increases, the cancellation of these effects among different experiments will increase as far as the determination of the most likely value for the parameters is concerned. Unfortunately, these unknown systematic effects have to be accounted for in the determination of parameter errors. We now discuss common methods for this in Sec. VI.C.

C. Propagation of experimental errors to fitted fragmentation functions

For Gaussian statistical errors and no correlations between data points, Eqs. (131) and (128) imply that the standard deviation error on f_i^t is σ_i. This error is equal to the amount by which f_i^t has to increase or decrease, with all other $f_{j\neq i}^t$ fixed, in order for χ^2 to increase by one from its minimum value of zero. More generally, the error on a quantity related to the f^t, such as a parameter a_i of the model, can be similarly determined. For simplicity, instead of a_i we work with the parameters

$$y_i = a_i - a_i^0, \tag{138}$$

where $a_i = a_i^0$ is the parameter space location of the minimum in χ^2 for these data. All following expressions are to lowest order in the y_i. The change in χ^2 from its minimum value at the origin $y_i = 0$ to any small values of the y_i is

$$\Delta\chi^2 = \sum_{ij} y_i H_{ij} y_j, \tag{139}$$

where the Hessian H is given by

$$H_{ij} = \frac{1}{2}\left(\frac{\partial^2 \chi^2}{\partial y_i \partial y_j}\right)\Bigg|_{y_k=0}. \tag{140}$$

The experimental error on a given a_i is equal to the magnitude of y_i that is required to make

$$\Delta\chi^2 = 1 \tag{141}$$

when all other $y_{j\neq i}$ are fixed. Thus, in the absence of correlations between the y_i, so that the off-diagonal elements of H vanish, the experimental error on y_i is $1/\sqrt{H_{ii}}$. More generally, according to Eq. (132), H is the inverse of the covariance matrix for the parameters,

$$\langle y_i y_j \rangle = (H^{-1})_{ij}. \tag{142}$$

According to Eq. (140), this covariance matrix can be determined numerically by calculating and then inverting the matrix of second derivatives of χ^2, which corresponds to the parabolic approximation of Eq. (139). If this approximation is not valid, the covariance matrix can be determined by the criterion of Eq. (141) directly, as done by Bourhis, Fontannaz, Guillet, and Werlen (2001).

The criterion of Eq. (141), however, is too idealistic for actual global fits. For example, Thorne (2002) highlighted the inconsistency between the resulting constraints on $\alpha_s(M_Z)$ determined from this criterion from different data sets used in the CTEQ6 extraction of PDFs (Pumplin, Stump, Huston, Lai, Nadolsky, and Tung, 2002). This is attributed by Botje (2002) and Thorne (2002) to various sources. First, the published statistical information on the experimental data may not be sufficiently reliable—errors, including systematic ones, may be inaccurate or not known at all or some errors may not be Gaussian distributed, let alone symmetric. Thus, for example, a fit to and extraction of parameter errors from data from one experiment in which the normalization error is underestimated may result in a good fit and apparently sensible results, but a similar analysis using data from two independent experiments suffering this problem will usually not. Second, the theory, including the parametrization used for the initial FFs and PDFs, may not be valid in all kinematic regions spanned by the data being fitted to. The simplest way to handle the reasons for the failure of the $\Delta\chi^2 = 1$ rule, whatever they may be, is to modify the criterion of Eq. (141) to (Pumplin, Stump, and Tung, 2002; Pumplin *et al.*, 2002; Stump *et al.*, 2002)

$$\Delta\chi^2 = T^2, \tag{143}$$

where the tolerance parameter T is a constant somewhat larger than 1. According to Eq. (137), this is equivalent to multiplying all errors, statistical and systematic, by a factor T. For example, Hirai, Kumano, Nagai, and Sudoh (2007) used $T^2 \sim 10$. This is significantly less than the choice $T^2 = 100$ in the CTEQ6 analysis (Pumplin, Stump, Huston, Lai, Nadolsky, and Tung, 2002), although the number of data points in the latter analysis exceeds that of the former by a factor of almost 10.

An alternative approach to Eq. (143) to handle unknown systematic effects is to take into account the degree of incompatibility of the data with one another. This is done in the neural network approach of Ball (2009), Honkanen (2009), and Ubiali (2009).

The statistical information on parameters of a theory from experimental data can be propagated to observables as follows. Consider a prediction X which depends on the FF parameters a_i. We determine the uncertainty on X, $\sqrt{\Delta X^2}$, resulting from the uncertainties on the experimental data which constrain the a_i. Since $\Delta X = \Sigma_i (\partial X/\partial y_i) y_i$ if the error $|y_i|$ is small,

$$\langle \Delta X^2 \rangle = \sum_{ij} \frac{\partial X}{\partial y_i} \frac{\partial X}{\partial y_j} \langle y_i y_j \rangle, \tag{144}$$

where $\langle y_i y_j \rangle = \int P(y|f_e) y_i y_j dy$. The probability distribution in y is chosen to be $P(y|f_e) \propto \exp[-\Delta\chi^2/(2T^2)]$, where $\Delta\chi^2$ is given by Eq. (139), which is the same as Eq. (132) except that the divisor T^2 has been introduced to ensure that the range of acceptable locations in parameter space are those for which $\Delta\chi^2 \leqslant T^2$ [recall Eq. (143)]. This modifies Eq. (142), the covariance matrix of the parameters, to $\langle y_i y_j \rangle = T^2 (H^{-1})_{ij}$.

A practical formula for calculating the error on a prediction is

$$\langle \Delta X^2 \rangle = \sum_{ij} \frac{X(y_k = \kappa\delta_{ki}) - X(y_k = -\kappa\delta_{ki})}{2\kappa} \times T^2 (H^{-1})_{ij} \frac{X(y_k = \kappa\delta_{kj}) - X(y_k = -\kappa\delta_{kj})}{2\kappa}, \tag{145}$$

where κ should be chosen to be less than or of the order of the error on each y_i but is otherwise arbitrary. In other words, constraints on a prediction are obtained by calculating it for each of the different sets of FFs for which $y_k = \pm\kappa\delta_{ki}$. Knowledge of the fitted a_i and their errors or even the choice of parametrization is not required.

Equation (145) can be simplified by diagonalization of the Hessian (Pumplin, Stump, and Tung, 2002; Pumplin *et al.*, 2002; Stump *et al.*, 2002), so that the parameters of the new basis are uncorrelated. The normalizations of these uncorrelated parameters z_i are chosen such that

$$\Delta\chi^2 = \sum_i z_i^2, \tag{146}$$

which is achieved through Eq. (139) by taking

$$z_i = \sum_j \sqrt{\epsilon_i} y_j v_{ji}, \tag{147}$$

where v_{lk} is the *kth* eigenvector of H_{ij} with eigenvalue ϵ_k,

$$\sum_j H_{ij} v_{jk} = \epsilon_k v_{ik}, \tag{148}$$

and the eigenvectors have been chosen to be orthonormal,

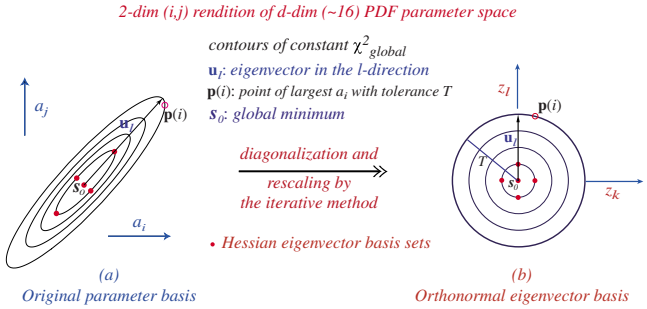

FIG. 24. (Color online) Illustration of the Hessian diagonalization of Pumplin, Stump, and Tung (2002), Pumplin *et al.* (2002), and Stump *et al.* (2002) for the case of two parameters for simplicity, showing contours of constant χ^2 in parameter space. In the new space of uncorrelated parameters (right), the contours are circles. From Pumplin *et al.*, 2002.

$$\sum_i v_{ij} v_{ik} = \delta_{jk}, \tag{149}$$

i.e., the matrix v obeys the orthonormal condition $v^T = v^{-1}$. This change in the parameter correlations due to the change of parameter basis is shown in Fig. 24.

Equation (145) is simplified to

$$\langle \Delta X^2 \rangle = \frac{1}{2} \frac{T^2}{4t^2} \sum_i \{X(y_k(z_l = t\delta_{li})) - X(y_k(z_l = -t\delta_{li}))\}^2, \tag{150}$$

where the choice $t \leqslant T$ should be made. Thus, for N free parameters, errors on predictions can be calculated from $2N$ sets $S_i^{\pm}$ of FFs at parameter values $y_k = y_k(z_l = \pm t\delta_{li})$, where $i = 1, \ldots, N$ as advocated by Soper and Collins (1994), Pumplin, Stump, and Tung (2002), Pumplin *et al.* (2002), and Stump *et al.* (2002) and is the current way in which PDFs are presented.

The Lagrange multiplier method (Pumplin, Stump, and Tung, 2002; Stump *et al.*, 2002), implemented in the global fit of de Florian, Sassot, and Stratmann (2007b), is a more reliable approach to obtaining errors on predictions because it avoids the assumption that χ^2 has a quadratic dependence on the parameters, as assumed in Eq. (139). The price is that it is computationally slower. The error on a prediction X is given by the range of its values for which the constrained minimum χ^2 (i.e., with the parameters constrained such that X is fixed to some value) is no greater than an amount T^2 above the unconstrained minimum χ^2. In practice, this is achieved by minimization of

$$F = \chi^2 + \lambda X \tag{151}$$

for a range of different values of λ because the corresponding minimized $\chi^2(\lambda)$ in each case is the minimum χ^2 given that the prediction takes the value $X(\lambda)$. To see this, take $dF = 0$ and choose the da_i such that $X(\lambda)$ is fixed, i.e., such that $\Sigma_i (\partial X/\partial a_i) da_i = 0$. Using this same reasoning, we see that Eq. (151) leads to the same results as the alternative form,

$$F = \chi^2 + \left(\frac{X - X_0}{\sigma_X}\right)^2, \tag{152}$$

with σ_X and X_0 varied, and therefore the Lagrange multiplier method is equivalent to the method of fictitious measurements discussed in the introduction to this section.

Although the Lagrange multiplier method avoids the quadratic approximation, it still suffers from the assumptions of Sec. VI.A such as no unknown systematic effects in the data, the linear dependence of the calculation on the parameters, and the independence of $P(f^i)$ on the calculation, which may not always be reliable. Furthermore, fits have to be repeated a number of times because the dependence of χ^2 on the parameters is unknown.

Figure 28 shows some results obtained with the Lagrange multiplier method and will be discussed in Sec. VII.B.

VII. CURRENT GLOBAL FITS

Recent global fits (de Florian, Sassot, and Stratmann, 2007a, 2007b; Hirai, Kumano, Nagai, and Sudoh, 2007; Albino, Kniehl, and Kramer, 2008b) made use of various experimental, computational, statistical, and theoretical advances. Data from e^+e^- reactions have provided accurate constraints on charge symmetry quark FFs. pp reaction data from RHIC provides better, and NLO, constraints on the gluon, and, along with HERMES data from HERA, is the only available data which can constrain the charge asymmetry FFs. However, due to the high accuracy and number of the e^+e^- reaction data relative to other data, charge asymmetry FFs remain much less constrained than charge symmetry FFs. This means that the prediction for a cross section for a particle of a given charge, which depends on $D_i^{h^+} = D_i^{h^\pm}/2 + D_i^{\Delta_c h^\pm}/2$ (or $D_i^{h^-} = D_i^{h^\pm}/2 - D_i^{\Delta_c h^\pm}/2$ for its antiparticle) will carry a large error coming from the charge asymmetry FFs $D_i^{\Delta_c h^\pm}$. It is therefore preferable to predict charge symmetry cross sections since they depend only on the charge symmetry FFs $D_i^{h^\pm}$, as shown in Sec. II.F, and therefore carry no large errors from the charge asymmetry FFs. Since charge asymmetry cross sections depend only on the charge asymmetry FFs, as also shown in Sec. II.F, a global fit can be separated into two fits, one for each type of FF and cross section, which disentangles the large charge asymmetry FFs' errors from the charge symmetry FFs' and allows for more efficient fitting.

Due to the large amount of data now available for constraining FFs, it is important that cross sections can be calculated quickly to ensure that the minimization of χ^2 occurs in a reasonable time. Exploiting multicore processors or multiple processors to perform the calculation of $f_i^t - f_i^e$ in Eq. (137) in parallel will substantially improve the minimization time because calculation of χ^2 is "embarrassingly parallel" (Foster, 1995). Calculating the cross section via the inverse Mellin transform, with the evolved Mellin space FFs obtained analytically according to the results of Sec. II.E, is faster than via the x-space convolution in Eq. (1) with the evolved FFs in z space via numerical integration of Eq. (3). However, the calculations of the partonic $d\sigma^i$ and partonic FFs E_{ij} [defined in Eq. (7)] in Mellin space can still be time consuming. Fortunately, since these quantities for each value of Mellin N which serves as the supports for the integration in the inverse Mellin transform [Eq. (D5)] are fixed during the fit, assuming of course that only the initial FFs' parameters are fitted but $\alpha_s(M_Z)$ is kept fixed, they can be calculated prior to fitting (Vogt, 2005; de Florian, Sassot, and Stratmann, 2007a). This precalculation is also suitable for adaptive integrations such as that used in the function GAUSS in the CERNLIB package because, for any given number of points used for the integration, each and every possible positioning of these points is predictable, the number of positionings being finite in number, and the values of $d\sigma^i$ and E_{ij} at each point need to be calculated only once as and when they are needed during the fitting and then stored. Most modern computers can manage the large amount of memory required for this precalculation for adaptive integrations. Although adaptive integration routines can take longer than integration routines which use the same points each time, they are more reliable. In the case that quantities such as $\alpha_s(M_z)$ and hadron mass are also fitted, $d\sigma^i$ in Mellin space will not themselves be fixed during the fit. Some improvement to this simple precalculation approach to handle such scenarios will usually be possible. Finally, note that it is not necessary for computational work to replace the infinite contour of integration in Mellin space by one of finite but large length because the infinite contour can be mapped to a finite range by a change of integration variable, and for most numerical integration methods the supports never approach the integration limits.

Analytic results for the $H^i_{h_1 h_2}$ in Mellin space do not exist. For example, they depend on PDFs which are normally extracted in x space from a numerical routine provided by the PDF Collaboration. An approximation to $H^i_{h_1 h_2}$ in Mellin space can be obtained by fitting them in x space to polynomials whose Mellin transform can be obtained analytically, with some modification to account for logarithmic singularities. Note that $H^i_{h_1 h_2}$ in x space are free of delta functions because these are integrated out in the convolution of $H^i_{1_{i_2}}$ with PDFs in Eq. (92). The use of the Chebyshev polynomials of the first kind (Press *et al.*, 2001) proves to be the best choice of polynomial type for speed and accuracy (Albino, Kniehl, and Kramer, 2008b). After performing the analytic Mellin transform of the Chebyshev expansions, Eq. (90) may be evaluated in Mellin space. This leads to an accuracy of a few parts per mil.

As well as these new experimental results and computational methods, the latest global fits of de Florian, Sassot, and Stratmann (2007a, 2007b), Hirai, Kumano, Nagai, and Sudoh (2007), and Albino, Kniehl, and Kramer

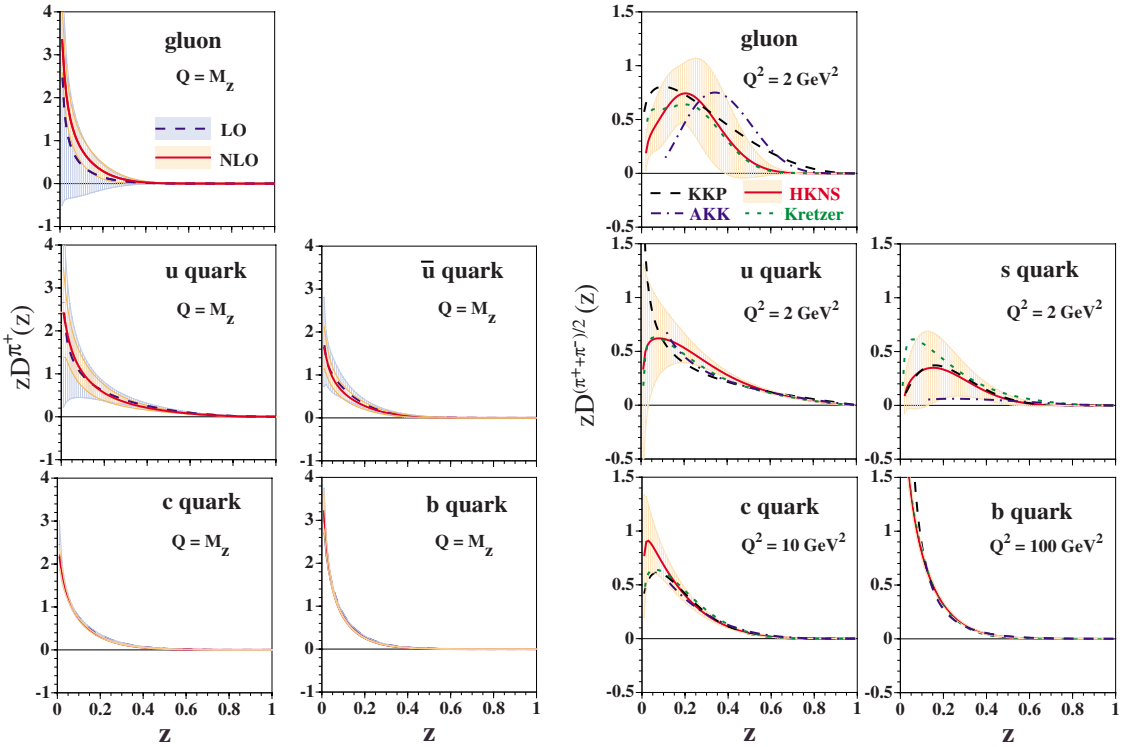

FIG. 25. (Color online) Errors on the fitted HKNS FFs for $\pi^{\pm}$ propagated from the errors on the data. Left: The results from a LO and NLO fit. Right: Comparison of the NLO HKNS FFs, with errors, with other FF sets. From Hirai, Kumano, Nagai, and Sudoh (2007).

(2008b), discussed in Secs. VII.A–VII.C, made use of the theoretical methods discussed in Sec. V and the statistical methods discussed in Sec. VI. We compare some of the results of these fits with one another in Sec. VII.D.

A. HKNS

The Hirai-Kumano-Nagai-Sudoh (HKNS) FF sets were obtained by Hirai, Kumano, Nagai, and Sudoh (2007) from global fits of FFs for $\pi^{\pm}$, $K^{\pm}$, and $p/\bar{p}$ to all available e^+e^- reaction data, excluding particle unidentified data because it may be contaminated with other particles beyond those just mentioned and also excluding the OPAL tagging probabilities of Abbiendi *et al.* (2000c), and the Hessian matrix of FF parameter errors was calculated. The results with errors for the FFs for $\pi^{\pm}$ are shown in Fig. 25. The plots on the left show a reduction in experimental errors propagated to FFs on going from LO to NLO. This is particularly significant in the case of the gluon FF probably because at LO the gluon only contributes through the evolution and therefore the cross section's dependence on it is less than at NLO. Furthermore, as can be seen by comparing these plots with the plots on the right, FF errors are relatively higher at lower factorization scales, and therefore FF errors may be particularly important in pp reaction data. The plots on the right suggest that the AKK, KKP, and Kretzer FF sets are generally consistent with the e^+e^- reaction data used in the HKNS analysis.

B. DSS

The DSS FF sets for $\pi^{\pm}$ and $K^{\pm}$ were obtained from global fits of de Florian, Sassot, and Stratmann (2007a), which also included ep reaction data from the HERMES Collaboration (Hillenbrand, 2005) at HERA and pp reaction data from the BRAHMS, PHENIX, and STAR Collaborations at RHIC. $pp(\bar{p})$ reaction data for $\pi^{\pm}$ and $K^{\pm}$ are summarized in Tables VIII and IX, respectively. Systematic errors due to normalization uncertainties on the data were accounted for. Although the HERMES data are measured for $Q \lesssim 2$ GeV, where low Q effects may be important, a good fit is obtained as shown in Fig. 15 for $\pi^{\pm}$. Since the particle charge is measured, these data also provide much needed constraints on the valence quark FFs or the charge asymmetry FFs which are the same functions. The large difference, relative to the experimental errors, between the calculations for the BRAHMS data using the DSS and Kretzer FF sets shown in Fig. 26 indicates that pp reaction data provide constraints not provided by e^+e^- reaction data, which were the only type of data used in the Kretzer analysis. Note, however, that the calculation using the Kretzer FF set is within the theoretical error, which is large compared to the theoretical error on calculations for e^+e^- reactions shown in Fig. 27.

The method of Lagrange multipliers discussed in Sec. VI.C to determine errors on predictions was applied in this analysis using the FFs at $\mu_f = 5$ GeV integrated from $z = 0.2$ to 1 as example predictions (for quark FFs, these

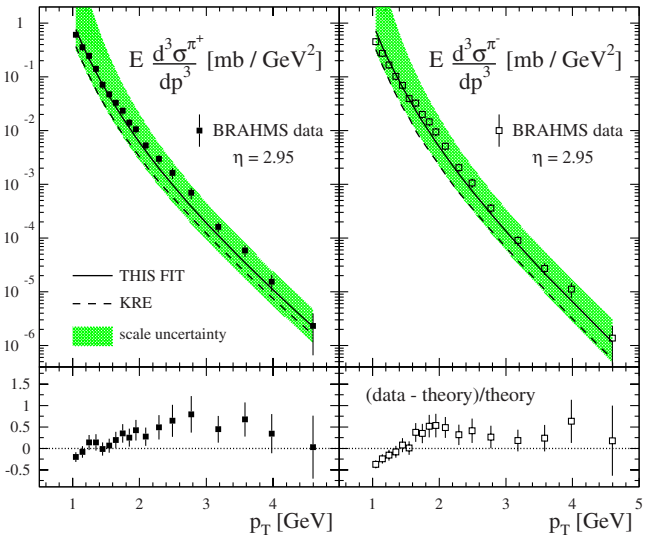

FIG. 26. (Color online) As in Fig. 15, but for the BRAHMS data. The shaded bands in the upper panels indicate theoretical uncertainties and are obtained by calculating in the range $1/2<\mu_f/p_T<2$, with $\mu=\mu_f$. From de Florian, Sassot, and Stratmann, 2007a.

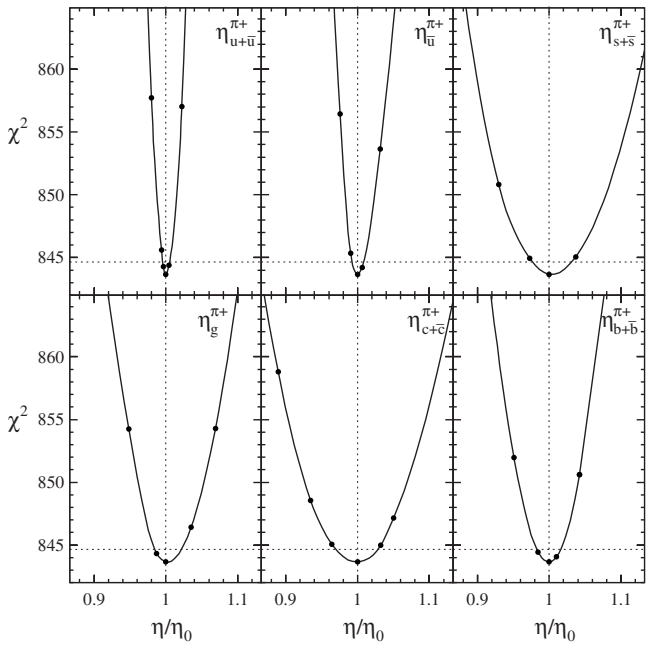

FIG. 28. Values of minimized χ^2 subject to fixed values of $\eta_i^{\pi^+}/\eta_{0i}^{\pi^+}$, where $\eta_i^{\pi^+}=\int_{0.2}^1 dz D_i^{\pi^+}(z,25\ \mathrm{GeV}^2)$ and $\eta_{0i}^{\pi^+}$ is the value of $\eta_i^{\pi^+}$ obtained when χ^2 is minimized without these constraints. From de Florian, Sassot, and Stratmann, 2007a.

are equal to the LO calculations of the OPAL tagging probabilities). The result of this study for π^+ is shown in Fig. 28. $\eta_{u+\bar{u}}^{\pi^+}$ has the smallest error, equal to 3%, if the tolerance parameter appearing in Eq. (143) is chosen to be $T=\sqrt{15}$. This is because all observables in the fit have a strong dependence on this FF. The error on $\eta_{\bar{u}}^{\pi^+}$, 5%, is not much larger. This quantity is expected to be well constrained by *ep* and *pp* reaction data due to the large PDFs for $\bar{u}$ at low x and for u at high x. Because using *pp* reaction data, the size of the error on $\eta_g^{\pi^+}$ relative to that on the other $\eta_i^{\pi^+}$ shows that the gluon FF is reasonably well constrained relative to the quark FFs. Presumably because b quark tagged observables can be measured more accurately than c quark tagged ones, $\eta_{b+\bar{b}}^{\pi^+}$ has a lower error than $\eta_{c+\bar{c}}^{\pi^+}$.

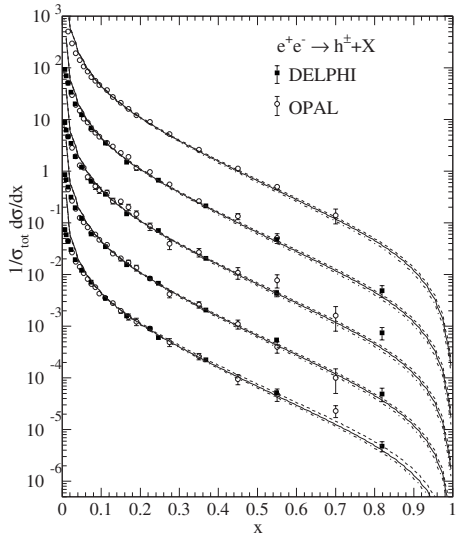

FIG. 27. NLO calculations using the KKP FF set with $\mu_f/\sqrt{s}=1/2$ (dashed lines), $\mu_f/\sqrt{s}=1$ (solid lines), and two (dot dashed lines) of the data from DELPHI (Abreu *et al.*, 1999b) and OPAL (Alexander, 1996; Ackerstaff *et al.*, 1997; Abbiendi *et al.*, 2000a) at energies $\sqrt{s}=133$, 161, 172, 183, and 189 GeV (from bottom to top in this order). From Kniehl, Kramer, and Pötter, 2001.

A global fit of FFs for $p/\bar{p}$ (and, separately, for unidentified particles) was performed by de Florian, Sassot, and Stratmann (2007b) including *pp* data from STAR. $pp(\bar{p})$ reaction data for $p/\bar{p}$ is summarized in Table X. BRAHMS data were excluded due to possible contamination of the sample by the beam from the large rapidity.

C. AKK08

The AKK08 FF sets were obtained by Albino, Kniehl, and Kramer (2008b) from global fits of FFs for $\pi^\pm$, $K^\pm$, $p/\bar{p}$, K_S^0, and $\Lambda/\bar{\Lambda}$ which included, as well as the usual e^+e^- reaction data, the *pp* reaction data from RHIC and $p\bar{p}$ reaction data from the CDF Collaboration at the Fermilab Tevatron (Acosta *et al.*, 2005). Due to the unreliability of perturbation theory at low p_T, a cut of $p_T>2$ GeV was imposed. We note that such data are dangerously close to the energy range $1\lesssim Q\lesssim 2$ GeV of the HERMES data of Fig. 15, which they omitted from the set of all data used in the fit. However, in contrast to the HERMES data, the $pp(\bar{p})$ reaction data are of much lower accuracy than the e^+e^- reaction data, so that the

TABLE I. Fitted particle masses used in the calculation of the hadron production from e^+e^- reactions in the AKK08 fit. For comparison, the true particle masses are also shown. From Albino, Kniehl, and Kramer, 2008b.

Particle	Fitted mass (MeV)	True mass (MeV)
$\pi^\pm$	154.6	139.6
$K^\pm$	337.0	493.7
$p/\bar{p}$	948.8	938.3
K_S^0	343.0	497.6
$\Lambda/\bar{\Lambda}$	1127.0	1115.7

TABLE II. The minimized χ^2 values in each of the charge summed AKK08 fits. For comparison, the χ^2 values for the unresummed fit are shown (under "Unres. fit"). From Albino, Kniehl, and Kramer, 2008b.

	χ^2	
H	Main fit	Unres. fit
$\pi^\pm$	518.7	519.0
$K^\pm$	416.6	439.4
$p/\bar{p}$	525.2	538.0
K_S^0	317.2	318.7
$\Lambda/\bar{\Lambda}$	273.1	325.7

constraints on the quark FFs still come essentially from the latter data only. The $pp(\bar{p})$ reaction data are included only to improve the constraints on the already poorly constrained gluon FF. As shown in Fig. 20 for the case of STAR data, the description of the RHIC data was good except in the case of the production of $\Lambda/\bar{\Lambda}$. Normalization errors were accounted for as systematic errors in a covariance matrix according to the procedure discussed in Sec. VI.B. λ_K at the location of the minimum value of χ^2 was determined according to Eq. (135) and was typically found to be in the expected range $|\lambda_K| \lesssim 2$. As for the DSS and HKNS fits, e^+e^- reaction data for x values as low as 0.05 and for $\sqrt{s} < M_Z$ were included with the LEP data at $\sqrt{s} = M_Z$, in contrast to the previous AKK fits (Albino, Kniehl, and Kramer, 2005, 2006) where a cutoff $x > 0.1$ was imposed on the data and only LEP data at $\sqrt{s} = M_Z$ and TPC data at $\sqrt{s} = 29$ GeV were used. Because of this additional lower $\sqrt{s}$ and smaller x data, the effect of hadron mass discussed in Sec. V.A was incorporated into the calculations of both the $pp(\bar{p})$ and the e^+e^- reaction data. The hadron mass appearing in the calculation of the e^+e^- reaction data was fitted and in this way absorbed approximately any other small x, low $\sqrt{s}$ effects such as higher twist. The results are shown in Table I.

The results for $\pi^\pm$, $p/\bar{p}$, and $\Lambda/\bar{\Lambda}$ suggest that hadron mass effects are important at small x, low $\sqrt{s}$ effects for the data considered. This is also consistent with the expectation that the contributions at higher twist fall off as $O(1/Q^2)$ (Balitsky and Braun, 1989, 1991) in the sense that if they fell slower, e.g., such as $O(1/Q)$, they would be expected to dominate over hadron mass effects, which fall as $O(1/Q^2)$. The slight excess in the fitted masses is expected because the overall production does not arise solely from direct partonic fragmentation but also includes contributions from decays of heavier particles. A full error analysis is required in order to determine whether the excess seen in the fitted masses is significant. The large undershoot in the fitted masses of $K^\pm$ and K_S^0 is likely due to physics effects not present in the production of $\pi^\pm$, $p/\bar{p}$, and $\Lambda/\bar{\Lambda}$, the most likely effect being the complicated production mechanisms of kaons from decays of heavier hadrons. Note that the undershoots in the fitted masses of $K^\pm$ and K_S^0, 156.7 and 154.6 MeV, respectively, are similar, which may be explained by similar production mechanisms, however complicated, for these two particles, as expected from SU(2) isospin symmetry. As discussed in Sec. III, this result suggests that the argument by Christova and Leader (2007, 2009) is unaffected by such production mechanisms. Again, a full error analysis is required here.

For reasons stated earlier, charge summed and charge asymmetry FFs were parametrized and fitted separately. The strongest nonperturbative assumption used in the AKK08 analysis is the parametrization of Eq. (59), taking $f_i(z) = 1 + c_i(1-x)^{d_i}$ for charge summed FFs and $f_i(z) = 1$ for the less well constrained charge asymmetry FFs. No further constraints among FFs were imposed other than Eq. (15), which is exact in QCD, and the SU(2) isospin symmetry conditions $D_u^{\pi^\pm/\Delta_c\pi^\pm}(z,\mu_f^2) = D_{\bar{d}}^{\pi^\pm/\Delta_c\pi^\pm}(z,\mu_f^2)$ which are also exact in QCD in the limit that the difference between u and d quark masses vanishes. This is in contrast to the DSS and HKNS analyses, where additional well-justified assumptions were also imposed, which provide additional nonphenomenological constraints on FFs.

The large x resummation discussed in Sec. V.B was incorporated into the calculations of the e^+e^- reaction data in the charge summed fits, made a significant improvement in the case of $K^\pm$, $p/\bar{p}$, and $\Lambda/\bar{\Lambda}$ as Table II shows, and does not worsen the fits for $\pi^\pm$ and K_S^0. Accurate large x, $\pi^\pm$, $K^\pm$, and $p/\bar{p}$ production data from BaBar at $\sqrt{s} = 10.54$ GeV (Anulli, 2004), shown in its preliminary form in Fig. 29, would further ascertain whether large x resummation improves the description of e^+e^- reaction data. In this case it would be interesting to determine whether it is in fact necessary either to implement or to not implement large x resummation.

We note that large x resummation was not implemented in the calculation of the $pp(\bar{p})$ reaction data, which in principle is inconsistent with the resummed calculation of the e^+e^- reaction data. However, as mentioned, the $pp(\bar{p})$ reaction data are of much lower accuracy and therefore do not significantly affect the quark FFs that are constrained by the e^+e^- reaction data. Fur-

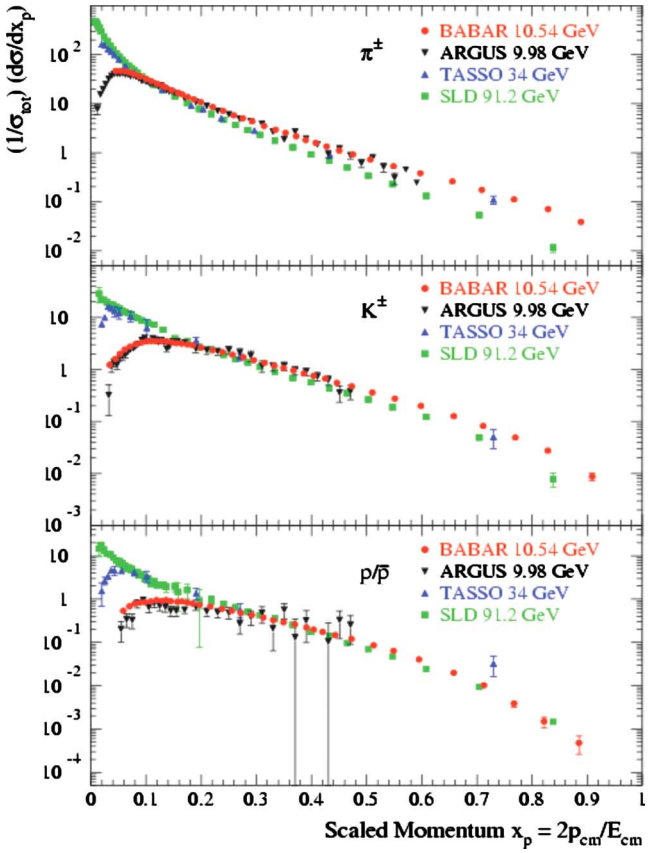

FIG. 29. (Color online) Preliminary data from e^+e^- reactions at BaBar for $\pi^{\pm}$, $K^{\pm}$, and $p/\bar{p}$. Also shown are some published data for comparison. From Arleo, 2009.

thermore, the gluon FF, which is important for the $pp(\bar{p})$ reaction data, is only weakly constrained by the e^+e^- reaction data.

D. Comparisons of the different FF sets

As an example of how the different FF sets compare, we show the FFs for $K^{\pm}$ from the different sets in Fig. 30. These represent an "average" comparison; i.e., better agreement is found among the different FF sets for $\pi^{\pm}$ and worse for $p/\bar{p}$. In Fig. 30, as well as Figs. 31–33, the scale μ_f=91.2 GeV has been chosen, although the FFs at this scale are not significantly different to FFs in the whole region $10 \leqslant \mu_f \leqslant 91.2$ GeV that is of experimental interest at present. Similar results are obtained at intermediate and large z for the u quark (except for DSS and for AKK at large z) which is favored and for the c and b quarks away from large z which is well constrained by c and b quark tagged measurements. For the d quark, which is unfavored, the results are very different. The large difference between the DSS and AKK08 gluon FFs suggests that the constraints on gluon fragmentation provided by pp reaction data are not as significant as might be hoped.

In Figs. 31–33 we show the charge asymmetry FF sets for $\pi^{\pm}$, $K^{\pm}$, and $p/\bar{p}$, respectively. The HKNS and DSS results are generally rather similar. However, no phenomenological constraints on the charge asymmetry FFs were applied in the HKNS analyses, so this similarity is most likely due to the similar nonperturbative assumptions used in the HKNS and DSS analyses, inspired by physical effects such as the suppression of nonfavored fragmentation, indicating that most of the constraint on the charge asymmetry FFs in these two analyses may come from these assumptions. These results show that the charge asymmetry FFs, which help to extract important information on nucleon PDFs (Gronau, Ravndal, and Zarmi, 1973; Arneodo, 1989; de Florian, Sampayo, and Sassot, 1998; Hasegawa, 1998; de Florian, 2003; Jager, Schafer, Stratmann, and Vogelsang, 2003; Airapetian *et al.*, 2004, 2005; de Florian, Navarro, and Sassot, 2005) as mentioned, are poorly constrained and highlight the need for data in which the hadron species and its charge are identified from, e.g., HERA and RHIC, as well as for measurements of the asymmetric cross section in e^+e^- reactions discussed in Sec. II.I.

Unfortunately, neither AKK nor DSS provides uncertainty estimates. The differences between the FFs for these sets shown in Figs. 30–33 provide the best error estimate of the latest FFs at present.

VIII. IMPROVING THE CALCULATION AT SMALL x

Perhaps the most serious limitation of the standard FO approach is its inability to describe a wealth of small x data from e^+e^- reactions, mainly as result of unresummed soft gluon logarithms (SGLs) in both the evolution and the coefficient functions spoiling the convergence of the perturbation series. This problem even renders some well-measured observable singular, such as the multiplicity in Eq. (43). For this reason, resummation of SGLs is more urgent than the treatment of other low E_s and small x effects. However, because of those effects, resummation of SGLs may be insufficient for at least some of the data at low E_s and small x. To date, the only way to determine which of these data can be described when SGLs are resummed is phenomenologically through fits. Resummation of SGLs extends the region of data that can be described by theory to smaller x values but still does not allow for all small x data to be described.

The advantage of SGL resummation is that it will allow use in global fits of data of lower x values than are currently used and thus not only would new constraints on FFs at smaller z be obtained but also, through the convolution in Eq. (1), further constraints on the FFs at intermediate and large z. This resummation also permits a calculation of the multiplicity.

In the DGLAP evolution, the largest of these SGLs, the double logarithms (DLs), can be calculated to all orders and then resummed using the results of the double logarithmic approximation (DLA). Since the only SGLs that appear at LO are DLs, a LO evolution of FFs that includes small z is now possible. However, at present the full DL contribution to the gluon coefficient function for e^+e^- reactions is unknown and is necessary

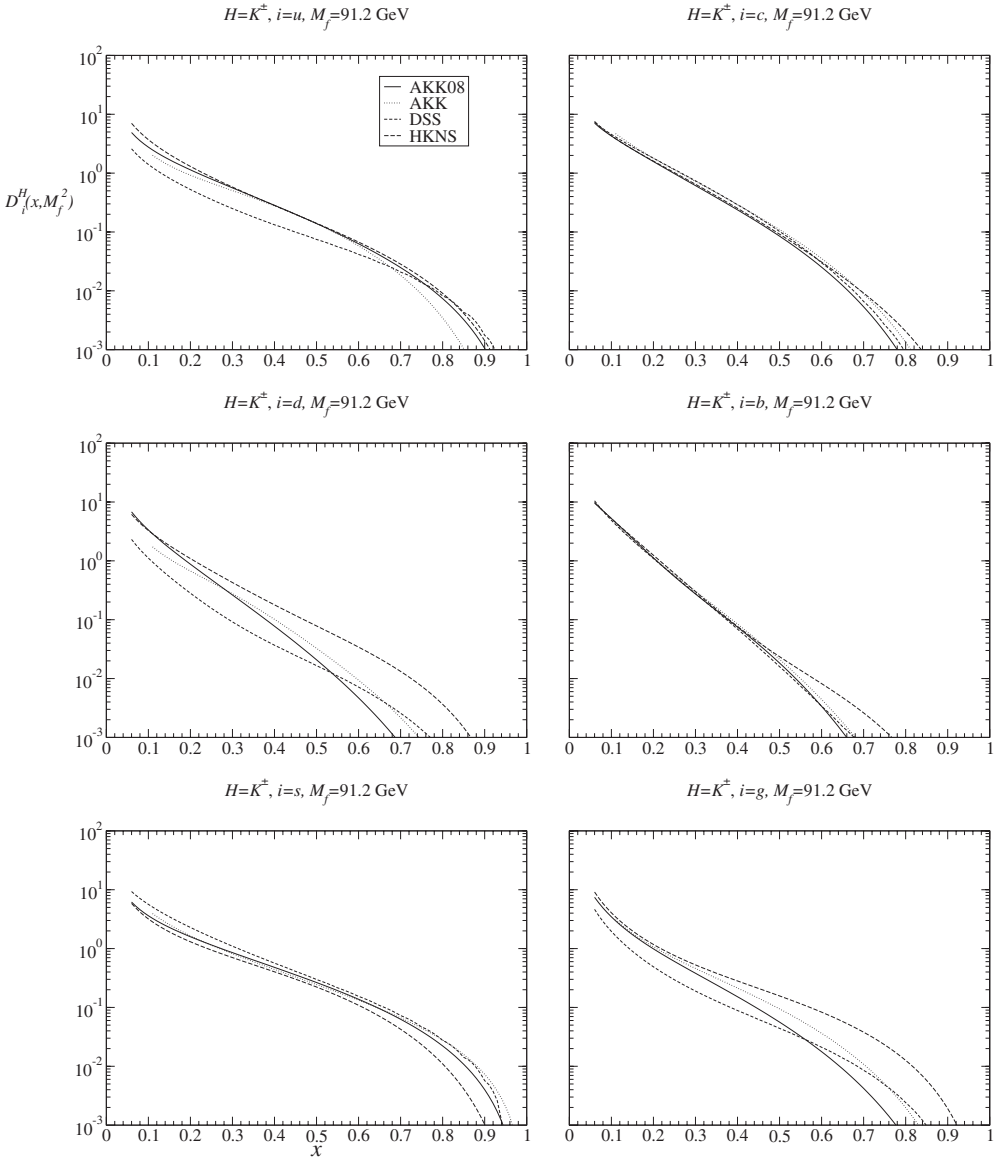

FIG. 30. The FFs for $K^{\pm}$ at μ_f=91.2 GeV.

for the calculation of the complete DL resummed cross section. In a LO calculation, it may be a reasonable approximation to neglect this DL contribution because the gluon contribution vanishes at this order. A consistent NLO fit including small x data is not possible at present because the next largest classes of SGLs after the DLs, which in order are the single logarithms (SLs), the subsingle logarithms (sSLs), and the subsubsingle logarithms (ssSLs), none of which are known in full, are all present at this order.

In addition to these shortcomings, the inclusive single hadron production data at small x is usually studied within a different framework to the standard FO approach, namely, the framework of the modified leading logarithmic approximation (MLLA) (Dokshitzer and Troian, 1984a, 1984b; Dokshitzer, Khoze, Mueller, and Troian, 1991; Dokshitzer and Olsson, 1993; Khoze and Ochs, 1997), in which both DLs and contributions from the SGL-free part of evolution are accounted for, leading to a good description of the data over the whole x range currently measured. In addition, in practical applications the nonperturbative components, the FFs, are usually fixed, up to an overall normalization, by the assumptions of local parton-hadron duality (LPHD) and the limiting spectrum (Azimov, Dokshitzer, Khoze, and Troian, 1985) rather than being fitted to experimental data: The LPHD states that sufficiently inclusive hadronic processes have similar properties to the equivalent partonic processes (except for particle number) at hadronic scales, which implies that the FFs are proportional to partonic FFs, i.e., $\delta(1-z)$, at $\mu_f \simeq \Lambda$. The limiting spectrum, which is a solution to the MLLA equation that is assumed to be valid in the region $\mu_f \simeq \Lambda$, can then be used to evolve the hadronic FFs to any scale. Perhaps the reason for this is that the way in which SGLs can be incorporated into the FO evolution was recently not known. A procedure for resumming SGLs in the evolution within the FO framework now exists: as for coeffi-

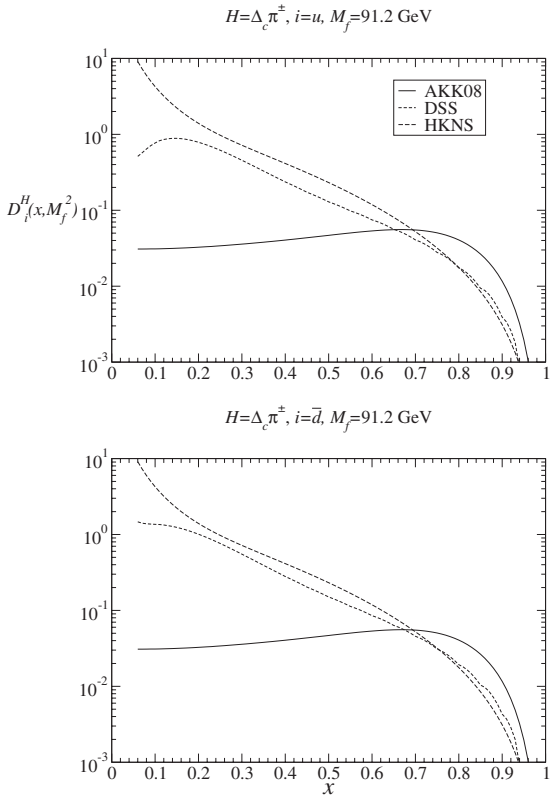

FIG. 31. The quark FFs for $\Delta_c\pi^{\pm}$ at μ_f=91.2 GeV.

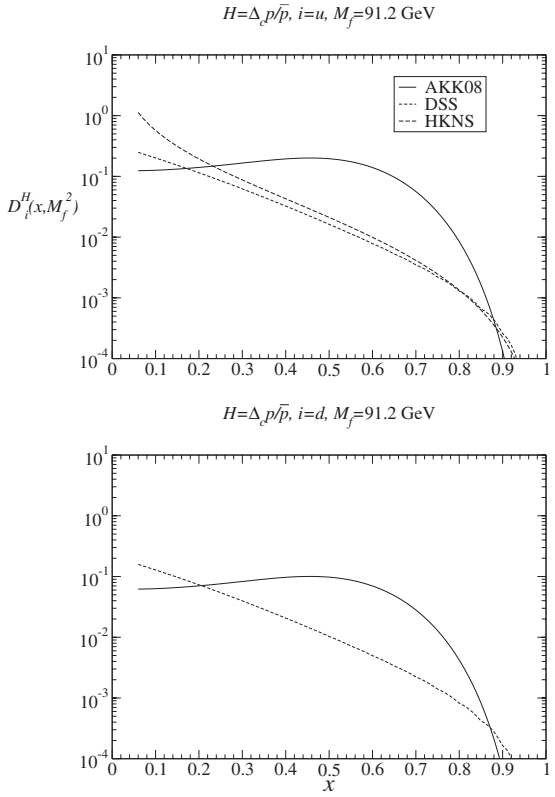

FIG. 33. The quark FFs for $\Delta_c p/\bar{p}$ at μ_f=91.2 GeV.

cient functions, for every class of SGLs in the FO splitting functions, the remaining SGLs to all orders are added. This approach reduces to the MLLA in certain approximations, but it provides an alternative to the MLLA because it is in principle complete: it contains the quark contribution to the evolution, and it can be systematically improved. However, the simplicity of the MLLA still makes the MLLA an attractive alternative for incorporating certain types of phenomenology such as medium effects or double hadron production at small x.

In this section, we discuss the present state of the art in the description of small x data from e^+e^- reactions. We first define, in Sec. VIII.A, the SGLs appearing in FO calculations and then, in Sec. VIII.B, derive the form

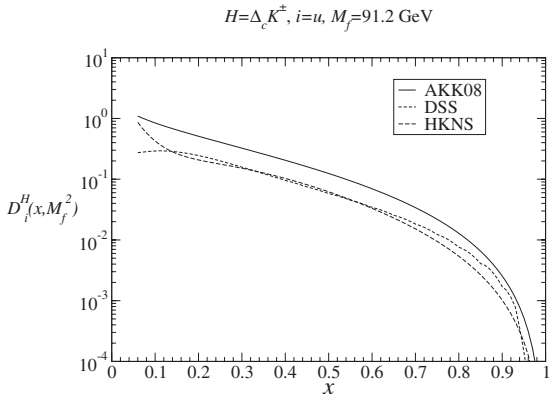

FIG. 32. The u quark FF for $\Delta_c K^{\pm}$ at μ_f=91.2 GeV.

taken by SGLs belonging to a specific class when they are summed to all orders within the FO framework. We discuss the DLA in Sec. VIII.C, which is crucial for determining the DLs to all orders in the splitting functions in the FO framework. By direct application of the DGLAP equation, we then generalize the DLA and FO approximations to a single approach in Sec. VIII.D. This approach incorporates both approximations and is the lowest-order approximation within the approach developed in Sec. VIII.B. It can be systematically improved both in the FO part and in the SGL part. We show in Sec. VIII.E that this approach reduces to the MLLA in certain limits used within that framework. Some discussion is then given on LPHD and the limiting spectrum which are used to fix the remaining, nonperturbative, degrees of freedom in the MLLA. Using the approach of SGL resummation within the FO framework, we are then able to give a perturbative argument for the results of the LPHD and limiting spectrum in Sec. VIII.F by studying the moments of the evolution.

A. The behavior of the evolution at small z

The approximation for P in Eq. (4) fails at small z due to the presence of terms which, in the limit $z\to 0$, behave as $(a_s^n/z)\ln^{2n-m-1} z$ for $m=1,\ldots,2n-1$. Such logarithms are called SGLs and m labels their class. The class of logarithms for which $m=1$ are the largest logarithms, known as DLs, while the next largest, for which $m=2$, are called SLs, the next largest sSLs, the next largest ssSLs, etc. As z decreases, these unresummed SGLs

will spoil the convergence of the FO series for $P(z,a_s)$ once $\ln(1/z) \geqslant O(a_s^{-1/2})$. Consequently, the evolution of $D_i(z,\mu_f^2)$ will not be valid at such small values of z since the range $z \leqslant z' \leqslant 1$ contributes in Eq. (3). Therefore, according to Eq. (1), the FO approach is only a good approximation for cross sections whose x value, being the minimum value of z, is sufficiently large, specifically it must obey $\ln(1/x) < O(a_s^{-1/2})$.

Using the result

$$\frac{1}{\omega^p} = \frac{1}{p!}\int_0^1 dz z^\omega \frac{\ln^{p-1}\frac{1}{z}}{z} \tag{153}$$

for $\mathrm{Re}(\omega) > 0$ and the integer $p \geqslant 1$, we find that in Mellin space these SGLs behave as a_s^n/ω^{2n-m} where $\omega = N - 1$; i.e., they become singular as $\omega \to 0$. Thus the standard FO approach in Mellin space will not be a valid approximation once $|\omega| \leqslant O(a_s^{1/2})$. Sometimes, those Mellin space terms for which $m = 2n$, i.e., which behave as a_s^n at small ω, are often included in the definition of SGLs. For example, in the MLLA, the $m = 2n = 2$ term in $P(z,a_s)$ at LO is referred to as an SL. Since such terms behave as $a_s^n \delta(1-z)$ in z space, i.e., do not affect the accuracy of the FO expansion at low z and so do not need to be resummed, we will not include such terms in our definition of SGLs, which will always be restricted to $m \leqslant 2n-1$.

By writing Eq. (44) as

$$\langle n^h(s)\rangle = \frac{Q_{q_J}}{\sum_{I=1}^{n_f} Q_{q_I}} D^h_{q_J/\bar{q}_J}(\omega = 0, s), \tag{154}$$

it is clear then that the multiplicity is undefined in the FO calculation because of the unresummed SGLs in the splitting functions. (More precisely, the multiplicity at any value of s cannot be determined from the multiplicity at a given value of s because its s dependence in the FO approach is singular if the SGLs are unresummed.) Beyond LO, unresummed SGLs in the coefficient functions will also give singular contributions to Eq. (154).

B. A unified formalism for small and large z evolution

The correct way to approximate $P(\omega,a_s)$ such that both the large and small $|\omega|$ regions (and hence the large and small z regions) of the evolution can be described by the DGLAP equation is to put it in the form (Albino, Kniehl, Kramer, and Ochs, 2005, 2006)

$$P(\omega,a_s) = P^{\not{\mathrm{SGL}}}(\omega,a_s) + P^{\mathrm{SGL}}(\omega,a_s), \tag{155}$$

where $P^{\not{\mathrm{SGL}}}$ is equal to P after all SGLs have been subtracted, so that it can be approximated in Mellin space for both large and small $|\omega|$ as the FO series

$$P^{\not{\mathrm{SGL}}}(\omega,a_s) = \sum_{n=1}^{\infty} a_s^n P^{\not{\mathrm{SGL}}(n-1)}(\omega), \tag{156}$$

truncated at some finite value for n, similar to Eq. (4) [note that $P^{\not{\mathrm{SGL}}(n-1)}(\omega) \propto \ln\omega$ at large ω, as discussed in Sec. V.B], and where P^{SGL} contains all SGLs in P and which therefore can be approximated in Mellin space by the series

$$P^{\mathrm{SGL}}(\omega,a_s) = \sum_{m=1}^{\infty} \left(\frac{a_s}{\omega}\right)^m g_m\left(\frac{a_s}{\omega^2}\right), \tag{157}$$

truncated at some finite value for m. For a given value of m, $(a_s/\omega)^m\, g_m(a_s/\omega^2)$ in Eq. (157) is obtained by resummation of all class m SGLs in P. Equation (157) is just the general result of expanding a function of a_s and ω in a_s/ω keeping a_s/ω^2 fixed (although it is not completely general because the series starts at $m=1$). Equation (157) should be a good asymptotic approximation in the region $|\omega| = O(a_s^{1/2})$, at least for sufficiently small a_s. In fact, from incomplete calculations up to the class $m=2$ (Dokshitzer, Khoze, Mueller, and Troian, 1991), in particular the splitting function for the MLLA evolution of the gluon FF in Eq. (188) below, P^{SGL} approximated as in Eq. (157) is believed to be valid for the region $|\omega| \leqslant O(a_s^{1/2})$ as well. In particular, at $\omega = 0$ it is expected to be a series in $\sqrt{a_s}$ with finite coefficients, beginning at $O(\sqrt{a_s})$. Note that P^{SGL} falls to zero as $|\omega| \to \infty$ because in this limit it is well approximated by an expansion in a_s keeping ω fixed. This condition is met by Eq. (188) below.

From Eq. (153), the inverse Mellin transform of Eq. (157) gives the z space result

$$P^{\mathrm{SGL}}(z,a_s) = \frac{1}{z\ln z}\sum_{m=1}^{\infty} (a_s \ln z)^m f_m(a_s \ln^2 z), \tag{158}$$

which can also be obtained by summing the SGLs in z space for each m. Equation (158) shows that the approximation of Eq. (157) is valid in the evolution of $D(z,Q^2)$ in the region $\ln(1/z) \leqslant O(a_s^{-1/2})$, which includes the small, but not arbitrarily small, z region $\ln(1/z) = O(a_s^{-1/2})$. Note that the usual condition $a_s \ll 1$ must still hold in order that the approximation in Eq. (156) holds everywhere in this range of z. If $P^{\mathrm{SGL}}(\omega,a_s)$ approximated as in Eq. (157) really is finite at $\omega = 0$, then $P^{\mathrm{SGL}}(z,a_s)$ in Eq. (158) must obey $zP^{\mathrm{SGL}}(z,a_s) \to 0$ as $z \to 0$.

Using the DLA, it is in fact possible to calculate the $m=1$ term in Eq. (157) or equivalently in Eq. (158), i.e., the complete DL contribution. We show how to do this in Sec. VIII.C.

C. The double logarithmic approximation

The DLA (Bassetto, Ciafaloni, Marchesini, and Mueller, 1982) states that if the evolution is written in the form

$$\frac{d}{d\ln\mu_f^2}D(z,\mu_f^2)=\int_z^1\frac{dz'}{z'}\frac{2C_A}{z'}Az'^{2(d/d\ln\mu_f^2)}\times\left[a_s(\mu_f^2)D\left(\frac{z}{z'},\mu_f^2\right)\right]+\int_z^1\frac{dz'}{z'}\bar{P}(z',a_s(\mu_f^2))D\left(\frac{z}{z'},\mu_f^2\right),\tag{159}$$

where $(2C_A/z)A=P^{\mathrm{DL}(0)}(z)$ is the LO term in the expansion in a_s of the full DL contribution to P, P^{DL}, where P^{DL} is equal to the $m=1$ term in Eq. (158), then $\bar{P}(z,a_s)$ is free of DLs. A will be given explicitly in the basis of singlet, nonsinglet, and valence quark FFs just now when we will see that A is a projection operator, its normalization being chosen such that it obeys $A^2=A$, and this property will make resummation calculations to appear later in this section easier. The solution to Eq. (159) leads to the famous *hump-backed plateau* in the cross section; i.e., the cross section can be approximated by a Gaussian in $\ln(1/x)$. This behavior is seen in the data (see Fig. 35).

We now give an outline of the derivation of Eq. (159), which is obtained from the generating functional technique (Dokshitzer, Khoze, Mueller, and Troian, 1991) in the context of angular ordering (Fadin, 1983) of successive emissions of gluons in the process $e^+e^-\to q+\bar{q}+Ng$, where Ng refers to N gluons in the final state: The double logarithms at small z are obtained by summing all processes involving the emission of gluons from parent gluons or the primary quark line because the probability that a gluon $i-1$ emits another gluon i at an angle θ_i and energy E_i is proportional to $a_s(d\theta_i/\theta_i)(dE_i/E_i)$. Since only the largest, double logarithmic, part of the probability is required, the strong ordering condition $(E,\theta)_i\ll(E,\theta)_{i-1}$ is imposed. These successive emissions of gluons from both gluons and the primary quark and antiquark will be described by the DGLAP equation [Eq. (3)] for small z and small z' (because the most important contribution of the integrand to the integral is in the region $z'\simeq z$), where μ_f on the left-hand side is the lower bound of the transverse energy $E_{i-1}\theta_{i-1}$ of the parent parton. However, since $E_i\theta_i\ll E_{i-1}\theta_{i-1}$, the lower bound on the right-hand side for the transverse energy $E_i\theta_i$ of the emitted parton should be chosen to be $z'\mu_f$ instead of μ_f as is done when z and z' are not small,

$$\frac{d}{d\ln\mu_f^2}D(z,\mu_f^2)=\int_z^1\frac{dz'}{z'}a_s(z'^2\mu_f^2)P^{(0)}(z')D\left(\frac{z}{z'},z'^2\mu_f^2\right).\tag{160}$$

At low z and z', $P^{(0)}(z')$ can be approximated by its double logarithm, where the right-hand side of Eq. (160) reduces to the first term in Eq. (159). The second term in Eq. (159) accounts for the remaining FO part of the evolution.

The quantity $\bar{P}$ is completely constrained by the DGLAP equation. It can be obtained in terms of P order by order in a_s by expanding the operator in Eq. (159) in the form

$$z'^{2(d/d\ln\mu_f^2)}=\exp\left[2\ln z'\frac{d}{d\ln\mu_f^2}\right]=\sum_{n=0}^{\infty}\frac{(2\ln z')^n}{n!}\left(\frac{d}{d\ln\mu_f^2}\right)^n\tag{161}$$

and then repeatedly applying the evolution equations [Eqs. (3) and (5)] to the $(d/d\ln\mu_f^2)^n[a_s(\mu_f^2)D(x/y,\mu_f^2)]$ operations in Eq. (159). For example, to $O(a_s^2)$ (NLO) one finds that

$$\bar{P}(z,a_s)=P(z,a_s)-2C_AA\left[\frac{a_s}{z}+2\beta(a_s)\frac{\ln z}{z}+\int_z^1\frac{dz'}{z'}\frac{2a_s\ln z'}{z'}P\left(\frac{z}{z'},a_s\right)\right]+O(a_s^3).\tag{162}$$

In the square brackets on the right-hand side of Eq. (162), only the first term contributes to the $O(a_s)$ (LO) part of $\bar{P}$, while the second and third terms contribute to the $O(a_s^2)$ part. To this accuracy, the third term is calculated with $P(z,a_s)=a_sP^{(0)}(z)$ (see Appendix C for the explicit functions). From Eq. (162) with P to NLO, we observe that $\bar{P}$ to NLO is free of DLs. The DLs in $P(z,a_s)$ to NLO are given by the NLO expansion of P^{DL},

$$P^{\mathrm{DL}}(z,a_s)=2C_A\frac{A}{z}a_s-4C_A^2\frac{A\ln^2 z}{z}a_s^2+O(a_s^3).\tag{163}$$

In Eq. (159), A is zero whenever D is a nonsinglet FF or valence quark FF. In this case, Eq. (3) implies $\bar{P}=P$, i.e., the splitting functions for such FFs are free of DLs. For $D=(D_\Sigma,D_g)$,

$$A=\begin{pmatrix}0 & \frac{2C_F}{C_A}\\ 0 & 1\end{pmatrix}.\tag{164}$$

Note in general that $A^2=A$, as mentioned earlier.

For consistency, resummation of the DLs in the hard partonic cross sections (i.e., the coefficient functions) of the process under consideration is also necessary. In principle, this has been done for e^+e^- reactions by Mueller (1983a, 1983b), the result being that C_{NS} and C_{PS} are free of DLs while

$$C_g(\omega,a_s)=\frac{2C_F}{C_A}\left[\frac{1}{2}\frac{\omega-\sqrt{\omega^2+16C_Aa_s}}{\sqrt{\omega^2+16C_Aa_s}}\right].\tag{165}$$

The expansion up to NNLO of this result,

$$C_g(\omega,a_s)=\frac{2C_F}{C_A}\left[-4C_A\frac{a_s}{\omega^2}-48C_A^2\left(\frac{a_s}{\omega^2}\right)^2\right], \tag{166}$$

may be compared with the small ω limit of the result of Blümlein and Ravindran (2006),

$$C_g(\omega,a_s)=\frac{2C_F}{C_A}\left[-4C_A\frac{a_s}{\omega^2}+40C_A^2\left(\frac{a_s}{\omega^2}\right)^2\right]. \tag{167}$$

There is clearly agreement at NLO but not at NNLO. The most likely reason is the difference in the choice of scheme or rather, since the DLs should be scheme independent, an ω dependent difference in the choice of normalization of C_g between the two approaches. Further studies of the factorization procedure used by Mueller (1983a, 1983b) are needed here. In any case, the coefficient functions for e^+e^- reactions at LO are free of DLs and so it may be a reasonable approximation to neglect them altogether. This is done in the MLLA, discussed in Sec. VIII.E.

The DLA implies a relation among quark and gluon FFs which simplifies calculations of cross sections. According to Eq. (159) with $\bar{P}$ neglected, which is a reasonable approximation at small z since it is free of DLs, the ratio of $dD_\Sigma/d\ln\mu_f^2$ to $dD_g/d\ln\mu_f^2$ is $2C_F/C_A$, while the operation of $d/d\ln\mu_f^2$ on the nonsinglet and valence quark FFs gives zero in this approximation. Integrating these results over $\ln\mu_f^2$ and neglecting the constants of integration relative to the FFs give

$$D_{q_J}=D_{\bar{q}_{J'}}=(C_F/C_A)D_g, \tag{168}$$

reducing the number of FFs required for the cross section to just one, D_g. Although we will not use Eq. (168) in this section, we consider an application of it in Sec. VIII.D.

The analytic solution to Eq. (159) can be obtained (Albino, Kniehl, Kramer, and Ochs, 2005, 2006) from its Mellin space form,

$$\left(\omega+2\frac{d}{d\ln\mu_f^2}\right)\frac{d}{d\ln\mu_f^2}D=2C_Aa_sAD+\left(\omega+2\frac{d}{d\ln\mu_f^2}\right)\bar{P}D, \tag{169}$$

where for brevity we have written $D=D(\omega,\mu_f^2)$, $a_s=a_s(\mu_f^2)$, and $\bar{P}=\bar{P}(\omega,a_s)$. Substituting Eq. (9) into Eq. (169) gives

$$\left(\omega+2\frac{d}{d\ln\mu_f^2}\right)(P-\bar{P})+2(P-\bar{P})P-2C_Aa_sA=0, \tag{170}$$

where again for brevity $P=P(\omega,a_s)$. Note that at this point we have not assumed anything about P. Thus Eq. (9) can be taken as a definition of P for now, in which case Eq. (170) is simply an alternative way of writing Eq. (169). In particular, $P(\omega,a_s)$ in Eq. (170) must not be seen as an expansion in a_s. To obtain P^{DL}, we split P into its DL and non-DL ($P^{\not{\mathrm{DL}}}$) parts,

$$P=P^{\not{\mathrm{DL}}}+P^{\mathrm{DL}}, \tag{171}$$

then expand Eq. (170) as a series in a_s/ω keeping a_s/ω^2 fixed [as in Eq. (157), noting that $P^{\not{\mathrm{DL}}}$ and $\bar{P}$ are of $O[(a_s/\omega)^2]$, which $\omega=(a_s/\omega)(a_s/\omega^2)^{-1}=O(a_s/\omega)$ and that $a_s=(a_s/\omega)^2(a_s/\omega^2)^{-1}=O[(a_s/\omega)^2]$] and finally extract the first, $O[(a_s/\omega)^2]$, term to find that the constraint on P^{DL} is exactly

$$2(P^{\mathrm{DL}})^2+\omega P^{\mathrm{DL}}-2C_Aa_sA=0. \tag{172}$$

Equation (172) gives two solutions for each component of P. Since P is never larger than a 2×2 matrix in the basis consisting of singlet, gluon, nonsinglet, and valence quark FFs, there are four solutions. The only solution which can be expanded in a_s and which reproduces the DLs in P at LO and NLO, given by

$$P^{\mathrm{DL}}(\omega,a_s)=\begin{pmatrix}0 & a_s\frac{4C_F}{\omega}-a_s^2\frac{16C_FC_A}{\omega^3}\\ 0 & a_s\frac{2C_A}{\omega}-a_s^2\frac{8C_A^2}{\omega^3}\end{pmatrix}+O(a_s^3), \tag{173}$$

is

$$P^{\mathrm{DL}}(\omega,a_s)=(A/4)(-\omega+\sqrt{\omega^2+16C_Aa_s}). \tag{174}$$

Equation (174) agrees with the results of Mueller (1983a, 1983b), which are derived using the conventional renormalization group approach and with the results from the generating functional technique of Dokshitzer, Khoze, Mueller, and Troian (1991). The remainder of P, i.e., $P^{\not{\mathrm{DL}}}$ in Eq. (171), can then be calculated in the FO approach, namely, as a series in a_s with ω fixed, obtained by subtracting the DLs from P in the FO approach, this form of P being already known in the literature to NLO.

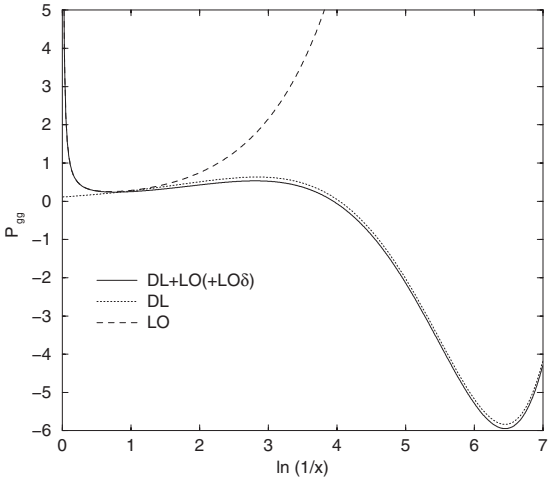

FIG. 34. The gluon splitting function in different approximations. (i) $P_{gg}(z,a_s)$ calculated as in Eq. (175) [labeled DL+LO(+LOδ)]: (ii) $P_{gg}(z,a_s)$ calculated to $O(a_s)$ in the FO approach (labeled LO): and (iii) $P_{gg}^{\mathrm{DL}}(z,a_s)$ (labeled DL). $a_s=0.118/(2\pi)$ and x is z. From Albino, Kniehl, Kramer, and Ochs, 2006.

D. Incorporating the DLA into the DGLAP equation

To a first approximation, the evolution valid for all $\ln(1/z)\leqslant O(a_s^{-1/2})$ takes the form of Eq. (3) with

$$P(z,a_s)=a_sP^{\mathrm{SGL}(0)}(z)+P^{\mathrm{DL}}(z,a_s). \tag{175}$$

Here P^{DL} in z space [the $m=1$ term in Eq. (158)] is given by

$$P^{\mathrm{DL}}(z,a_s)=\frac{A\sqrt{C_Aa_s}}{z\ln\frac{1}{z}}J_1\left(4\sqrt{C_Aa_s}\ln\frac{1}{z}\right), \tag{176}$$

where $J_1(y)$ is the Bessel function of the first kind, which can be calculated from

$$J_1(y)=\frac{1}{\pi}\int_0^\pi d\theta\cos(y\sin\theta-\theta). \tag{177}$$

In Fig. 34, we show that $P_{gg}(z,a_s)$ calculated as in Eq. (175) interpolates well between its $O(a_s)$ approximation in the FO approach, $a_sP_{gg}^{(0)}$, at large z and, $P_{gg}^{\mathrm{DL}}(z,a_s)$, at small z [the small difference here comes from $P^{\mathrm{SGL}(0)}(z)$ at small z]. DL resummation clearly makes a large difference to P at small z.

Higher order calculations in the FO approach with no resummation should extend the validity of the FO calculation of the evolution to smaller z values. However, for sufficiently small z, the improvement to the calculation due to SGL resummation will be better. The reason is that, as z decreases, the order required for the evolution in the FO approach to be reasonably accurate will eventually become higher than the order available. We can use Eq. (176) to illustrate this point. Using the expansion

$$J_1(y)=\frac{y}{2}\sum_{r=0}^{\infty}\frac{(-y^2/4)^r}{r!(r+1)!}, \tag{178}$$

the series for $P^{\mathrm{DL}}(z,a_s)$ in a_s reads

$$P^{\mathrm{DL}}(z,a_s)=\frac{2C_Aa_sA}{z}\sum_{r=0}^{\infty}\frac{(-1)^r}{r!(r+1)!}(4C_Aa_s\ln^2z)^r. \tag{179}$$

The series in Eq. (179) may also be obtained by expanding Eq. (174) to infinite order in a_s. For $z>0$, Eq. (179) converges rapidly at sufficiently large r, but the value of r around which this convergence sets in increases with decreasing z. For example, for $z=0.01$, the accuracy of the series reaches the level of a few percent only at $r=7$, i.e., P in the FO approach would need to be known to $O(a_s^8)$ before evolution at z values as low as $z=0.01$ could be performed.

Using Eq. (174) for P in the DGLAP equation (9) the dependence of the multiplicity in Eq. (154) on s is found to be

$$\langle n^h(s)\rangle\propto\exp\left[\frac{2\sqrt{C_A}}{\beta_0}\frac{1}{\sqrt{a_s(s)}}\right], \tag{180}$$

i.e., the calculation of the s dependence of the multiplicity is finite once the DLs have been resummed. Of course, the DL contribution from the gluon coefficient function has been neglected, but this is probably negligible relative to the LO quark coefficient function.

We now discuss how Eq. (175) was used in the phenomenological studies of Albino, Kniehl, Kramer, and Ochs (2006). From Eqs. (29) (with tagged quarks q_J summed over) and (30), the LO cross section for e^+e^- reactions reads

$$\frac{1}{\sigma(s)}\frac{d\sigma^h}{dx}(x,s)=\frac{1}{n_f\langle Q(s)\rangle}\sum_{J=1}^{n_f}Q_{q_J}(s)D^h_{q_J/\bar{q}_J}(x,\mu_f^2), \tag{181}$$

where $\langle Q(s)\rangle=(1/n_f)\Sigma_{J=1}^{n_f}Q_{q_J}(s)$ is the average electroweak coupling of quarks. Using Eq. (181), fits to e^+e^- reaction data were performed by Albino, Kniehl, Kramer, and Ochs (2006). The initial FFs were parametrized as

$$D_i^h(z,\mu_{f0}^2)=N\exp[-c\ln^2z]z^\alpha(1-z)^\beta \tag{182}$$

because at large z its behavior is similar to Eq. (59) (with $f_i=1$), which has so far sufficed for global fits to large x data, while at small z Eq. (182) reduces, for $c>0$, to a Gaussian in $\ln 1/z$,

$$D_i^h(z,\mu_{f0}^2)\approx N\exp\left[-c\ln^2\frac{1}{z}-\alpha\ln\frac{1}{z}\right], \tag{183}$$

which is the empirical behavior of the cross section at small $x=z$. As shown in Sec. VIII.F, Eq. (183) is also the large μ_{f0} behavior of the FFs predicted by the DLA and MLLA, with $\alpha<0$ to ensure that the center in $\ln 1/x$ is

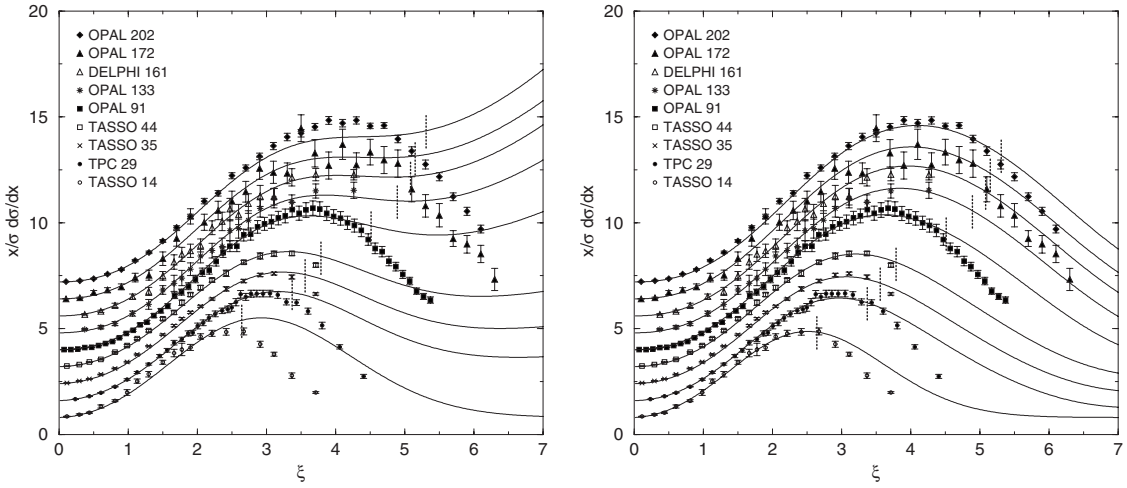

FIG. 35. Fit to data using DGLAP evolution in the FO approach to LO (left) and using DGLAP evolution in the FO approach to LO but with DLs resummed (right). The variable $\xi=\ln 1/x$. Only some of the data sets used for the fit are shown, together with their theoretical predictions from the results of the fit. Data to the right of the horizontal dotted lines have not been used in the fit. Each curve is shifted up by 0.8 for clarity.

at $-\alpha/(2c)>0$. The values of α and c were chosen to be the same for the FFs of all partons, as dictated by the DLA result in Eq. (168). The choice $\mu_f=\sqrt{s}$ was made, as well as the large value $\mu_{f0}=14$ GeV, to ensure that the form of Eq. (183) predicted by the DLA at large μ_{f0} is valid.

Data for unidentified hadron production at e^+e^- reactions over a large range of values of $\sqrt{s}$ were used, being composed of the sets from TASSO at $\sqrt{s}=14,35,44$ (Braunschweig *et al.*, 1990b), and 22 GeV (Althoff *et al.*, 1984), MARK II (Petersen *et al.*, 1988) and TPC (Aihara *et al.*, 1988b) at 29 GeV, TOPAZ at 58 GeV (Itoh *et al.*, 1995), ALEPH (Barate *et al.*, 1998), DELPHI (Abreu *et al.*, 1996), L3 (Adeva *et al.*, 1991), OPAL (Akrawy *et al.*, 1990), and SLC (Abrams *et al.*, 1990) at 91 GeV, ALEPH (Buskulic *et al.*, 1997) and OPAL (Alexander *et al.*, 1996) at 133 GeV, DELPHI at 161 GeV (Ackerstaff *et al.*, 1997), and OPAL at 172, 183, 189 (Abbiendi *et al.*, 2000a), and 202 GeV (Abbiendi *et al.*, 2003). These data also span a wide range in x, from large to small values, as is usually the case with inclusive single hadron production measurements. The level of accuracy of the calculations of Albino, Kniehl, Kramer, and Ochs (2006) was such that the possible contamination of these hadron unidentified data as discussed in Sec. III was not considered a problem. However, such data are probably not suited to a NLO fit because of this possible contamination. The *unresummed* fit, i.e., using $P=a_sP^{(0)}$ in Eq. (3) fails at the small x values around and to the right of the maximum, as shown in Fig. 35 (left). On the other hand, the *resummed* fit, i.e., using Eq. (175) for the splitting functions appearing in the evolution, of Fig. 35 (right) succeeds much better at these small x values, while the large x description remains intact. The fitted value of $\Lambda_{\rm QCD}$ in the unresummed fit was 388 MeV, which is fairly reasonable, but the resummed fit gave $\Lambda_{\rm QCD}=801$ MeV, which is somewhat larger than expected. This may not be serious since $\Lambda_{\rm QCD}$ carries a multiplicative error of $O(1)$: Multiplying $\Lambda_{\rm QCD}$ by a factor is equivalent to dividing the choices above for μ_{f0} and μ_f by this factor, which by factorization scale independence and perturbative convergence is allowed provided that this factor is of $O(1)$.

To further improve the small x description, hadron mass effects were accounted for as discussed in Sec. V.A. The hadron mass was fitted and thus would absorb any other low $\sqrt{s}$, small x effects such as higher twist. In the case of the unresummed fit, the description of all fitted data was as good as the resummed fit of Fig. 35 (right), while the resummed fit did not improve substantially. However, the resummed fit gave the reasonable values $\Lambda_{\rm QCD}=399$ MeV and $m_h=252$ MeV (assuming the hadron sample is composed mostly of $\pi^{\pm}$), while the unresummed fit gave the unreasonable value $\Lambda_{\rm QCD}=1308$ MeV and perhaps slightly too large value $m_h=408$ MeV. Thus the conclusion from these analyses is that both DL resummation and treatment of hadron mass effects are needed in order to achieve a reasonable fitted value of $\Lambda_{\rm QCD}$ and to improve the description of the data at smaller x values.

Calculations with SGLs resummed should be valid down to small x because Eq. (157) is expected to be valid for all ω including as $\omega\to 0$. Thus the small x data may be described by performing the calculation with the complete SL contribution to the evolution and/or the complete DL contribution in the gluon coefficient function. There may, however, also be a discrepancy between the theoretical and experimental definitions of the cross section, such as the effective exclusion, in experiment, of partons emitted outside the jet, which are included in the theoretical calculation. Such effects become more important with decreasing x.

E. The modified leading logarithmic approximation

Equation (3) with P given by Eq. (175) reduces to the MLLA master equation (Dokshitzer and Olsson, 1993), differentiated with respect to the factorization scale (Lupia and Ochs, 1998), if $P^{\not{SGL}(0)}$ in Eq. (175) is replaced, in Mellin space, by its value at $\omega=0$, i.e.,

$$P(\omega,a_s)=a_sP^{\not{SGL}(0)}(\omega=0)+P^{\mathrm{DL}}(\omega,a_s). \tag{184}$$

In discussions of the MLLA, the term

$$P^{\not{SGL}(0)}(\omega=0)=\begin{pmatrix}0 & -3C_F\\ \frac{2}{3}T_Rn_f & -\frac{11}{6}C_A-\frac{2}{3}T_Rn_f\end{pmatrix} \tag{185}$$

is usually referred to as the SL term, as discussed following Eq. (153). At small ω, the accuracy of Eq. (184) is similar to the accuracy of Eq. (175), while for all ω, Eq. (184) is still a better approximation for P than $P=P^{\mathrm{DL}}$ is. By coincidence (Dokshitzer, Khoze, Mueller, and Troian, 1991), Eq. (184) leads to a similar result at large z as Eq. (175) or (4) does. In any case, the approach of Eq. (175) or more generally Eq. (155) incorporates more information than the MLLA, in particular in the large ω region, and should therefore be more accurate.

In many applications of the MLLA, Eq. (168) is used. Together with the gluon component of Eq. (169) with $D=(D_\Sigma,D_g)$, it implies that the gluon FF evolves according to

$$D_g(\omega,\mu_f^2)=E'_{gg}(\omega,a_s(\mu_f^2),a_s(\mu_{f0}^2))D_g(\omega,\mu_{f0}^2), \tag{186}$$

where writing

$$E'_{gg}(\omega,a_s(\mu_f^2),a_s(\mu_{f0}^2))=\exp\left[\int_{M=\mu_{f0}}^{M=\mu_f}d\ln\mu_f^2P'_{gg}(\omega,a_s(\mu_f^2))\right], \tag{187}$$

the splitting function P'_{gg} expanded in the form in Eq. (156) is given by (Dokshitzer, Khoze, Mueller, and Troian, 1991)

$$\begin{aligned}P'_{gg}(\omega,a_s)=&\frac{1}{4}(-\omega+\sqrt{\omega^2+16C_Aa_s})\\&+a_s\left[\left(\frac{11C_A}{6}-\frac{2n_fT_R}{3}\right)\frac{4C_Aa_s}{\omega^2+16C_Aa_s}\right.\\&-\frac{1}{2}\left(\frac{11C_A}{6}+\frac{2n_fT_R}{3C_A^2}\right)\\&\left.\times\left(1+\frac{\omega}{\sqrt{\omega^2+16C_Aa_s}}\right)\right]\\&+O\left(\left(\frac{a_s}{\omega}\right)^3\left(\frac{a_s}{\omega^2}\right)^n\right).\end{aligned} \tag{188}$$

As for P^{DL}, $P'_{gg}(\omega,a_s)$ is finite as $\omega\to0$. Furthermore, Eq. (168) reduces Eq. (181) to

$$\frac{1}{\sigma(s)}\frac{d\sigma^h}{dx}(x,s)=\frac{2C_F}{C_A}D_g(x,s). \tag{189}$$

We have derived these MLLA results using the DLA and the FO approximation results, but they were first derived as a correction to the derivation of the DLA using the generating functional technique mentioned in Sec. VIII.C.

It is often convenient and simpler to study the *moments* of the cross section. The nth moment of a function $f(z)$ is given by

$$K_n=\left(-\frac{d}{d\omega}\right)^n\ln f(\omega)\bigg|_{\omega=0}. \tag{190}$$

According to Eq. (186), the μ_f^2 dependence of the nth moment of $f(z)=D_g(z,\mu_f^2)$ is given by

$$K_n(\mu_f^2)=\Delta K_n(a_s(\mu_f^2),a_s(\mu_{f0}^2))+K_n(\mu_{f0}^2), \tag{191}$$

where $\Delta K_n(a_s(\mu_f^2),a_s(\mu_{f0}^2))$ is the nth moment of $E'_{gg}(z,a_s(\mu_f^2),a_s(\mu_{f0}^2))$, given by

$$\begin{aligned}\Delta K_n(a_s(\mu_f^2),a_s(\mu_{f0}^2))=&\int_{M=\mu_{f0}}^{M=\mu_f}d\ln M^2\left(-\frac{d}{d\omega}\right)^n\\&\times P'_{gg}(\omega,a_s(M^2)).\end{aligned} \tag{192}$$

From Eq. (188), for $n\geqslant1$,

$$\begin{aligned}\Delta K_n(a_s(\mu_f^2),a_s(\mu_{f0}^2))=&a_s^{-(n+1)/2}(\mu_f^2)(C_n^{(0)}+C_n^{(1)}a_s^{1/2}(\mu_f^2)\\&+O(a_s))-\{a_s(\mu_f^2)\leftrightarrow a_s(\mu_{f0}^2)\}.\end{aligned} \tag{193}$$

The explicit results for the $C_n^{(0,1)}$ can be calculated from Eq. (188) and are presented by Fong and Webber (1989) for the first few values of n. For $n\geqslant3$ and odd, $C_n^{(0)}=0$. Equation (193) also applies for $n=0$ but with the presence of a term proportional to $\ln a_s$.

F. Local parton-hadron duality and the limiting spectrum

Perturbative QCD is incomplete in that it cannot describe the physics of hadrons entirely. An intuitive solution to this problem is provided by the LPHD, which states that the distribution of partons in inclusive processes with a sufficiently low energy scale is similar to the distribution of hadrons, up to the number of particles actually produced (the multiplicity). This implies that the hadronic FF is proportional to the partonic FF at a factorization scale of $O(\Lambda_{\mathrm{QCD}})$. In other words, assuming that Eq. (168) is valid at such low scales, we must ensure that our initial gluon FF obeys

$$D_g(z,\mu_{f0}^2)=N\delta(1-z) \tag{194}$$

if we choose $\mu_{f0}=O(\Lambda_{\mathrm{QCD}})$. Ordinarily, evolution at such low scales will not be possible in perturbation theory because the convergence of the perturbation series is spoilt and can even be singular. However, using hypergeometric functions, it is possible to write the MLLA evolution of D_g and therefore the s dependence of the cross section in Eq. (189), such that the calculation is

well defined at $\mu_f=\Lambda_{\rm QCD}$. This calculation is known as the *limiting spectrum*. In this section we show how the limiting spectrum and the result of the LPHD in Eq. (194) arise as accidental consequences of truncated perturbation theory.

According to Eq. (193) and the result $a_s(M^2)\to 0$ as $M\to\infty$, for sufficiently large μ_f we may neglect $K_n(\mu_{f0}^2)$ relative to $\Delta K_n(a_s(\mu_f^2),a_s(\mu_{f0}^2))$ except for $n=0$ because the cross section is sensitive to $N=\exp[K_0(\mu_{f0}^2)]$. From Eq. (190) with $f(z)=D_g(z,\mu_{f0}^2)$ and $K_n(\mu_{f0}^2)=0$ for $n\geqslant 1$, we see that $D_g(z,\mu_{f0}^2)$ takes the form in Eq. (194). In other words, at high energies it appears as if the initial FF at low energy is a delta function (Albino, Kniehl, and Kramer, 2004), even though it could be a different function.

The second, μ_{f0} dependent, part of K_n in Eq. (193) may also be neglected relative to the first, μ_f dependent, part for sufficiently large μ_f because in this limit $a_s(\mu_f^2)\ll a_s(\mu_{f0}^2)$. Coincidentally, because $a_s(M^2)\to\infty$ as $M\to\Lambda_{\rm QCD}$, the neglect of the second, μ_{f0} dependent, part of K_n Eq. (193) is equivalent to choosing $\mu_{f0}=\Lambda_{\rm QCD}$, provided that the series in $a_s^{1/2}$ is terminated at $O(a_s^{n/2})$ because the next term will be finite and the terms following that will be singular. In other words, at high energies, it appears as if the choice $\mu_{f0}=\Lambda_{\rm QCD}$ is justified (Albino, Kniehl, and Kramer, 2004) even though it is in fact not.

We conclude that the LPHD and limiting spectrum in the context of hadron production can only be verified using low energy data because their consequences at high energy are also implied by perturbation theory alone.

With the two approximations above, Eq. (191) finally becomes

$$K_n(\mu_f^2)\approx\Delta K_n(a_s(\mu_f^2),\infty)\quad\text{for } n\geqslant 1, \tag{195}$$

which are the moments of the limiting spectrum. Equation (195) implies an interesting large μ_f behavior of the gluon FF and hence, from Eq. (168), of all quark FFs. The inverse Mellin transform of the gluon FF,

$$zD_g(z,\mu_f^2)=\frac{1}{2\pi i}\int_C d\omega\exp[\omega\xi]D_g(\omega,\mu_f^2), \tag{196}$$

where $\xi=\ln(1/z)$, may by making the replacement $y=i\omega\sigma$ where $\sigma^2=K_2(\mu_f^2)$, be written as

$$zD_g(z,\mu_f^2)=\frac{\mathcal{N}}{\sigma\sqrt{2\pi}}\exp\left[-\frac{\delta^2}{2}\right]R(\delta,\{\kappa_n\}), \tag{197}$$

where $\mathcal{N}=\exp[K_0(\mu_f^2)]$ [so that $\mathcal{N}(\mu_{f0}^2)=N$ in Eq. (194)], $\delta=(\xi-\bar{\xi})/\sigma$ with $\bar{\xi}=K_1(\mu_f^2)$ as the average value of ξ, the real quantity R is given by

$$R(\delta,\{\kappa_n\})=\frac{e^{\delta^2/2}}{\sqrt{2\pi}}\int_{-\infty}^{\infty}dy\exp\left[\sum_{n=3}^{\infty}\kappa_n\frac{(-iy)^n}{n!}\right]\times\exp\left[iy\delta-\frac{y^2}{2}\right], \tag{198}$$

and

$$\kappa_n=\frac{K_n(\mu_f^2)}{K_2^{n/2}(\mu_f^2)}=a_s^{(n-2)/4}(\mu_f^2)[1+O(a_s^{1/2}(\mu_f^2))]. \tag{199}$$

Equation (193) has been used for the second equality in Eq. (199). Because of that property, we can expand the κ_n-dependent exponential in Eq. (198) in powers of the κ_n up to the required accuracy and perform the integral for each term. Then, writing R as an exponential of the form

$$R=\exp\left[\sum_{i=0}^{\infty}A_i\delta^i\right], \tag{200}$$

we find that the series in the exponent will terminate at a finite value of i when it is expanded in a_s to some finite order even if $\delta=O(1)$. In particular, if $\kappa_n=0$ for $n\geqslant 3$, which is always a reasonable approximation because of Eq. (199), then all $A_i=0$ so that $R=1$. Therefore, from Eq. (197) the gluon FF at large μ_f and therefore the cross section at large $\sqrt{s}$ will be a (distorted) Gaussian over the range from large to small x. This justifies the choice for the small z behavior of Eq. (183) used for the FFs in the fits of Albino, Kniehl, Kramer, and Ochs (2006).

IX. OUTLOOK

A. Possible experimental results for the future

Accurate measurements of light charged and neutral hadron production at HERA are now possible. As noted by Albino, Kniehl, Kramer, and Sandoval (2007) and Jung *et al.* (2008), such data in which the hadron species is identified, which do not yet exist and which may only be possible for short lived particles such as the neutral hadrons K_S^0 and $\Lambda/\bar{\Lambda}$, would make a significant improvement to the current knowledge of FFs. In particular, such data together with data from e^+e^- reactions already used in global fits could significantly improve the flavor separation of the FFs for each hadron species if the ep reaction data are in similar kinematic regions to the e^+e^- ones and the validity of the quark tagging often performed in measurements of e^+e^- reactions can be studied. By identification of the charge of the detected hadrons as well, perhaps the greatest improvement to the current constraints on FFs that ep reaction data could provide is on the valence quark FFs, which at present are only constrained by similar but relatively much less accurate data from RHIC. The accurate set of measurements from BaBar (Anulli, 2004) mentioned in Sec. VII.C should appear in the next year or so and will provide much needed constraints on FFs at large z that are not provided by any current data sets. Because these data are taken at a different $\sqrt{s}$ to that of the currently most accurate data, which is at $\sqrt{s}=91.2$ GeV, such data will also significantly improve the constraints on $\alpha_s(M_Z)$. In addition, new more accurate pp reaction data are being taken at RHIC which includes larger p_T values than before and hence will also improve the large z con-

straints. Furthermore, the inclusion of these BaBar data in global fits could help to determine whether there are any general problems with the factorization framework at large x, a possibility suggested by the inconsistency found between high energy (ALEPH and OPAL) and low energy (Belle and CLEO) data for charmed meson production (Cacciari, Nason, and Oleari, 2006; Kneesch, Kniehl, Kramer, and Schienbein, 2008).

In the further future, accurate results for e^+e^- reactions may be extracted from the raw data taken at CLEO, Belle, and LEP. The constraints on valence quark FFs could also be improved by measurements of the asymmetric cross section in e^+e^- reactions. Further ep reaction data could be taken at the proposed eRHIC and LHeC colliders. Finally, measurements of pp reactions at the LHC, which at present could be obtained from the first run at $\sqrt{s}=900$ GeV, would likely be of sufficiently high accuracy to significantly improve the FF constraints.

B. Future theoretical input to global fits

A number of improvements which global fits may benefit from are possible, and we list those which are most likely to be available first:

(1) The inclusion of heavy quarks and heavy quark masses in the partonic cross sections.

(2) The application of large x resummation to pp reaction calculations for a finite rapidity range and also for ep reactions both with and without cuts in p_T.

(3) The calculation of the NNLO off-diagonal splitting functions, as well as the NNLO partonic cross sections in ep and pp reactions.

(4) The calculation of the full DL contribution to the gluon coefficient function in e^+e^- reactions data, and possibly further SGLs here, and in the splitting functions, with the incorporation of these improvements in global fits to e^+e^- reaction data including more of the data at small x that have previously been excluded. The resummation of the same classes of SGLs in other types of processes may also be beneficial if there exist measurements of those processes whose calculations would improve due to the resummation.

Of course, a simultaneous treatment of the above improvements simultaneously in a single global fit would be an additional goal, but one which is further into the future.

Global fits of FFs can be further improved by fitting other quantities not determinable in perturbation theory, such as higher twist contributions, intrinsic FFs, fracture functions, and the modifications associated with hadronic decay channels, whose fitted results would contribute significantly to the current knowledge of QCD physics.

X. SUMMARY

We have given a comprehensive account of important methods and results in the phenomenological extraction of FFs from experimental data. Many FF components for many particles are now well constrained. FFs have been useful in the study of other phenomena and in the extraction of other physical quantities, some examples are given in Sec. I, and the number and intensity of such applications is expected to increase as the constraints on FFs improve. The best constraints on FFs at present come from e^+e^- reaction data. However, these data do not constrain the valence quark FFs (or charge asymmetry FFs), and to a large degree the gluon FF, which can be at least weakly constrained by current data from RHIC. Theoretically, calculations of inclusive single hadron production in all reactions that have been performed experimentally can be calculated to NLO, and the effects of large x resummation in e^+e^- reactions and heavy quarks effects in all reactions can be included at this level of accuracy. The deviation of the fitted detected hadron mass from its true value gives a quantification of how important the production of this particle from decays of heavier hadrons instead of from direct partonic fragmentation. We note here that the production of particles such as pions from direct partonic fragmentation only could be determined in the future by subtracting the contribution to pion production coming from the decays of resonances such as ρ, K^*, ϕ, etc., which requires measuring the production of these resonances. In global fits, systematic errors are now accounted for through a covariance matrix, and various sound approaches for propagating experimental errors from measurements to predictions have been applied.

There is a lot of room for improvement in this program, perhaps the most important being the eventual incorporation in global fits of future accurate measurements of hadron production at HERA in which both the species and charge of the hadrons are measured in order to significantly improve the constraints on the differences between FFs of different quark flavors (the nonsinglet quark FFs) and of different quark charges (the valence quark FFs), respectively. Such FF components are currently constrained by intuitive but experimentally untested nonperturbative assumptions. A significant improvement in the extraction of $\alpha_s(M_Z)$ would also result from such fits relative to previous fits. Because of the theoretical similarity between charge summed data from e^+e^- and ep reactions, further tests on FF universality would also result from the inclusion of hadron species identified data from HERA in global fits together with data from e^+e^- reactions.

Note that FF universality tests are provided by the inclusion of $pp(\bar{p})$ reaction data but, because of their much lower accuracy, to a much lesser degree than by the inclusion of ep reaction data. At present, $pp(\bar{p})$ reaction data are crucial for the extraction of the currently badly constrained gluon and valence quark FFs, and therefore future accurate measurements from RHIC and LHC will be most welcome. We note that the con-

straints on these FFs could also be significantly improved by measurements of the longitudinal and asymmetric cross sections (with hadron species identification, of course) in e^+e^- reactions, respectively.

ACKNOWLEDGMENTS

I thank G. Kramer for a thorough reading of the paper and J. C. Collins for valuable discussions and criticisms concerning Appendix A.

APPENDIX A: DERIVATION OF THE QCD FACTORIZATION THEOREM

In this appendix, we discuss the factorization theorem applied to inclusive single hadron production. That is, we show how such processes can be calculated in the form in Eq. (1), where the hard partonic cross sections $d\sigma^i$ and the μ_f^2 dependence of the universal FFs D_i^h are perturbatively calculable, i.e., are nonsingular and remain so as the first n_f quark masses vanish and/or the remaining quark masses approach infinity. We restrict our discussion to the process $e^+e^- \to \gamma^* \to h+X$ of Fig. 2, although it can be applied to other inclusive single hadron production processes. This cross section can be decomposed as

$$d\sigma = L^{\mu\nu} W_{\mu\nu}, \tag{A1}$$

where $L^{\mu\nu}$ is the well-known tensor describing the process $e^+e^- \to \gamma^*$ (we work to LO in QED), while the tensor

$$W_{\mu\nu}(q,p_h) = \frac{1}{2\pi} \int d^4x e^{iqx} \langle 0|J_\mu(x) a_h^\dagger(p_h)|X\rangle \times \langle X|a_h(p_h) J_\nu(0)|0\rangle, \tag{A2}$$

where $a_h^{(\dagger)}(p_h)$ is the annihilation (creation) operator for a hadron h with momentum p_h (we do not assume a massless hadron in this appendix) describes the hadronic process $\gamma^* \to h+X$ and is the quantity in which we are interested. W may be partially calculated using perturbation theory by decomposing it into the form (omitting the space-time indices $\mu\nu$ for brevity)

$$W = wD + r, \tag{A3}$$

where the remainder r is *power suppressed*, i.e.,

$$r = O((\Lambda_{\rm QCD}/\sqrt{s})^p), \tag{A4}$$

w is a vector of the equivalent, factorized, full partonic processes w_i [where the parton species label i includes (combinations of) the spin state(s) and charge(s) as discussed in Sec. II.F] for the processes $\gamma^* \to i+X$ and D is a vector of factorized FFs D_i. Equation (A3) is then the same as Eq. (1). The "product" wD involves sums and integrations over all species of the "detected" final state parton of w, which is a real particle moving spatially parallel to the detected hadron. Note that the momentum integration is precisely the convolution of Eq. (1), i.e., over the momentum fraction z and not over all four components of momentum. In the language of the OPE (Georgi and Politzer, 1974; Gross and Wilczek, 1974; Floratos, Ross, and Sachrajda, 1977; Buras, 1980; Reya, 1981; Sterman, 1995; Weinberg, 1996; Moch and Vermaseren, 2000), Eq. (A3) corresponds to a twist expansion, the term wD being referred to as the leading twist component. The variable $p \geqslant 1$ in Eq. (A4), so at large enough energy the higher twist terms are smaller than the radiative corrections of $O(1/\ln\sqrt{s})$.

In the remainder of this appendix, we outline the formal derivation of the factorization theorem of Collins (1998b), where full details and more references may be found. In Appendix A.1, we outline the steps given by Collins (1998b) for separating the nonleading twist part, whose order of magnitude can be reliably estimated from the cross section such that it is suitable for factorization. In Appendix A.2, we discuss the factorization approach of Collins (1998b), which is essentially a generalization of former approaches. Then, in Appendix A.3, we connect it with the older factorization approach of Ellis, Georgi, Machacek, Politzer, and Ross (1978, 1979), Curci, Furmanski, and Petronzio (1980), and Furmanski and Petronzio (1980, 1982). Because the manner in which a parton should be treated in factorization depends on the magnitude of its mass relative to the hard scale, different schemes are appropriate for different energies and therefore, in Appendix A.5, we discuss matching conditions between quantities in these different schemes. However, we note there that the correct treatment of quarks with mass much greater than the hard scale has not been specified so far, and we indicate how this may be remedied. Finally, in Appendix A.6, we summarize the open issues remaining in the factorization theorem.

1. Twist expansion

For now, assume that all partons have masses less than or of the order of the hard scale $\sqrt{s}$. We return to the case that there are also quarks with masses much greater than $\sqrt{s}$ in Appendix A.4. Collins (1998b) derived the form of Eq. (A3) for DIS, $eh \to e+X$ (in which case D is a vector of PDFs), by starting from an expansion in graphs which are two-particle irreducible (2PI), i.e., cannot be disconnected by cutting through two internal lines, in the t channel and then using the result that all graphs that contribute at leading twist are two-particle reducible (Libby and Sterman, 1978a, 1978b). There are many subtleties involved in getting to this result; see Sec. IV.A of Collins (1998b) for details and references. By repeating these arguments but with the negative virtuality of the exchanged boson replaced with positive virtuality and the incoming hadron replaced with an outgoing hadron, one obtains the factorized form of the cross section $e^+e^- \to \gamma^* \to h+X$. The expansion is shown in Fig. 36 which, using the shorthand $1+K_0+K_0^2+\cdots = 1/(1-K_0)$, may be represented as

$$W = C_0 \frac{1}{1-K_0} T_0 + B. \tag{A5}$$

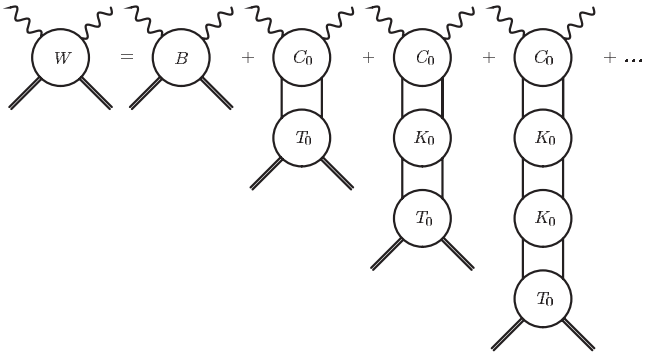

FIG. 36. 2PI t-channel expansion of the cross section for $e^+e^- \to \gamma^* \to h+X$ (with the electron and positron legs removed for simplicity). The left-hand side is the modulus squared of the amplitude shown in Fig. 2, i.e., the external wavy legs represent the virtual photon γ^* and the external double lines the detected hadron h. On the right-hand side, the lines between 2PI graphs are virtual partons in loops (i.e., summed and integrated over all quantum numbers). C_0 and K_0 represent all 2PI t-channel contributions to the processes $\gamma^* \to j+X$ and $i \to j+X$, respectively. B and T_0 represent all 2PI t-channel contributions to $\gamma^* \to h+X$ and $j \to h+X$, where in this case 2PI must be defined by nonperturbative external field methods. Strictly speaking, all graphs have a cut down the middle signifying the final state and on which all particles must be real. Alternatively, we may forget the cut if these graphs may be regarded as forward amplitudes, whose imaginary component also gives the cross section as dictated by the optical theorem.

As it stands, Eq. (A5) is no use for practical calculations. First, T_0 and B contain hadron legs for which no perturbative or other analytic representation exists. Second, perturbation theory cannot be applied even to calculate the equivalent purely partonic cross section $C_0/(1-K_0)$: In general, each parton species contributes potential mass singularities, which are logarithms of each parton mass that becomes singular as that mass approaches zero. The potential mass singularities of any quark then will not be singular if all quarks are taken to be massive, but they will be large if this quark's mass m_i is much less than $\sqrt{s}$, i.e., in the limit that this mass be neglected. However, neglecting the mass m_i of a parton i should only introduce a relative error of $O(m_i^2/s)$ on the cross section as dictated by the *decoupling theorem* (Appelquist and Carazzone, 1975). In fact, because the potential mass singularities are raised to a power that increases with the order in a_s, for sufficiently large s they will cause the perturbative calculation to diverge. Third, the products in Eq. (A5) are rather complicated, containing sums and integrations over all virtual partons connecting 2PI graphs, which we call connecting partons. To tackle the second and third problems, we begin with the observation that, in a physical gauge such as the light-cone gauge, which we use from now on, the 2PI graphs are free of potential mass singularities (Ellis, Georgi, Machacek, Politzer, and Ross, 1978, 1979), which therefore arise from those connecting partons which are in the vicinity of being real, i.e., on shell and with physical spin, and moving spatially parallel to the

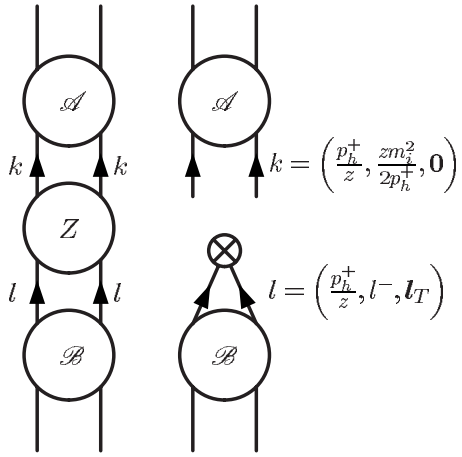

FIG. 37. The action of Z on the connecting partons of mass m_i between any graphs $\mathcal{A}$ and $\mathcal{B}$. The momentum integration is over the variables z, l^-, and $\mathbf{l}_T$.

detected hadron. These 2PI graphs are also free of UV singularities after renormalization of the strong coupling and quark masses. Thus we introduce a projection operator $Z=Z^2$ which projects onto the connecting partons in a manner which includes all those partons with momenta responsible for the potential mass singularities. The operator $1-Z$ therefore annihilates the potential mass singularity between any two 2PI graphs. Now we give one explicit definition of such an operator. We use light-cone coordinates (defined in Appendix B) and work in a frame for which the detected hadron's momentum is given by Eq. (97) and the virtual boson's momentum by Eq. (96). Considering only massless partons for simple illustration, mass singularities arise from connecting partons with physical spins and physical momenta obeying

$$k = (p_h^+/z, 0, \mathbf{0}). \tag{A6}$$

Then

$$Z_{\alpha\alpha';\beta,\beta'}(k,l) = \tfrac{1}{4}\gamma^-_{\alpha\alpha'}\gamma^+_{\beta\beta'}(2\pi)^4\delta(k^+ - l^+)\delta(k^-)\delta^{(2)}(\boldsymbol{k}_T) \tag{A7}$$

and something similar for gluons. Note that Eq. (A7) is consistent with the projection operator property $Z=Z^2$. The extension of Eq. (A7) to massive quarks (we assume all quarks' and the detected hadron's masses are nonnegligible) is quite straightforward, in particular the $-$ component of Eq. (A6) becomes $zm_i^2/(2p_h^+)$ and the mass singularities become potential mass singularities. Like K_0, Z can be regarded as a graph with two partons at the top, each with momentum k, and two with momentum l at the bottom. As shown in Fig. 37, the insertion of Z between two graphs reduces the sums and integrations in the product between them to an integration over z of the pair of connecting partons at the bottom of the top graph, which have momenta given by Eq. (A6), i.e., they are on shell, and an integration over the momenta l^- and $\boldsymbol{l}_T$ of the pair of connecting partons at the top of the bottom graph, whose $+$ component of mo-

mentum is the same as that in Eq. (A6), i.e., $l^+=p_h^+/z$. This is the case, for example, in the product between wD in Eq. (A3)—in practice it is usually not necessary to show explicitly the l^- and $\boldsymbol{l}_T$ integrations over the initial state partons in D.

The Z operator is used to put Eq. (A5) into the form of Eq. (A3) in Sec. V.B of Collins (1998b), where the remainder r is shown to be power suppressed [i.e., to obey Eq. (A4)]. A general graph such as W, containing a hard and a soft scale such as $\sqrt{s}$ and $\Lambda_{\rm QCD}$, respectively, will in general contain a leading region, i.e., a part which is not power suppressed, coming from graphs which can be expressed as a graph coupled to the hard scale, called the hard graph, joined to a graph coupled to the soft scale, called the soft graph, by two real partons of mass much less than the hard scale (Libby and Sterman, 1978a, 1978b) which are collinear to the detected hadron. Being 2PI, B does not contain such graphs and therefore does not contain a leading region, i.e., it is power suppressed. This will not be the case in a general gauge because additional gluon exchanges between the hard and soft graphs are allowed. However, it is assumed, without proof, that a suitable light-cone gauge exists such that such graphs are power suppressed. At least this is known to be true for the $A^+=0$ gauge used and in the case that these gluons' momenta are almost collinear with the detected hadron's. In the leading region, lines in the hard graph will have much larger virtualities than lines in the soft graph, from which we conclude that, again in the leading region, all lines in a 2PI graph must have similar virtualities to one another. Since Z projects out connecting partons which are real and collinear to the detected hadron, a $1-Z$ insertion between two graphs removes the contribution to the leading region, so the result is of order (highest virtuality in graph below to lowest virtuality in graph above)^p (Collins, 1998b). Successive insertions of $1-Z$ between all 2PI graphs in Eq. (A5) will give successive factors of this suppression leading an overall power suppression. Consequently,

$$r = C_0(1-Z)\frac{1}{1-K_0(1-Z)}T_0 + B \tag{A8}$$

obeys Eq. (A4), so r may be taken to represent all higher twist terms in W. All potential mass singularities in r are annihilated by the $1-Z$ insertions. All UV singularities in r cancel: in the quantity $(1-Z)/[1-K_0(1-Z)]$, the action on partons from the left with Z introduces a UV singularity, which is then canceled by the power-suppressing $1-Z$ factors in essentially the same way as these factors remove the potential mass singularities. The leading twist component of W is therefore $W-r$, which we now factorize in order to express it in its familiar form in Eq. (A3).

2. The modern approach to factorization

The approach to factorization of Collins (1998b) considered in this section is a generalization of previous approaches such as the OPE. Most importantly, it implicitly uses the cut vertices (Mueller, 1978, 1981) and nonlocal operators (Balitsky and Braun, 1989, 1991) that were necessary in modifying the Wilson expansion in local operators on the light cone, which can be applied to, e.g., the time ordered product of currents appearing in $ep\to e+X$ to the time ordered product of currents appearing in $e^+e^-\to h+X$, which is subtle due to its nonlocal operator structure. The result that $r=O((\Lambda_{\rm QCD}/Q)^2)$, i.e., that $p=2$ in Eq. (A3), found by Balitsky and Braun (1989, 1991), using an expansion in nonlocal operators, should be obtainable using the approach of Collins (1998b). Using the Z operator, Eq. (A5) may be rewritten in the form

$$W - r = w_B D_B. \tag{A9}$$

In this expression, the vector

$$w_B = C_0\frac{1}{1-(1-Z)K_0}Z \tag{A10}$$

contains the equivalent "UV bare" (containing UV divergences) partonic processes. It is clearly free of potential mass singularities. Note that the "detected" parton is real due to the presence of Z on the right-hand side. The UV bare FFs

$$D_B = Z\frac{1}{1-K_0}T_0 \tag{A11}$$

appearing in Eq. (A9) describe the fragmentation of partons. Clearly, D_B contains all processes contributing to the process $i\to h+X$ (i is in fact a virtual parton, but its $+$ component of momentum is fixed to that of the real parton lines at the top of Z, while its remaining components are integrated over) and may therefore be written as a matrix element of unrenormalized operators. In a general gauge, it is given by (Collins and Soper, 1981, 1982; Collins, 1993)

$$D^h_{Bq_I}(z) = \frac{z^{d-3}}{4\pi}\int dx^- e^{-iP^+x^-/z}\frac{1}{3}\mathrm{tr}_{\rm color}\frac{1}{3}\mathrm{tr}_{\rm spin}\left\{\gamma^+\langle 0|\psi^{(0)}_{q_I}(0,0,\mathbf{0})\bar{\mathcal{T}}\exp\left[ig^{(0)}\int_0^\infty dy^- A_a^{(0)+}(0,y^-,\mathbf{0})t_a^T\right]\right.$$
$$\left.\times a_h^\dagger(P^+,0,\mathbf{0})a_h(P^+,0,\mathbf{0})\mathcal{T}\exp\left[-ig^{(0)}\int_{x^-}^\infty dy^- A_a^{(0)+}(0,y^-,\mathbf{0})t_a^T\right]\bar{\psi}^{(0)}_{q_I}(0,x^-,\mathbf{0})|0\rangle\right\}, \tag{A12}$$

for a quark of flavor q_I, where ψ_{q_I} is the spinor field for quarks of flavor I, g is the strong coupling, $t_a=\lambda_a/2$ where λ_a are the Gell-Mann matrices, and A_a^μ is the field for gluons of color charge a. The operator $\mathcal{T}(\bar{\mathcal{T}})$ orders the field operators $A_a^+(0,y^-,0)$ in the products in each term of the exponential expansion in g such that an operator is always to the left (right) of any other operator with a lower (higher) value of y^-. The superscript (0) on $\psi_{q_I}^{(0)}$ implies that the operator (e.g., $\psi_{q_I}^{(0)}$) or quantity (e.g., $g^{(0)}$) is unrenormalized. The expression for the gluon FF is similar, obtained essentially by replacing $\psi_{q_I}^{(0)}$ everywhere with the gluon field strength tensor. The Wilson lines are not present in Eq. (A12) in the $A^+=0$ gauge that we have been using, i.e., the exponentials are equal to unity. Their direct derivation involves going beyond the 2PI expansion in a nontrivial way. Since the UV divergences of the bare operators are subtracted by ordinary multiplicative renormalization, the renormalized FFs take the form

$$D = GD_B, \tag{A13}$$

where $G=GZ$ renormalizes UV divergences in the operator in D_B in the standard way of operator renormalization [see, e.g., Peskin and Schroeder (1995)] and therefore introduces a dependence of D on some operator renormalization scale μ_f. G is nonsingular as parton masses vanish, as shown later [in the text following Eq. (A25)]. Dimensional regularization is necessary to implement the CWZ schemes (Collins, Wilczek, and Zee, 1978), in which case G will be singular as the number of dimensions approaches 4. As usual in operator renormalization, the dependence of G on μ_f is governed by the renormalization group equation

$$dG/d\ln\mu_f^2 = PG, \tag{A14}$$

where the components of the matrix P are the relevant perturbatively calculable anomalous dimensions for the operators in D_B and are known as splitting functions. Therefore from Eq. (A13),

$$dD/d\ln\mu_f^2 = PD, \tag{A15}$$

which is the DGLAP equation. In studies using the OPE, Eq. (A15) appears in Mellin space, where the Mellin space variable N is an integer equal to the spin of the given operator in the OPE, which is equivalent to Eq. (A15) in z space just derived by applying the inverse Mellin transform of Eq. (D5).

We finally arrive at Eq. (A3) from Eq. (A9) by making the identity

$$w = w_B G^{-1}, \tag{A16}$$

where G^{-1} is defined such that $GG^{-1}=Z$. Since w_B and G are free of potential mass singularities, so are the factorized partonic processes w. In practice, w can be calculated as follows: we may write

$$w_0 = w_B K_B, \tag{A17}$$

where

$$w_0 = C_0 \frac{1}{1-K_0} Z \tag{A18}$$

is the equivalent partonic process in which the detected parton is real. Because w_0 is a matrix element of unrenormalized operators, it is free of UV divergences after renormalization of the coupling constant. However, w_0 contains potential mass singularities. The quantities represented by

$$K_B = Z \frac{1}{1-K_0} Z \tag{A19}$$

are the bare FFs for partons to fragment to partons. They are renormalized in the same way as D_B defined in Eq. (A11) was in Eq. (A13),

$$\Gamma = GK_B, \tag{A20}$$

which is nonsingular as the regulator of UV singularities is removed, but is singular as any parton masses vanish. Note that K_B and Γ are written by Collins (1998b), as A_{Bp} and A_{Rp}, respectively. Then, instead of calculating w via Eq. (A16), w may be explicitly calculated from w_0 according to

$$w = w_0 \Gamma^{-1}, \tag{A21}$$

where Γ^{-1} is defined such that $\Gamma\Gamma^{-1}=\Gamma^{-1}\Gamma=Z$. Equation (A21), which is equivalent to Eq. (65) of Collins (1998b) (after expanding in a_s), makes it clear that the purpose of Γ is to remove from w_0 the potential mass singularities. In other words, each potential mass singularities in w_0 is canceled by *counterterms* in Γ. Γ may be chosen, through the choice of G and Z in Eq. (A20), to depend on parton masses only through mass logarithms, which will be the case for the CWZ schemes (Collins, Wilczek, and Zee, 1978). The precise form of this Γ [Eq. (A34)] will be derived later.

To summarize, w and the μ_f dependence of D are perturbatively calculable. The components of w are the standard coefficient functions up to electroweak couplings, etc. Like D_B, the factorized FFs D in Eq. (A26) are universal since all details of the initial state are contained in C_0.

3. Connection with the older approach to factorization

Finally, we make some connections between the above approach and the earlier approach of Ellis, Georgi, Machacek, Politzer, and Ross (1978, 1979), Curci, Furmanski, and Petronzio (1980), and Furmanski and Petronzio (1980, 1982). The latter approach was formulated for the case of massless quarks only, so we need to make some modifications to these earlier approaches to account for massive quarks as well. In addition, our definitions of bare FFs will need to differ from the earlier approach in order to obtain reliable results. We begin with an alternative to Eq. (A9) which corresponds to the starting point of calculations in the literature [i.e., Eq. (A21)],

$$W - r = w_0 D_0, \tag{A22}$$

where the "bare" FF in this case is

$$D_0 = Z \frac{1}{1 - K_0(1 - Z)} T_0, \tag{A23}$$

which is free of UV singularities because the UV singularity introduced by acting from the left with Z is canceled by $1-Z$ insertions occurring to the right, similar to the cancellation of UV singularities in r discussed in the text following its definition in Eq. (A8). We define a projection operator $\mathcal{P}=\mathcal{P}^2$ which projects in the same way as Z on parton lines above (so that $Z\mathcal{P}=\mathcal{P}$) and which projects in a similar way as Z on parton lines below except that, in contrast to Z, it becomes sufficiently suppressed for increasing momenta of these lines such that it does not introduce UV singularities. The scale at which this suppression sets in is called the factorization scale, which is written as μ_f since it will turn out to be identical to the operator renormalization scale defined above. Thus, for example, we may choose $\mathcal{P}$ (in the case of massless quarks for simplicity) to be given by Eq. (A7) multiplied by a function $f(k^-/\mu_f, \mathbf{k}_T/\mu_f)$ such that $f(0,0)=1$ and $f(\infty,\infty)=0$. A more explicit definition of $\mathcal{P}$ (or f) is not required since an implicit definition will be given later. Note that, like Z, $\mathcal{P}$ is flavor diagonal. As a projection operator, $\mathcal{P}^2=\mathcal{P}$, and insertion of $1-\mathcal{P}$ between two 2PI graphs annihilates the potential mass singularity due to the connecting partons.

The momentum dependence of $\mathcal{P}$ can lead to problems with gauge invariance and with rapidity divergences (Collins, 2003, 2008). Such problems were not considered by Ellis, Georgi, Machacek, Politzer, and Ross (1978, 1979), Curci, Furmanski, and Petronzio (1980), and Furmanski and Petronzio (1980, 1982), which were limited to the case of massless quarks. We assume that some suitable choice for the remaining degrees of freedom in $\mathcal{P}$ exists such that these problems do not arise in the case of massive quarks. Further work is needed here to prove that such a $\mathcal{P}$ exists.

The dependence of Γ, which was introduced in Eq. (A20), on $\mathcal{P}$ is

$$\Gamma = \left(1 + \mathcal{P} K_0 \frac{1}{1 - K_0}\right) Z, \tag{A24}$$

which can be interpreted as the FFs for hard partons fragmenting to on-shell soft partons. Using Eq. (A20), we may write

$$G = \left(1 + (\mathcal{P} - Z) K_0 \frac{1}{1 - (1 - Z) K_0}\right) Z, \tag{A25}$$

i.e., G is free of potential mass singularities because, in the $\mathcal{P}-Z$ operator, those potential mass singularities projected out by Z are identical to those projected out by $\mathcal{P}$. This behavior was noted just after Eq. (A13). According to Eqs. (A3) and (A21), the factorized FFs defined in Eq. (A13) may also be written as

$$D = \Gamma D_0. \tag{A26}$$

Using Eq. (A21), the hard partonic cross section in terms of $\mathcal{P}$ reads

$$w = C_0 \frac{1}{1 - (1 - \mathcal{P}) K_0} Z, \tag{A27}$$

which is free of both UV singularities and potential mass singularities. $\Gamma = Z\Gamma = \Gamma Z$ is a function only of the ratio of the + component of light-cone momenta of its initial and final partons, as well as of parton masses and indices. By giving this function explicitly, Eq. (A24) defines $\mathcal{P}$ implicitly. The simplest possible choice for Γ, which occurs for the CWZ schemes (Collins, Wilczek, and Zee, 1978), is when the coefficients in the perturbative series for Γ are themselves finite series in $\ln \mu_f^2/m_i^2$, where i runs over all partons. Although the gluon mass must be zero for renormalizability, connecting gluons can be given a small mass after renormalization has been performed within the 2PI graphs. Although the perturbative approximation for Γ fails in the numerical sense, its μ_f dependence does not because

$$d\Gamma/d \ln \mu_f^2 = P\Gamma, \tag{A28}$$

where the splitting functions

$$P = \left(\frac{d}{d \ln \mu_f^2} \mathcal{P}\right) K_0 \frac{1}{1 - (1 - \mathcal{P}) K_0} Z \tag{A29}$$

are free of UV and potential mass singularities. This is obviously true since the perturbatively calculable w must obey a similar equation to Eq. (A28) in order for Eq. (A3), in particular wD, to be independent of μ_f. Thus, when Γ is chosen to depend on parton masses only through finite powers of potential mass singularities, as discussed in the text preceding Eq. (A28), P will be independent of all parton masses. The DGLAP equation (A15) may be obtained from Eqs. (A26) and (A28).

4. Treatment of nonpartonic quarks

Up to this point, all results are only valid when no parton mass is much greater than $\sqrt{s}$. Because the potential mass singularities of quarks with mass much greater than $\sqrt{s}$ are power suppressed by $O(s/m_i^2)$, where m_i is the mass of any such quark, they must not be subtracted by a large counterterm, i.e., they must be treated differently. Thus partons must be distinguished according to how they are treated: the partons that are treated as discussed in the last three sections are called *active* partons, while the rest, which should include those for which $m_i \gg \sqrt{s}$, are called *nonpartonic* quarks. Note that a quark for which $m_i = O(\sqrt{s})$ can be treated as either active or nonpartonic since its potential mass singularities and their corresponding counterterms are not large. We define the 2PI graphs to be 2PI in nonpartonic quarks as well. The choice of Z on nonpartonic quarks must be that r remains both power suppressed and free of UV singularities; i.e., Z on nonpartonic quarks must

be that the arguments around Eq. (A8) still hold. Choosing $Z=0$ when acting on nonpartonic quark lines as is done by Collins (1998b) leads to UV singularities in r and therefore is not a valid possibility. One possibility which is valid is to choose $Z(k,l)$ when the magnitude of l is large to behave in the same way on nonpartonic quark lines as on active quark lines, i.e., to choose Eq. (A7) to hold for nonpartonic quarks as well, thus guaranteeing the cancellation of UV divergences in r, while the $Z(k,l)$ on nonpartonic quark lines vanishes as l becomes small both to guarantee the power suppression of r and to ensure that no large counterterms are introduced for potential mass singularities due to nonpartonic quarks, which are suppressed or not large. In other words, Z on nonpartonic quark lines may be chosen in a similar way to how $\mathcal{P}$ acting on active quark lines was in the text following Eq. (A23), except that now $f(k^-/\mu_f,\boldsymbol{k}_T/\mu_f)$ is replaced with another function, $g(k^-/\mu_f,\boldsymbol{k}_T/\mu_f)$ say, where μ_f is another arbitrary scale at which the suppression of Z acting on nonpartonic quark lines sets in, which obeys $g(0,0)=0$ and $g(\infty,\infty)=1$. In this case, Z would no longer be a projection operator and r is now scheme and scale dependent; i.e., it depends on the number of flavors and on μ_f. Neither of these two facts presents any problems. However, as noted in the text preceding Eq. (A24), introducing a momentum dependence into a projection operator can lead to problems with gauge invariance and with rapidity divergences, so further work is needed to prove that a Z exists for which these problems do not arise.

The other types of potential mass singularity that a nonpartonic quark contributes, namely, logarithms of its mass m_{q_I} that become singular as $m_{q_I}\gg\sqrt{s}$, are absorbed into the strong coupling constant in, e.g., a CWZ scheme (Collins, Wilczek, and Zee, 1978). Note that for active partons, for which $m_i\ll\sqrt{s}$, such logarithms are power suppressed by $O(m_i^2/s)$.

5. Matching conditions

Next we consider the relation or *matching conditions* between D and w, in schemes that differ by the number of active partons. For simplicity, we choose Z on nonpartonic quark lines to be the same as Z on active quark lines [i.e., the massive quark equivalent of Eq. (A7)]. Note that in this case r is free of UV singularities but is no longer power suppressed. Then, in the presence of nonpartonic quarks, all results derived so far still hold except that the sum over partons in all products such as that in Eq. (A3) includes nonpartonic quarks. In certain physical schemes, defined in Sec. II.G such as the CWZ schemes (Collins, Wilczek, and Zee, 1978) in which no subtraction is made on quantities which are free of UV singularities, G depends on nonpartonic quark masses only and is singular as such masses vanish (recall from Appendix A.2 that G is nonsingular as active parton masses vanish), while Γ is independent of nonpartonic quark masses. When acting on nonpartonic quark lines, $\mathcal{P}$ must be chosen such that it does not introduce large counterterms to cancel power suppressed potential mass singularities, e.g., $\mathcal{P}$ can be chosen to vanish on nonpartonic quark lines.

Taking all previous factorized quantities to be defined for n_f active quark flavors and using primes to denote quantities defined with n_f+1 active quark flavors, Eq. (A13) implies that the matching conditions for FFs and coefficient functions are

$$D' = AD \tag{A30}$$

and

$$w' = wA^{-1}, \tag{A31}$$

respectively, where $A=G'G^{-1}=\Gamma'\Gamma^{-1}$ is a function only of the ratio of the $+$ component of light-cone momenta of its initial and final partons, as well as of parton masses and indices. Diagrammatically it is given by

$$A = Z\left[1+(\mathcal{P}'-\mathcal{P})\frac{1}{1-K_0(1-\mathcal{P})}K_0\right]Z. \tag{A32}$$

Note that A remains nonsingular as the regulator of UV singularities is removed, in contrast to G, and, as for G, contains no potential mass singularities due to active parton masses. G can be chosen such that A depends on nonpartonic quark masses only and only through mass logarithms. This is the case in the CWZ schemes (Collins, Wilczek, and Zee, 1978). Recall that some modifications of our incomplete results are needed to ensure that r is properly power suppressed. Again, similar to P above, if Γ is chosen to have the simplest possible form as discussed in the text preceding Eq. (A28), the only parton mass that A can depend on is m_{n_f+1}. Since the series for K_0 starts at $O(a_s)$, since $\mathcal{P}'-\mathcal{P}$ projects out a potential mass singularity from the (n_f+1)th quark, and since n factors of K_0 contain $n-1$ pairs of connecting partons and therefore a product of $n-1$ potential mass singularities, A in Mellin space and as a matrix in parton species can be chosen to take the simplest form

$$A(N,\mu_f^2) = 1+\sum_{n=1}^{\infty} a_s^n(\mu_f^2)\sum_{m=0}^{n} A_m^{(n)}(N)\ln^m\frac{\mu_f^2}{m_{n_f+1}^2}. \tag{A33}$$

From this we obtain the simplest possible form for Γ,

$$\Gamma = \prod_{i=0}^{n_f}\left(1+\sum_{n=1}^{\infty} a_s^n(\mu_f^2)\sum_{m=0}^{n} A_m^{(n)}(N)\ln^m\frac{\mu_f^2}{m_i^2}\right). \tag{A34}$$

In practice, $A_m^{(n)}$ are chosen such that w in Eq. (A21) is finite in the limit that active parton masses vanish (although these limits do not of course need to be taken in the actual cross section calculations). The CWZ scheme (Collins, Wilczek, and Zee, 1978) is obtained by choosing $A_m^{(n)}$ such that w in Eq. (A21) reduces to the $\overline{\text{MS}}$ scheme for a theory with n_f massless flavors only in the limits that active parton masses vanish and nonpartonic masses approach infinity (which again do not need to be taken in actual applications).

In calculations of light hadron production, it may or may not be possible to neglect the contribution of intrin-

sic fragmentation, namely, the nonpartonic components in the product in Eq. (A3). In the case of PDFs, according to the decoupling theorem those graphs that contain a nonpartonic quark i will be suppressed by a power of $\Lambda_{\rm QCD}/m_i$ (Witten, 1976), which is therefore the relative error on the cross section due to the neglect of the intrinsic PDF of parton i. If such a suppression also occurs for FFs then as for PDFs D_{n_f+1} can be neglected, in which case Eq. (A30) implies that D'_{n_f+1} is determined entirely from the D_i for $i=0,\ldots,n_f$. This component of D'_{n_f+1} describes the extrinsic fragmentation of parton n_f+1. However, the results of Witten (1976) only apply to the case of local operators, such as those relevant to DIS, but not necessarily to FFs for which nonlocal operators must be used, as mentioned. If the intrinsic fragmentation of a nonpartonic quark is deemed important (e.g., charm fragmentation in a three flavor scheme), calculations would need to be made in which Z acting on nonpartonic lines takes the form discussed in Appendix A.4 that leads to a power suppressed remainder r. In the meantime, a quark whose intrinsic fragmentation is large must be treated as an active parton, with an intrinsic FF that can be fitted to experimental data as is the case for the light partons and thus $\sqrt{s}$ cannot be too small relative to its mass.

6. Open issues

We have given a summary of the current status of factorization which was developed by Collins (1998b). This approach both generalizes earlier approaches and solves a number of issues therein. However, some issues remain. In particular, the necessary modification proposed here to the behavior of Z on nonpartonic quark lines given by Collins (1998b) as well as our proposed relations between the results of Collins (1998b) and those of the earlier approach of Ellis, Georgi, Machacek, Politzer, and Ross (1978, 1979) Curci, Furmanski, and Petronzio (1980), and Furmanski and Petronzio (1980, 1982) in terms of $\mathcal{P}$ need more explicit study in order to ensure that there are no problems with gauge invariance or rapidity divergences, which are a general consequence of momentum dependent projection operators. Furthermore, while it has been proved that graphs in which there is an exchange between the hard and soft graphs of gluons collinear to the detected hadron are power suppressed, a proof is lacking for the cases where these gluons are not collinear.

APPENDIX B: MOMENTUM FRACTION

The light-cone momentum fraction x of the detected particle h plays a central role in the factorization theorem as the scaling variable of single hadron inclusive production processes. Specifically, defining light-cone coordinates $V=(V^+=(V^0+V^3)/\sqrt{2}, V^-=(V^0-V^3)/\sqrt{2}, \boldsymbol{V}_T=(V_1,V_2))$ for any vector V, x is the fraction of the available+component of momentum that h carries away from some process, i.e.,

TABLE III. Summary of the measurements for inclusive single $\pi^{\pm}$ production in e^+e^- reactions. The column labeled "# data" gives the number of data for which $x \geqslant 0.05$. The last column refers to the normalization uncertainty on the data.

Collaboration	Tagging	$\sqrt{s}$ (GeV)	# data	Norm. (%)
TASSO[a]	Untagged	12	5	20
TASSO[b]	Untagged	14	10	8.5
TASSO[b]	Untagged	22	1	6.3
HRS[c]	Untagged	29	6	
TPC[d]	l tagged	29	9	
TPC[d]	c tagged	29	9	
TPC[d]	b tagged	29	9	
TPC[e]	Untagged	29	27	
TASSO[a]	Untagged	30	4	20
TASSO[f]	Untagged	34	10	6
TASSO[f]	Untagged	44	7	6
TOPAZ[g]	Untagged	58	8	
ALEPH[h]	Untagged	91.2	22	3
DELPHI[i]	l tagged	91.2	17	
DELPHI[i]	b tagged	91.2	17	
DELPHI[i]	Untagged	91.2	17	
OPAL[j]	u tagged	91.2	5	
OPAL[j]	d tagged	91.2	5	
OPAL[j]	s tagged	91.2	5	
OPAL[j]	c tagged	91.2	5	
OPAL[j]	b tagged	91.2	5	
OPAL[k]	Untagged	91.2	20	
SLD[l]	l tagged	91.2	28	
SLD[l]	c tagged	91.2	28	
SLD[l]	b tagged	91.2	28	
SLD[l]	Untagged	91.2	28	
DELPHI[m]	Untagged	189	3	
Total			338	

[a] Brandelik, (TASSO Collaboration), 1980.
[b] Althoff, (TASSO Collaboration) (1983).
[c] Derrick, (HRS Collaboration) (1987).
[d] Aihara, (TPC/Two-Gamma Collaboration) (1987); Lu (1986).
[e] Aihara, (TPC/Two-Gamma Collaboration) (1988a, 1988b).
[f] Braunschweig, (TASSO Collaboration) (1989a).
[g] Itoh, (TOPAZ Collaboration) (1995).
[h] Buskulic, (ALEPH Collaboration) (1995a).
[i] Abreu, (DELPHI Collaboration) (1998).
[j] Abbiendi, (OPAL Collaboration) (2000c).
[k] Akers, (OPAL Collaboration) (1994).
[l] Abe, (SLD Collaboration) (2004).
[m] Abreu, (DELPHI Collaboration) (2000).

$$x = (p_{3h} + E_h)/(p_{3h\,\max} + E_{h\,\max}). \tag{B1}$$

Here E_h is the particle's energy, $p_{h3}>0$ its z component of the spatial momentum $\mathbf{p}_h$, and the subscript max refers to the maximum value that the variable can take, in other words the amount of this variable available to the particle. For example, in $e^+e^-\to h+X$ reactions, E_h is

TABLE IV. As in Table III, but for $K^{\pm}$.

Collaboration	Tagging	$\sqrt{s}$ (GeV)	# data	Norm. (%)
TASSO[a]	Untagged	12	3	20
TASSO[b]	Untagged	14	9	8.5
TASSO[b]	Untagged	22	7	6.3
HRS[c]	Untagged	29	7	
MARKII[d]	Untagged	29	2	12
TPC[e]	Untagged	29	26	
TASSO[a]	Untagged	30	2	20
TASSO[f]	Untagged	34	5	6
TOPAZ[g]	Untagged	58	5	
ALEPH[h]	Untagged	91.2	18	3
DELPHI[i]	l tagged	91.2	17	
DELPHI[i]	b tagged	91.2	17	
DELPHI[i]	Untagged	91.2	17	
OPAL[j]	u tagged	91.2	5	
OPAL[j]	d tagged	91.2	5	
OPAL[j]	s tagged	91.2	5	
OPAL[j]	c tagged	91.2	5	
OPAL[j]	b tagged	91.2	5	
OPAL[k]	Untagged	91.2	10	
SLD[l]	l tagged	91.2	28	
SLD[l]	c tagged	91.2	28	
SLD[l]	b tagged	91.2	28	
SLD[l]	Untagged	91.2	28	
DELPHI[m]	Untagged	189	3	
Total			286	

[a]Brandelik, (TASSO Collaboration), 1980.
[b]Althoff, (TASSO Collaboration) (1983).
[c]Derrick, (HRS Collaboration) (1987).
[d]Schellman, (MARK II Collaboration) (1985).
[e]Aihara, (TPC/Two-Gamma Collaboration) (1988a, 1988b).
[f]Braunschweig, (TASSO Collaboration) (1989a).
[g]Itoh, (TOPAZ Collaboration) (1995).
[h]Barate, (ALEPH Collaboration) (1998a); Buskulic, (ALEPH Collaboration) (1995a).
[i]Abreu, (DELPHI Collaboration) (1998).
[j]Abbiendi, (OPAL Collaboration) (2000c).
[k]Akers, (OPAL Collaboration) (1994).
[l]Abe, (SLD Collaboration) (2004).
[m]Abreu, (DELPHI Collaboration) (2000).

TABLE V. As in Table III, but for $p/\bar{p}$.

Collaboration	Tagging	$\sqrt{s}$ (GeV)	# data	Norm. (%)
TASSO[a]	Untagged	12	3	20
TASSO[b]	Untagged	14	9	8.5
TASSO[b]	Untagged	22	9	6.3
HRS[c]	Untagged	29	7	
TPC[d]	Untagged	29	20	
TASSO[a]	Untagged	30	3	20
JADE[e]	Untagged	34	2	14
TASSO[f]	Untagged	34	7	6
TOPAZ[g]	Untagged	58	5	
ALEPH[h]	Untagged	91.2	18	3
DELPHI[i]	l tagged	91.2	17	
DELPHI[i]	b tagged	91.2	17	
DELPHI[i]	Untagged	91.2	17	
OPAL[j]	u tagged	91.2	5	
OPAL[j]	d tagged	91.2	5	
OPAL[j]	s tagged	91.2	5	
OPAL[j]	c tagged	91.2	5	
OPAL[j]	b tagged	91.2	5	
OPAL[k]	Untagged	91.2	10	
SLD[l]	l tagged	91.2	29	
SLD[l]	c tagged	91.2	29	
SLD[l]	b tagged	91.2	29	
SLD[l]	Untagged	91.2	29	
DELPHI[m]	Untagged	189	3	
Total			289	

[a]Brandelik, (TASSO Collaboration), 1980.
[b]Althoff, (TASSO Collaboration) (1983).
[c]Derrick, (HRS Collaboration) (1987).
[d]Aihara, (TPC/Two-Gamma Collaboration) (1988a, 1988b).
[e]Bartel, (JADE Collaboration) (1981).
[f]Braunschweig, (TASSO Collaboration) (1989a).
[g]Itoh, (TOPAZ Collaboration) (1995).
[h]Barate, (ALEPH Collaboration) (1998a); Buskulic, (ALEPH Collaboration) (1995a).
[i]Abreu, (DELPHI Collaboration) (1998).
[j]Abbiendi, (OPAL Collaboration) (2000c).
[k]Akers, (OPAL Collaboration) (1994).
[l]Abe, (SLD Collaboration) (2004).
[m]Abreu, (DELPHI Collaboration) (2000).

maximal when $X=\bar{h}$, so that the energy available to the particle is $E_{h\,\max}=\sqrt{s}/2$. Other convenient "momentum" fractions can be defined, such as the fraction of available energy

$$x_E = E_h/E_{h\,\max}, \tag{B2}$$

which for $e^+e^-\to h+X$ reactions is then $2E_h/\sqrt{s}$, and the ratio of the particle's spatial momentum to the available energy

$$x_p = |\mathbf{p}_h|/E_{h\,\max}, \tag{B3}$$

which for $e^+e^-\to h+X$ reactions is then $2|\mathbf{p}_h|/\sqrt{s}$. If the hadron's mass can be neglected, $x_E=x_p=x=p_h/p_{h\,\max}$. Note that the definitions of x_E and x_p in Eqs. (B2) and (B3) are frame dependent. Although the definition of x in Eq. (B1) is also frame dependent, it is invariant with respect to boosts in the 3-direction since in that case $\pm$components change by the same factor.

APPENDIX C: LEADING ORDER SPLITTING FUNCTIONS

The LO coefficients of the splitting functions are given by

TABLE VI. As in Table III, but for K_S^0.

Collaboration	Tagging	$\sqrt{s}$ (GeV)	# data	Norm. (%)
TASSO[a]	Untagged	14	8	15
TASSO[b]	Untagged	14.8	8	
TASSO[b]	Untagged	21.5	5	
TASSO[a]	Untagged	22	5	15
HRS[c]	Untagged	29	12	
MARK II[d]	Untagged	29	17	12
TPC[e]	Untagged	29	7	
TASSO[f]	Untagged	33.3	7	15
TASSO[a]	Untagged	34	13	15
TASSO[b]	Untagged	34.5	13	
CELLO[g]	Untagged	35	9	
TASSO[b]	Untagged	35	13	
TASSO[b]	Untagged	42.6	13	
TOPAZ[h]	Untagged	58	4	
ALEPH[i]	Untagged	91.2	16	2
DELPHI[j]	Untagged	91.2	13	
OPAL[k]	u tagged	91.2	5	
OPAL[k]	d tagged	91.2	5	
OPAL[k]	s tagged	91.2	5	
OPAL[k]	c tagged	91.2	5	
OPAL[k]	b tagged	91.2	5	
OPAL[l]	Untagged	91.2	16	6
SLD[m]	l tagged	91.2	9	
SLD[m]	c tagged	91.2	9	
SLD[m]	b tagged	91.2	9	
SLD[m]	Untagged	91.2	9	
DELPHI[n]	Untagged	183	2	
DELPHI[n]	Untagged	189	3	
Total			252	

[a]Althoff, (TASSO Collaboration) (1985).
[b]Braunschweig, (TASSO Collaboration) (1990a).
[c]Derrick, (HRS Collaboration) (1987).
[d]Schellman, (MARK II Collaboration) (1985).
[e]Aihara, (TPC/Two-Gamma Collaboration) (1984).
[f]Brandelik (TASSO Collaboration) (1981).
[g]Behrend, (CELLO Collaboration) (1990).
[h]Itoh, (TOPAZ Collaboration) (1995).
[i]Barate, (ALEPH Collaboration) (1998a).
[j]Abreu, (DELPHI Collaboration) (1995).
[k]Abbiendi, (OPAL Collaboration) (2000c).
[l]Abbiendi, (OPAL Collaboration) (2000a).
[m]Abe, (SLD Collaboration) (1999).
[n]Abreu, (DELPHI Collaboration) (2000).

$$P_{\Sigma\Sigma}^{(0)}(z) = C_F\left(-1-z+2\left[\frac{1}{1-z}\right]_+ + \frac{3}{2}\delta(1-z)\right),$$

$$P_{\Sigma g}^{(0)}(z) = 2C_F\frac{1+(1-z)^2}{z}, \tag{C1}$$

TABLE VII. As in Table III, but for $\Lambda/\bar{\Lambda}$.

Collaboration	Tagging	$\sqrt{s}$ (GeV)	# data	Norm. (%)
TASSO[a]	Untagged	14	3	20
TASSO[a]	Untagged	22	4	20
HRS[b]	Untagged	29	12	
MARK II[c]	Untagged	29	15	
TASSO[d]	Untagged	33.3	6	15
TASSO[a]	Untagged	34	6	20
TASSO[e]	Untagged	34.8	9	9
CELLO[f]	Untagged	35	7	
TASSO[g]	Untagged	42.1	4	9
ALEPH[h]	Untagged	91.2	16	4
DELPHI[i]	Untagged	91.2	7	
OPAL[j]	u tagged	91.2	5	
OPAL[j]	d tagged	91.2	5	
OPAL[j]	s tagged	91.2	5	
OPAL[j]	c tagged	91.2	5	
OPAL[j]	b tagged	91.2	5	
OPAL[k]	Untagged	91.2	12	
SLD[l]	l tagged	91.2	4	
SLD[l]	c tagged	91.2	4	
SLD[l]	b tagged	91.2	4	
SLD[l]	Untagged	91.2	9	
DELPHI[m]	Untagged	183	3	
DELPHI[m]	Untagged	189	3	
Total			145	

[a]Althoff, (TASSO Collaboration) (1985).
[b]Baringer, (HRS Collaboration) (1986a).
[c]de la Vaissiere, (MARK II Collaboration) (1985).
[d]Brandelik (TASSO Collaboration) (1981).
[e]Braunschweig, (TASSO Collaboration) (1989b).
[f]Behrend, (CELLO Collaboration) (1990).
[g]Braunschweig, (TASSO Collaboration) (1989a).
[h]Barate, (ALEPH Collaboration) (1998a).
[i]Abreu, (DELPHI Collaboration) (1993).
[j]Abbiendi, (OPAL Collaboration) (2000c).
[k]Alexander, (OPAL Collaboration) (1997).
[l]Abe, (SLD Collaboration) (1999).
[m]Abreu, (DELPHI Collaboration) (2000).

$$P_{g\Sigma}^{(0)}(z) = T_R n_f[z^2+(1-z)^2],$$

$$P_{gg}^{(0)}(z) = 2C_A\left(\frac{1}{z}-2+z-z^2+\left[\frac{1}{1-z}\right]_+\right) + \left(\frac{11}{6}C_A - \frac{2}{3}T_R n_f\right)\delta(1-z),$$

where $T_R=1/2$ and, for the color gauge group SU(3), $C_A=3$ and $C_F=4/3$. The $[f(z)]_+$ operation occurs often in perturbative calculations and can be most usefully defined by its behavior in a convolution (in which it will always appear)

$$\int_x^1 \frac{dz}{z}[f(z)]_+ D\left(\frac{x}{z}\right) = \int_x^1 \frac{dz}{z} f(z)\left[D\left(\frac{x}{z}\right) - zD(x)\right] - D(x)\int_0^x dz f(z) \tag{C2}$$

for any functions $f(z)$ and $D(z)$. Supposing that $f(z)$ may contain a singularity as $z \to 1$ but nowhere else, Eq. (C2) is nonsingular provided $f(z)$ is less singular than $1/(1-z)^2$ because the quantity in square brackets in the first integral on the right-hand side falls to zero as fast as $1-z$ in this limit. On the other hand, without the $[\,]_+$ operation, Eq. (C2) is only nonsingular provided $f(z)$ is less singular than $1/(1-z)$. By choosing $D(z)=z^{-N}$, removing the common factor x^{-N}, and then replacing the lower limit of the integration on the left-hand side with 0, we find the Mellin transform of $[f(z)]_+$ to be

$$\{[f(z)]_+\}(N) = \int_0^1 dz(z^{N-1}-1)f(z). \tag{C3}$$

Transforming Eq. (C1) to Mellin space gives

$$\begin{aligned} P_{\Sigma\Sigma}^{(0)}(N) &= C_F\left[\frac{3}{2} + \frac{1}{N(N+1)} - 2S_1(N)\right], \\ P_{\Sigma g}^{(0)}(N) &= 2C_F\frac{N^2+N+2}{(N-1)N(N+1)}, \\ P_{g\Sigma}^{(0)}(N) &= T_R n_f \frac{N^2+N+2}{N(N+1)(N+2)}, \\ P_{gg}^{(0)}(N) &= 2C_A\left[\frac{11}{12} + \frac{1}{N(N-1)} + \frac{1}{(N+1)(N+2)} - S_1(N)\right] - \frac{2}{3}T_R n_f, \end{aligned} \tag{C4}$$

where for integer N, the harmonic sum

$$S_1(N) = \sum_{k=1}^{N} \frac{1}{k}. \tag{C5}$$

Equation (C5) can be analytically continued to complex $N \neq -1, -2, \ldots$ (Albino, Kniehl, and Kramer, 2005) by making the replacement $\Sigma_{k=1}^{N} \to \Sigma_{k=1}^{\infty} - \Sigma_{k=N+1}^{\infty}$ and then making the replacement $k \to k-N$ in the second sum. The result is

$$S_1(N) = \sum_{k=1}^{\infty} \frac{N}{k(k+N)}. \tag{C6}$$

This sum converges but rather slowly. For numerical work, $S_1(N)$ should be calculated using the result (Albino, Kniehl, and Kramer, 2005)

$$S_1(N) = S_1(N+r) - \sum_{k=1}^{r} \frac{1}{k+N}, \tag{C7}$$

which follows from Eq. (C5), where r should be chosen such that $|N+r|$ is large and then calculating $S_1(N+r)$ as an expansion in $1/(N+r)$ (Abramowitz and Stegun, 1965; Albino, 2009).

APPENDIX D: MELLIN SPACE

Any succession of convolutions, which may be written as

$$f(z) = \int_z^1 \frac{dz_1}{z_1}\int_{z_1}^1 \frac{dz_2}{z_2}\cdots\int_{z_{n-2}}^1 \frac{dz_{n-1}}{z_{n-1}} f_1\left(\frac{z}{z_1}\right) \times f_2\left(\frac{z_1}{z_2}\right)\cdots f_{n-1}\left(\frac{z_n}{z_{n-1}}\right) f_n(z_{n-1}), \tag{D1}$$

is converted by the Mellin transform, defined by the integral transformation

TABLE VIII. As in Table III, but for $pp(\bar{p})$ reactions. In the case of the BRAHMS data, the values in brackets are the normalization errors below 3 GeV.

Collaboration	Rapidity	$\sqrt{s}$ (GeV)	# data	Norm. (%)
	$y \in [2.9,3]$		8	11,7,8(13),2,1(3)
BRAHMS[a]	$y \in [3.25,3.35]$	200	7	
PHENIX[b] (π^0)	$\lvert\eta\rvert < 0.35$	200	13	9.7
STAR[c] (π^0)	$\eta = 3.3$	200	4	16
STAR[c] (π^0)	$\eta = 3.8$	200	2	16
STAR[d]	$\lvert y\rvert < 0.5$	200	10	11.7
Total			44	

[a] Arsene, (BRAHMS Collaboration) (2007).
[b] Adler, (PHENIX Collaboration) (2003b).
[c] Adams, (STAR Collaboration) (2006b).
[d] Adams, (STAR Collaboration) (2006a).

TABLE IX. As in Table VIII, but for $K^{\pm}$.

Collaboration	Rapidity	$\sqrt{s}$ (GeV)	# data	Norm. (%)
	$y \in [2.9,3]$		8	11,7,8(13),2,1(3)
BRAHMS[a]	$y \in [3.25,3.35]$	200	6	
CDF[b] (K^0_S)	$\lvert\eta\rvert<1$	630	37	10
STAR[c] (K^0_S)	$\lvert y\rvert<0.5$	200	9	11.7
Total			60	

[a]Arsene, (BRAHMS Collaboration) (2007).
[b]Acosta, (CDF Collaboration) (2005).
[c]Adams, (STAR Collaboration) (2006a).

$$f(N) = \int_0^1 \frac{dz}{z} z^N f(z), \tag{D2}$$

into an analytically more manageable succession of products

$$f(N) = f_1(N) f_2(N) \cdots f_n(N). \tag{D3}$$

Equation (D3) is most easily proved by applying the Mellin transform to an alternative form of Eq. (D1),

$$f(z) = \int_0^1 dz_1 \int_0^1 dz_2 \cdots \int_0^1 dz_n \delta(z - z_1 z_2 \cdots z_n) \times f_1(z_1) f_2(z_2) \cdots f_n(z_n). \tag{D4}$$

The Mellin transform is invertible via the inverse Mellin transform

$$f(z) = \frac{1}{2\pi i} \int_C dN z^{-N} f(N), \tag{D5}$$

where C is a contour in complex N space which starts from a point at $\mathrm{Im}(N) = -\infty$, ends at a point at $\mathrm{Im}(N) = \infty$, and passes to the right of all poles in $f(N)$. According to Cauchy's theorem, the contour C may be deformed provided that it does not pass through any poles in the process. The numerical evaluation of the integration in Eq. (D5) converges fastest when a contour for which $\mathrm{Re}(-N) \to \infty$ is used because then z^{-N} falls exponentially to zero along it.

Often in a convolution of two functions,

TABLE X. As in Table VIII, but for $p(\bar{p})$.

Collaboration	Rapidity	$\sqrt{s}$ (GeV)	# data	Norm. (%)
	$y \in [2.9,3]$		7	
BRAHMS[a]	$y \in [3.25,3.35]$	200	5	11,7,8(13),2,1(3)
STAR[b]	$\lvert y\rvert<0.5$	200	8	11.7
Total			20	

[a]Arsene, (BRAHMS Collaboration) (2007).
[b]Adams, (STAR Collaboration) (2006a).

TABLE XI. As in Table VIII, but for K^0_S.

Collaboration	Rapidity	$\sqrt{s}$ (GeV)	# data	Norm. (%)
($K^{\pm}$)	$y \in [2.9,3]$		8	
BRAHMS[a]	$y \in [3.25,3.35]$	200	6	11,7,8(13),2,1(3)
CDF[b]	$\lvert\eta\rvert<1$	630	48	
STAR[c]	$\lvert y\rvert<0.5$	200	9	11.7
Total			71	

[a]Arsene, (BRAHMS Collaboration) (2007).
[b]Acosta, (CDF Collaboration) (2005).
[c]Adams, (STAR Collaboration) (2006a).

$$g(z) = \int_z^1 \frac{dz'}{z'} g_1(z') g_2\left(\frac{z}{z'}\right) = \frac{1}{2\pi i} \int_C dN z^{-N} g_1(N) g_2(N), \tag{D6}$$

the analytic Mellin transform of one of these functions, g_1 say, may not be calculable. [Note that Eq. (D6) includes the cases of multiple convolutions in Eq. (D1) since g_1 can be equated with a subset of the convolutions in Eq. (D1) and g_2 with the rest.] An example is the $F^i_{h_1 h_2}$ appearing in Eq. (92). In this case the Mellin transform of $g_1 = F^i_{h_1 h_2}$ may be performed numerically but only after dealing with a subtlety: Eq. (D2) with $f \to g_1$ implies that the second equality in Eq. (D6) has a divergent contribution proportional to $\int_C dN (z/z')^{-N} g_2(N)$ whenever $0 < z' < z$ if the contour C is chosen as discussed. However, inspection of the first equality in Eq. (D6) reveals that $f(z)$ is independent of $g_1(z')$ in this region. Thus $g_1(N)$ in the second equality in Eq. (D6) must be replaced with the modified Mellin transform

$$g_1(N;z) = \int_z^1 \frac{dz'}{z'} z'^N g_1(z'). \tag{D7}$$

It can sometimes happen that the analytic Mellin transform of the other function, g_2, cannot also be obtained. Unfortunately, Eq. (D7) cannot be used to also calculate the Mellin transform of g_2 because then the inverse Mellin transform does not converge: as well as Eq. (D7), assume a second result which is the same as Eq. (D7) but with $g_1 \to g_2$ and $z' \to z''$. Then Eq. (D6) has a divergent

TABLE XII. As in Table VIII, but for $\Lambda/\bar{\Lambda}$.

Collaboration	Rapidity	$\sqrt{s}$ (GeV)	# data	Norm. (%)
CDF[a]	$\lvert\eta\rvert<1$	630	34	10
STAR[b]	$\lvert y\rvert<0.5$	200	9	11.7
Total			43	

[a]Acosta, (CDF Collaboration) (2005).
[b]Abelev, (STAR Collaboration) (2007).

contribution proportional to $\int_C dN(z/z'z'')^{-N}$ from the region $z'z''<z$, which exists even though $z'>z$ and $z''>z$. One solution is instead to approximate g_2 in z space as, e.g., an expansion in Chebyshev polynomials and then analytically Mellin transform it.

APPENDIX E: SUMMARY OF INCLUSIVE SINGLE HADRON PRODUCTION MEASUREMENTS

Here we list all $\pi^{\pm}$, $K^{\pm}$, $p/\bar{p}$, K_S^0, and $\Lambda/\bar{\Lambda}$ data which can be reasonably reliably calculated and which are therefore suitable for global fits.

1. e^+e^- reactions

Tables III–VII show a summary of the measurements for inclusive $\pi^{\pm}$ reactions.

2. $pp(\bar{p})$ reactions

Tables VIII–XII show a summary of the measurements for inclusive $\pi^{\pm}$ production in $pp(\bar{p})$ reactions.

REFERENCES

Aaron, F. D., *et al.* (H1 Collaboration), 2007, Phys. Lett. B **654**, 148.
Abbiendi, G., *et al.* (OPAL Collaboration), 2000a, Eur. Phys. J. C **16**, 185.
Abbiendi, G., *et al.* (OPAL Collaboration), 2000b, Eur. Phys. J. C **17**, 373.
Abbiendi, G., *et al.* (OPAL Collaboration), 2000c, Eur. Phys. J. C **16**, 407.
Abbiendi, G., *et al.* (OPAL Collaboration), 2003, Eur. Phys. J. C **27**, 467.
Abe, K., *et al.* (SLD Collaboration), 1999, Phys. Rev. D **59**, 052001.
Abe, K., *et al.* (SLD Collaboration), 2004, Phys. Rev. D **69**, 072003.
Abelev, B. I., *et al.* (STAR Collaboration), 2007, Phys. Rev. C **75**, 064901.
Abramowitz, M., and I. A. Stegun, 1965, *Handbook of Mathematical Functions with Formulas (Graphs and Mathematical Tables)* (Dover, New York).
Abrams, G. S., *et al.* (SLC Collaboration), 1990, Phys. Rev. Lett. **64**, 1334.
Abreu, P., *et al.* (DELPHI Collaboration), 1993, Phys. Lett. B **318**, 249.
Abreu, P., *et al.* (DELPHI Collaboration), 1995, Z. Phys. C **65**, 587.
Abreu, P., *et al.* (DELPHI Collaboration), 1996, Z. Phys. C **73**, 11.
Abreu, P., *et al.* (DELPHI Collaboration), 1998, Eur. Phys. J. C **5**, 585.
Abreu, P., *et al.* (DELPHI Collaboration), 1999a, Eur. Phys. J. C **6**, 19.
Abreu, P., *et al.* (DELPHI Collaboration), 1999b, Phys. Lett. B **459**, 397.
Abreu, P., *et al.* (DELPHI Collaboration), 2000a, Eur. Phys. J. C **18**, 203; **25**, 493(E) (2000b).
Ackerstaff, K., *et al.* (OPAL Collaboration), 1997, Z. Phys. C **75**, 193.
Ackerstaff, K., *et al.* (OPAL Collaboration), 1999, Eur. Phys. J. C **7**, 369.
Acosta, D. E., *et al.* (CDF Collaboration), 2005, Phys. Rev. D **72**, 052001.
Adams, J., *et al.* (STAR Collaboration), 2006a, Phys. Lett. B **637**, 161.
Adams, J., *et al.* (STAR Collaboration), 2006b, Phys. Rev. Lett. **97**, 152302.
Adcox, K., *et al.* (PHENIX Collaboration), 2005, Nucl. Phys. A **757**, 184.
Adeva, B., *et al.* (L3 Collaboration), 1991, Phys. Lett. B **259**, 199.
Adler, S. S., *et al.* (PHENIX Collaboration), 2003a, Phys. Rev. Lett. **91**, 072301.
Adler, S. S., *et al.* (PHENIX Collaboration), 2003b, Phys. Rev. Lett. **91**, 241803.
Adloff, C., *et al.* (H1 Collaboration), 1997, Nucl. Phys. B **504**, 3.
Aihara, H., *et al.* (TPC/Two-Gamma Collaboration), 1984, Phys. Rev. Lett. **53**, 2378.
Aihara, H., *et al.* (TPC/Two-Gamma Collaboration), 1987, Phys. Lett. B **184**, 299.
Aihara, H., *et al.* (TPC/Two-Gamma Collaboration), 1988a, Report No. LBL-23737 UC-34D.
Aihara, H., *et al.* (TPC/Two Gamma Collaboration), 1988b, Phys. Rev. Lett. **61**, 1263.
Airapetian, A., *et al.* (HERMES Collaboration), 2004, Phys. Rev. Lett. **92**, 012005.
Airapetian, A., *et al.* (HERMES Collaboration), 2005, Phys. Rev. D **71**, 012003.
Aivazis, M. A. G., J. C. Collins, F. I. Olness, and W. K. Tung, 1994, Phys. Rev. D **50**, 3102.
Aivazis, M. A. G., F. I. Olness, and W. K. Tung, 1994, Phys. Rev. D **50**, 3085.
Akers, R., *et al.* (OPAL Collaboration), 1994, Z. Phys. C **63**, 181.
Akers, R., *et al.* (OPAL Collaboration), 1995, Z. Phys. C **68**, 203.
Akrawy, M. Z., *et al.* (OPAL Collaboration), 1990, Phys. Lett. B **247**, 617.
Albino, S., 2009, Phys. Lett. B **674**, 41.
Albino, S., and R. D. Ball, 2001, Phys. Lett. B **513**, 93.
Albino, S., and E. Christova, 2010, Phys. Rev. D **81**, 094031.
Albino, S., B. A. Kniehl, and G. Kramer, 2004, Eur. Phys. J. C **38**, 177.
Albino, S., B. A. Kniehl, and G. Kramer, 2005, Nucl. Phys. B **725**, 181.
Albino, S., B. A. Kniehl, and G. Kramer, 2006, Nucl. Phys. B **734**, 50.
Albino, S., B. A. Kniehl, and G. Kramer, 2008a, Phys. Rev. Lett. **100**, 192002.
Albino, S., B. A. Kniehl, and G. Kramer, 2008b, Nucl. Phys. B **803**, 42.
Albino, S., B. A. Kniehl, G. Kramer, and W. Ochs, 2005, Phys. Rev. Lett. **95**, 232002.
Albino, S., B. A. Kniehl, G. Kramer, and W. Ochs, 2006, Phys. Rev. D **73**, 054020.
Albino, S., B. A. Kniehl, G. Kramer, and C. Sandoval, 2007, Phys. Rev. D **75**, 034018.
Albino, S., *et al.*, 2008, e-print arXiv:0804.2021.
Albrecht, H., *et al.* (ARGUS Collaboration), 1989, Z. Phys. C **44**, 547.
Alexander, G., *et al.* (OPAL Collaboration), 1996, Z. Phys. C

72, 191.
Alexander, G., *et al.* (OPAL Collaboration), 1997, Z. Phys. C **73**, 569.
Aloisio, R., V. Berezinsky, and M. Kachelriess, 2004, Phys. Rev. D **69**, 094023.
Altarelli, G., R. K. Ellis, G. Martinelli, and S. Y. Pi, 1979, Nucl. Phys. B **160**, 301.
Altarelli, G., and G. Parisi, 1977, Nucl. Phys. B **126**, 298.
Althoff, M., *et al.* (TASSO Collaboration), 1983, Z. Phys. C **17**, 5.
Althoff, M., *et al.* (TASSO Collaboration), 1984, Z. Phys. C **22**, 307.
Althoff, M., *et al.* (TASSO Collaboration), 1985, Z. Phys. C **27**, 27.
Amsler, C., *et al.* (Particle Data Group), 2008, Phys. Lett. B **667**, 1.
Anselmino, M., P. Kroll, and E. Leader, 1983, Z. Phys. C **18**, 307.
Anulli, F., 2004, e-print arXiv:hep-ex/0406017.
Appelquist, T., and J. Carazzone, 1975, Phys. Rev. D **11**, 2856.
Aranda, C. P., 1995, Ph.D. thesis (Universitat Autònoma de Barcelona).
Arleo, F., 2009, Eur. Phys. J. C **61**, 603.
Arneodo, M., *et al.* (European Muon Collaboration), 1989, Nucl. Phys. B **321**, 541.
Arsene, I., *et al.* (BRAHMS Collaboration), 2007, Phys. Rev. Lett. **98**, 252001.
Ashman, J., *et al.* (European Muon Collaboration), 1991, Z. Phys. C **52**, 361.
Aurenche, P., R. Basu, M. Fontannaz, and R. M. Godbole, 2004, Eur. Phys. J. C **34**, 277.
Aversa, F., P. Chiappetta, M. Greco, and J. P. Guillet, 1988a, Phys. Lett. B **210**, 225.
Aversa, F., P. Chiappetta, M. Greco, and J. P. Guillet, 1988b, Phys. Lett. B **211**, 465.
Aversa, F., P. Chiappetta, M. Greco, and J. P. Guillet, 1989, Nucl. Phys. B **327**, 105.
Azimov, Y. I., Y. L. Dokshitzer, V. A. Khoze, and S. I. Troian, 1985, Z. Phys. C **27**, 65.
Baier, R., J. Engels, and B. Petersson, 1979, Z. Phys. C **2**, 265.
Baier, R., and K. Fey, 1979, Z. Phys. C **2**, 339.
Balitsky, I. I., and V. M. Braun, 1989, Phys. Lett. B **222**, 123.
Balitsky, I. I., and V. M. Braun, 1991, Nucl. Phys. B **361**, 93.
Ball, R. D., *et al.* (NNPDF Collaboration), 2009, Nucl. Phys. B **809**, 1; **816**, 293(E) 2009.
Barate, R., *et al.* (ALEPH Collaboration), 1998, Phys. Rep. **294**, 1.
Baringer, P., *et al.* (HRS Collaboration), 1986, Phys. Rev. Lett. **56**, 1346.
Bartel, W., *et al.* (JADE Collaboration), 1981, Phys. Lett. B **104B**, 325.
Bassetto, A., M. Ciafaloni, G. Marchesini, and A. H. Mueller, 1982, Nucl. Phys. B **207**, 189.
Beenakker, W., H. Kuijf, W. L. van Neerven, and J. Smith, 1989, Phys. Rev. D **40**, 54.
Beenakker, W., W. L. van Neerven, R. Meng, G. A. Schuler, and J. Smith, 1991, Nucl. Phys. B **351**, 507.
Behrend, H. J., *et al.* (CELLO Collaboration), 1990, Z. Phys. C **46**, 397.
Binnewies, J., 1997, Ph.D. thesis (University of Hamburg).
Binnewies, J., B. A. Kniehl, and G. Kramer, 1995a, Z. Phys. C **65**, 471.
Binnewies, J., B. A. Kniehl, and G. Kramer, 1995b, Phys. Rev. D **52**, 4947.
Binnewies, J., B. A. Kniehl, and G. Kramer, 1996, Phys. Rev. D **53**, 3573.
Blokzijl, R., *et al.* (Amsterdam-CERN-Nijmegen Collaboration), 1975, Nucl. Phys. B **98**, 401.
Blümlein, J., H. Böttcher, and A. Guffanti, 2004, Nucl. Phys. B, Proc. Suppl. **135**, 152.
Blümlein, J., H. Böttcher, and A. Guffanti, 2007, Nucl. Phys. B **774**, 182.
Blümlein, J., and V. Ravindran, 2006, Nucl. Phys. B **749**, 1.
Blümlein, J., and A. Vogt, 1998, Phys. Rev. D **58**, 014020.
Botje, M., 2002, J. Phys. G **28**, 779.
Bourhis, L., M. Fontannaz, J. P. Guillet, and M. Werlen, 2001, Eur. Phys. J. C **19**, 89.
Bourrely, C., and J. Soffer, 2003, Phys. Rev. D **68**, 014003.
Braaten, E., and J. Lee, 2002, Phys. Rev. D **65**, 034005.
Brandelik, R., *et al.* (DASP Collaboration), 1979, Nucl. Phys. B **148**, 189.
Brandelik, R., *et al.* (TASSO Collaboration), 1980, Phys. Lett. B **94B**, 444.
Brandelik, R., *et al.* (TASSO Collaboration), 1981, Phys. Lett. B **105B**, 75.
Braunschweig, W., *et al.* (TASSO Collaboration), 1989a, Z. Phys. C **42**, 189.
Braunschweig, W., *et al.* (TASSO Collaboration), 1989b, Z. Phys. C **45**, 209.
Braunschweig, W., *et al.* (TASSO Collaboration), 1990a, Z. Phys. C **47**, 167.
Braunschweig, W., *et al.* (TASSO Collaboration), 1990b, Z. Phys. C **47**, 187.
Breitweg, J., *et al.* (ZEUS Collaboration), 1997, Phys. Lett. B **414**, 428.
Breitweg, J., *et al.* (ZEUS Collaboration), 1999, Eur. Phys. J. C **11**, 251.
Brzozowska, B. (ZEUS Collaboration), 2007, *Proceedings of the 15th International Workshop on Deep-Inelastic Scattering and Related Subjects (DIS2007), Munich, Germany* (Atlantic Press, Amsterdam).
Buras, A. J., 1980, Rev. Mod. Phys. **52**, 199.
Buskulic, D., *et al.* (ALEPH Collaboration), 1995a, Z. Phys. C **66**, 355.
Buskulic, D., *et al.* (ALEPH Collaboration), 1995b, Phys. Lett. B **357**, 487; **364**, 247(E) 1995.
Buskulic, D., *et al.* (ALEPH Collaboration), 1997, Z. Phys. C **73**, 409.
Cacciari, M., and S. Catani, 2001, Nucl. Phys. B **617**, 253.
Cacciari, M., P. Nason, and C. Oleari, 2005, J. High Energy Phys. **0510**, 034.
Cacciari, M., P. Nason, and C. Oleari, 2006, J. High Energy Phys. **0604**, 006.
Cafarella, A., 2006, Ph.D. thesis (Università Degli Studi di Lecce).
Catani, S., D. de Florian, G. Rodrigo, and W. Vogelsang, 2004, Phys. Rev. Lett. **93**, 152003.
Catani, S., M. L. Mangano, P. Nason, and L. Trentadue, 1996, Nucl. Phys. B **478**, 273.
Catani, S., and L. Trentadue, 1989, Nucl. Phys. B **327**, 323.
Ceccopieri, F. A., and L. Trentadue, 2008, Phys. Lett. B **668**, 319.
Chang, C. H., J. K. Chen, Z. Y. Fang, B. Q. Hu, and X. G. Wu, 2007, Eur. Phys. J. C **50**, 969.
Chiappetta, P., M. Greco, J. P. Guillet, S. Rolli, and M. Werlen, 1994, Nucl. Phys. B **412**, 3.

Christova, E., and E. Leader, 2007, Eur. Phys. J. C **51**, 825.
Christova, E., and E. Leader, 2009, Phys. Rev. D **79**, 014019.
Christova, E., E. Leader, and S. Albino, 2010, e-print arXiv:1001.1859.
Collins, J. C., 1993, Nucl. Phys. B **396**, 161.
Collins, J. C., 1998a, Phys. Rev. D **57**, 3051; **61**, 019902(E) 2000.
Collins, J. C., 1998b, Phys. Rev. D **58**, 094002.
Collins, J. C., 2003, Acta Phys. Pol. B **34**, 3103.
Collins, J. C., 2008, PoS LC2008, 028.
Collins, J. C., and J. Pumplin, 2001, e-print arXiv:hep-ph/0105207.
Collins, J. C., and J. W. Qiu, 1989, Phys. Rev. D **39**, 1398 (the singularities at $z=1$ are derived diagrammatically rather than imposed by hand using the momentum sum rule).
Collins, J. C., and D. E. Soper, 1981, Nucl. Phys. B **193**, 381; **213**, 545(E) (1983).
Collins, J. C., and D. E. Soper, 1982, Nucl. Phys. B **194**, 445.
Collins, J. C., F. Wilczek, and A. Zee, 1978, Phys. Rev. D **18**, 242.
Consoli, M., and W. Hollik, 1989, CERN Yellow Report No. 89-08.
Coriano, C., and A. E. Faraggi, 2002, Phys. Rev. D **65**, 075001.
Cowan, G. D. (ALEPH Collaboration), 1994, *Proceedings of the 27th International Conference on High Energy Physics (ICHEP)*, Glasgow, Scotland (Institute of Physics, Bristol, UK).
Curci, G., W. Furmanski, and R. Petronzio, 1980, Nucl. Phys. B **175**, 27.
Dainton, J. B., M. Klein, P. Newman, E. Perez, and F. Willeke, 2006, JINST **1**, 10001.
Daleo, A., D. de Florian, and R. Sassot, 2005, Phys. Rev. D **71**, 034013.
de Florian, D., 2003, Phys. Rev. D **67** 054004.
de Florian, D., G. A. Navarro, and R. Sassot, 2005, Phys. Rev. D **71**, 094018.
de Florian, D., O. A. Sampayo, and R. Sassot, 1998, Phys. Rev. D **57**, 5803.
de Florian, D., R. Sassot, and M. Stratmann, 2007a, Phys. Rev. D **75**, 114010.
de Florian, D., R. Sassot, and M. Stratmann, 2007b, Phys. Rev. D **76**, 074033.
de Florian, D., M. Stratmann, and W. Vogelsang, 1998, Phys. Rev. D **57**, 5811.
de Florian, D., and W. Vogelsang, 2005, Phys. Rev. D **71**, 114004.
de la Vaissiere, C., *et al.* (MARK II Collaboration) 1985, Phys. Rev. Lett. **54**, 2071; **55**, 263(E) (1985).
Derrick, M., *et al.* (HRS Collaboration), 1987, Phys. Rev. D **35**, 2639.
Derrick, M., *et al.* (ZEUS Collaboration), 1996, Z. Phys. C **70**, 1.
Deshpande, A., R. Milner, R. Venugopalan, and W. Vogelsang, 2005, Annu. Rev. Nucl. Part. Sci. **55**, 165.
Dixon, P., 1997, Ph.D. thesis (University of Lancaster).
Dixon, P., D. Kant, and G. Thompson, 1999, J. Phys. G **25**, 1453.
Dokshitzer, Y. L., 1977, Zh. Eksp. Teor. Fiz. **73**, 1216 [Sov. Phys. JETP **46**, 641 (1977)].
Dokshitzer, Y. L., V. A. Khoze, A. H. Mueller, and S. I. Troian, 1991, *Basics of Perturbative QCD* (Editions Frontières, Gif-sur-Yvette, France).
Dokshitzer, Y. L., G. Marchesini, and G. P. Salam, 2006, Phys. Lett. B **634**, 504.
Dokshitzer, Y. L., and M. Olsson, 1993, Nucl. Phys. B **396**, 137.
Dokshitzer, Y. L., and S. I. Troian, 1984a, *Proceedings of the 19th Winter School of the LNPI* (Leningrad Nuclear Physics Institute, Leningrad), Vol. 1, p. 144.
Dokshitzer, Y. L., and S. I. Troian, 1984b, *Proceedings of the LNPI-922* (Leningrad Nuclear Physics Institute, Leningrad).
Dokshitzer, Y. L., and B. R. Webber, 1998, Discussion at Third UK Phenomenology Workshop on HERA Physics, Durham, U.K. (unpublished).
Ellis, R. K., M. A. Furman, H. E. Haber, and I. Hinchliffe, 1980, Nucl. Phys. B **173**, 397.
Ellis, R. K., H. Georgi, M. Machacek, H. D. Politzer, and G. G. Ross, 1978, Phys. Lett. B **78B**, 281.
Ellis, R. K., H. Georgi, M. Machacek, H. D. Politzer, and G. G. Ross, 1979, Nucl. Phys. B **152**, 285.
Ellis, R. K., Z. Kunszt, and E. M. Levin, 1994, Nucl. Phys. B **420**, 517; **433**, 498(E) (1995).
Ellis, R. K., and J. C. Sexton, 1986, Nucl. Phys. B **269**, 445.
Ellis, R. K., W. J. Stirling, and B. R. Webber, 1996, Cambridge Monogr. Part. Phys., Nucl. Phys., Cosmol. **8**, 1.
Fadin, V. S., 1983, Yad. Fiz. **37**, 408 [Sov. J. Nucl. Phys. **37**, 245 (1983)].
Field, R. D., and R. P. Feynman, 1977, Phys. Rev. D **15**, 2590.
Field, R. D., and R. P. Feynman, 1978, Nucl. Phys. B **136**, 1.
Floratos, E. G., D. A. Ross, and C. T. Sachrajda, 1977, Nucl. Phys. B **129**, 66; **139**, 545(E) (1978).
Fodor, Z., and S. D. Katz, 2001, Phys. Rev. Lett. **86**, 3224.
Fong, C. P., and B. R. Webber, 1989, Phys. Lett. B **229**, 289.
Fontannaz, M., 2004, Eur. Phys. J. C **38**, 297.
Foster, I., 1995, *Designing and Building Parallel Programs* (Addison-Wesley, Reading, MA), Sec. 1.4.4.
Furmanski, W., and R. Petronzio, 1980, Phys. Lett. B **97B**, 437.
Furmanski, W., and R. Petronzio, 1982, Z. Phys. C **11**, 293.
Furry, W., 1937, Phys. Rev. **51**, 125.
Georgi, H., and H. D. Politzer, 1974, Phys. Rev. D **9**, 416.
Georgi, H., and H. D. Politzer, 1976, Phys. Rev. D **14**, 1829.
Giele, W. T., and S. Keller, 1998, Phys. Rev. D **58**, 094023.
Gluck, M., E. Reya, and A. Vogt, 1993, Phys. Rev. D **48**, 116; **51**, 1427(E) (1995).
Graudenz, D., 1994, Nucl. Phys. B **432**, 351.
Graudenz, D., 1997, Fortschr. Phys. **45**, 629.
Greco, M., and S. Rolli, 1993, Z. Phys. C **60**, 169.
Greco, M., and S. Rolli, 1995, Phys. Rev. D **52**, 3853.
Greco, M., S. Rolli, and A. Vicini, 1995, Z. Phys. C **65**, 277.
Gribov, V. N., and L. N. Lipatov, 1972, Sov. J. Nucl. Phys. **15**, 438; **15**, 675(E) (1972).
Gronau, M., F. Ravndal, and Y. Zarmi, 1973, Nucl. Phys. B **51**, 611.
Gross, D. J., and F. Wilczek, 1974, Phys. Rev. D **9**, 980.
Hasegawa, T. (Spin Muon Collaboration), 1998, Nucl. Phys. A **629**, 273C.
Hillenbrand, A., 2005, Ph.D. thesis (DESY).
Hirai, M., S. Kumano, T. H. Nagai, and K. Sudoh, 2007, Phys. Rev. D **75**, 094009.
Hirai, M., S. Kumano, M. Oka, and K. Sudoh, 2008, Phys. Rev. D **77**, 017504.
Honkanen, H., *et al.*, 2009, Phys. Rev. D **79**, 034022.
Itoh, R., *et al.* (TOPAZ Collaboration), 1995, Phys. Lett. B **345**, 335.
Jager, B., A. Schafer, M. Stratmann, and W. Vogelsang, 2003, Phys. Rev. D **67**, 054005.
Jager, B., M. Stratmann, and W. Vogelsang, 2003, Phys. Rev. D **68**, 114018.

Jager, B., M. Stratmann, and W. Vogelsang, 2005, Eur. Phys. J. C **44**, 533.
James, F., 1998, CERN Program Library Long Writeup D506, http://wwwasdoc.web.cern.ch/wwwasdoc/minuit/minmain.html.
James, F., and M. Roos, 1975, Comput. Phys. Commun. **10**, 343.
Jones, D. L., and J. F. Gunion, 1979, Phys. Rev. D **19**, 867.
Jung, H., *et al.*, 2008, e-print arXiv:0809.0549.
Kalinowski, J., K. Konishi, P. N. Scharbach, and T. R. Taylor, 1981, Nucl. Phys. B **181**, 253.
Kant, D., 1995, Ph.D. thesis (University of London).
Katsoufis, E. C., and S. D. P. Vlassopulos, 1985, Nuovo Cimento Soc. Ital. Fis., A **86**, 87.
Khoze, V. A., and W. Ochs, 1997, Int. J. Mod. Phys. A **12**, 2949.
Kneesch, T., B. A. Kniehl, G. Kramer, and I. Schienbein, 2008, Nucl. Phys. B **799**, 34.
Kniehl, B. A., G. Kramer, and M. Maniatis, 2005, Nucl. Phys. B **711**, 345; **720**, 231(E) (2005).
Kniehl, B. A., G. Kramer, and B. Pötter, 2000, Nucl. Phys. B **582**, 514.
Kniehl, B. A., G. Kramer, and B. Pötter, 2001, Nucl. Phys. B **597**, 337.
Kniehl, B. A., G. Kramer, I. Schienbein, and H. Spiesberger, 2005a, Phys. Rev. D **71**, 014018.
Kniehl, B. A., G. Kramer, I. Schienbein, and H. Spiesberger, 2005b, Eur. Phys. J. C **41**, 199.
Kniehl, B. A., G. Kramer, I. Schienbein, and H. Spiesberger, 2008, Phys. Rev. D **77**, 014011.
Koller, K., T. F. Walsh, and P. M. Zerwas, 1979, Z. Phys. C **2**, 197.
Korchemsky, G. P., 1989, Mod. Phys. Lett. A **4**, 1257.
Kramer, G., and H. Spiesberger, 2001 Eur. Phys. J. C **22**, 289.
Kramer, G., and H. Spiesberger, 2003, Eur. Phys. J. C **28**, 495.
Kramer, G., and H. Spiesberger, 2004, Eur. Phys. J. C **38**, 309.
Krämer, M., F. I. Olness, and D. E. Soper, 2000, Phys. Rev. D **62**, 096007.
Kretzer, S., 2000, Phys. Rev. D **62**, 054001.
Kretzer, S., E. Leader, and E. Christova, 2001, Eur. Phys. J. C **22**, 269.
Kretzer, S., and I. Schienbein, 1999, Phys. Rev. D **59**, 054004.
Lafferty, G. D., P. I. Reeves, and M. R. Whalley, 1995, J. Phys. G **21**, A1.
Libby, S. B., and G. Sterman, 1978a, Phys. Rev. D **18**, 3252.
Libby, S. B., and G. Sterman, 1978b, Phys. Rev. D **18**, 4737.
Lipatov, L. N., 1974, Yad. Fiz. **20**, 181 [Sov. J. Nucl. Phys. **20**, 94 (1975)].
Lu, X.-Q., 1986, Ph.D. thesis (Johns Hopkins University).
Lupia, S., and W. Ochs, 1998, Eur. Phys. J. C **2**, 307.
Marciano, W. J., 1984, Phys. Rev. D **29**, 580.
Martin, A. D., R. G. Roberts, W. J. Stirling, and R. S. Thorne, 2002, Eur. Phys. J. C **23**, 73.
Mele, B., and P. Nason, 1991, Nucl. Phys. B **361**, 626.
Mitov, A., and S. Moch, 2006, Nucl. Phys. B **751**, 18.
Mitov, A., S. Moch, and A. Vogt, 2006, Phys. Lett. B **638**, 61.
Moch, S., and J. A. M. Vermaseren, 2000, Nucl. Phys. B **573**, 853.
Moch, S., and A. Vogt, 2008, Phys. Lett. B **659**, 290.
Mocioiu, I., Y. Nara, and I. Sarcevic, 2003, Phys. Lett. B **557**, 87.
Mueller, A. H., 1978, Phys. Rev. D **18**, 3705.
Mueller, A. H., 1981, Phys. Rep. **73**, 237.
Mueller, A. H., 1983a, Nucl. Phys. B **213**, 85.
Mueller, A. H., 1983b, Nucl. Phys. B **228**, 351.
Nadolsky, P. M., D. R. Stump, and C. P. Yuan, 2001, Phys. Rev. D **64**, 114011.
Nason, P., S. Dawson, and R. K. Ellis, 1989, Nucl. Phys. B **327**, 49; **335**, 260(E) (1990).
Nason, P., and B. R. Webber, 1994, Nucl. Phys. B **421**, 473; **480**, 755(E) (1996).
Peskin, M. E., and D. V. Schroeder, 1995, *An Introduction To Quantum Field Theory* (Addison-Wesley, Reading, MA), Sec. 12.4.
Petersen, A., *et al.* (MARK II Collaboration), 1988, Phys. Rev. D **37**, 1.
Press, W. H., *et al.*, 2001, *Numerical Recipes*, 2nd ed. (Cambridge University Press, Cambridge, England), Sec. 5.8.
Pumplin, J., D. R. Stump, J. Huston, H. L. Lai, P. Nadolsky, and W. K. Tung, 2002, J. High Energy Phys. **0207**, 012.
Pumplin, J., D. R. Stump, and W. K. Tung, 2002, Phys. Rev. D **65**, 014011.
Pumplin, J., *et al.*, 2002, Phys. Rev. D **65**, 014013.
Qiu, J. W., and X. F. Zhang, 2001, Phys. Rev. D **64**, 074007.
Reya, E., 1981, Phys. Rep. **69**, 195.
Rijken, P. J., 1997, Ph.D. thesis (Rijksuniversiteit te Leiden).
Rijken, P. J., and W. L. van Neerven, 1996, Phys. Lett. B **386**, 422.
Rijken, P. J., and W. L. van Neerven, 1997a, Phys. Lett. B **392**, 207.
Rijken, P. J., and W. L. van Neerven, 1997b, Nucl. Phys. B **487**, 233.
Rodrigo, G., S. Catani, D. de Florian, and W. Vogelsang, 2004, Nucl. Phys. B, Proc. Suppl. **135**, 188.
Sakai, N., 1979, Phys. Lett. B **85B**, 67.
Sandoval, C., 2009, Thesis (DESY).
Schellman, H., *et al.* (MARK II Collaboration), 1985, Phys. Rev. D **31**, 3013.
Schienbein, I., *et al.*, 2008, J. Phys. G **35**, 053101.
Schierholz, G., and D. H. Schiller, 1980, Thesis (DESY).
Soper, D. E., and J. C. Collins, 1994, e-print arXiv:hep-ph/9411214.
Sterman, G., *et al.* (CTEQ Collaboration), 1995, Rev. Mod. Phys. **67**, 157.
Stratmann, M., and W. Vogelsang, 1997, Nucl. Phys. B **496**, 41.
Stump, D., *et al.*, 2002, Phys. Rev. D **65**, 014012.
Thorne, R. S., *et al.*, 2002, J. Phys. G **28**, 2717.
Trentadue, L., and G. Veneziano, 1994, Phys. Lett. B **323**, 201.
Tung, W. K., S. Kretzer, and C. Schmidt, 2002, J. Phys. G **28**, 983.
Ubiali, M., 2009, Nucl. Phys. B, Proc. Suppl. **186**, 62.
Vlassopulos, S. D. P., 1985, Lett. Nuovo Cimento Soc. Ital. Fis. **42**, 225.
Vogt, A., 2005, Comput. Phys. Commun. **170**, 65.
Weinberg, S., 1996, *Modern Applications: The Quantum Theory of Fields* (Cambridge University Press, Cambridge, England), Vol. 2, Chap. 20.
Witten, E., 1976, Nucl. Phys. B **104**, 445.